YRKESHÖGSKOLAN
NOVIA

Engine Laboratory Remodel

Modification of the Bench Test for the Adaptation of the SISU 420 DWRIE and Opel Z16XEP Engines

Pablo Guillén Moralejo

Pol Criado Martínez

Thesis for a Novia UAS degree

Degree Programme in Energy Technology

Vaasa, Finland, 2022

DEGREE THESIS

Author: Pablo Guillén Moralejo & Pol Criado Martínez

Degree Programme: Mechanical Engineering

Specialization: Energy Technology

Supervisors: Philip Hollins & Tobias Ekfors

Title: Engine Laboratory Remodel

Date	Number of pages	Appendices
May 17, 2022	91	18

Abstract

Engine testing is a tool to compare the performance of different states of tune and different types of engines. The aim of this thesis is to remodel the engine laboratory in Technobothnia so that the engine testbed can operate in optimal conditions with two different engines, these being SISU 420 DWRIE, a diesel engine, and Opel Z16XEP, a gas-operating engine.

The thesis reviewed a range of different things that could be changed in the engine laboratory, including the dynamometer, the shape of the testbed, the mountings and the coupling between the engine and the dynamometer.

As a result, it was found that the engine laboratory could be arranged such as it could test the two different engines on the same testbed. This was accomplished by enlarging the structure from 740mm to 855mm and replacing one side of the bed with two beam assemblies where the SISU engine will lie. This model was simulated using Siemens NX, giving a maximum deformation of 0.004mm, which is correct for the operation. The dynamometer was replaced by a Lanmec DW250 which can reach the Opel maximum (6500rpm) and the SISU maximum torque (503Nm). The mountings were also replaced, using for each engine a model that isolates the vibrations at idle speeds. The coupling also needed to be replaced as the current coupling could not be used for both engines. This is because of the SAE size, being the Opel engines' flywheel 7 ½ and the SISUs' 11 ½. To solve this, the coupling was substituted for the CENTAX-TEST, which can operate with both engines and the critical speeds of the shaft are 262.45rpm for the SISU engine and 244.05rpm for the Opel engine, which are both below the idle speeds of the engine, which is correct for the operation. The overall cost of the laboratory remodel would be 22720€, which is within the 30000€ budget cap.

Language: English

Keywords: Testbed, Opel, SISU, NX, Dynamometer, Coupling, Mounting, Engine Testing, Structure, Simulation, Vibrations, Power

Table of contents

List of figures

List of tables

1 Introduction

Currently, the engine laboratory of Technobothnia building in Vaasa owns three different engine benches that have been in operation for the last years. However, the appearance of new technologies, opportunities and also certain limitations with the operation of one of the tools, have motivated the approach of this project. At the moment, the existing engine used for testing is limited in terms of its study. The issue regarding it corresponds to the dynamometer that is being used to brake the engine while it is being tested, which cannot offer as much braking torque as needed for stopping the engine leading to complete analysis of the power and torque that it can produce. At the same time, the laboratory has the opportunity of changing the current water brake dynamometer for an eddy current based.

Also, the laboratory team is interested in testing different engines on the bench, increasing that way the data that could be extracted and also increasing the quality of the tests that could be done. In this case, the engines are the SISU 420 DWRIE diesel engine and the Opel Z16XEP, which operates with petrol.

The purpose of engine testing is to compare performance in different states of tune, meaning that the engine needs to be tested at its whole operating range. As said before the main issue with the current dynamometer is the braking power is not enough to fully brake the engine, so this thesis covers a study regarding the dynamometer, the possible dynamometer options regarding the torque and the power and also the economics of the new option.

With regards to the possibility of testing different engines in the same bench test, a design of a new bed and its calculations, being the structural analysis and vibration analysis, will be presented, to fit the engines without having to change the bed. Also, a new coupling design for the new shaft and dynamometer will be presented.

In order to accomplish all these things, the engine laboratory team accorded a budget of 30000€.

2 Aim and objectives

The aim of this thesis is based on the remodel and modularity of one of the three engine laboratory's bench tests available in Novia UAS' placed in the Technobotnia building. Currently, the engine laboratory facility in question lacks a good dynamometer, thus being limited in terms of testing.

To achieve the aim of this thesis, the following objectives were set:

- Analysis of the existing dynamometers and their feasible alternatives existing in the market (water dynamometer and eddy current dynamometer respectively).
- Investigate the economic feasibility of the alternative dynamometers in case the existing ones cannot be used as a solution.
- Analysis of the existing mountings and couplings and their feasible alternatives existing in the market
- Design of the engine bed and structural simulations.

2.1 Document structure

The first section (Section 3) provides an overview of the theory involved in the project, including an introduction to engine testing, and the theory behind the dynamometers, mountings and couplings. Sections 4, 5 and 6 describe the methodology used for the selection of the dynamometer, mountings and coupling in the new setup respectively. Section 7 describes the process of the remodelling of the testbed, including the build-in NX as well as deformation simulations. Finally, the last three sections (Sections 8, 9 and 10) evaluate the outcome of the project, whether the objectives have been accomplished and further research.

3 Study background

The first stage of the project is based on the research of literature for the correct understanding of all the involved elements that later are going to be an object of study and practice. As mentioned before, the focal points for the project are, firstly, the research and study of engine test benches, focusing especially on the parts that need to be replaced. Thus, dynamometers that could replace the actual model for carrying on tests for the available engines, are going to be an object of literature study too.

This would regard the first block of the project. After the study of dynamometers, the literature will focus on the related aspects for the second block of the work, based on the coupling and mounting of the engine, which will lead to the familiarization with the required concepts previous to the design phase.

3.1 SISU diesel 420 DWRIE engine

The available laboratory engine in Novia UAS that is going to be talked about in this project is a SISU diesel engine. Concretely, the engine is called SISU diesel 420 DWRIE and it is located in the Energy Technology and Automotive Technology laboratory in the basements of the Technobothnia building in the Finnish city of Vaasa.

3.1.1 SISU diesel 420 DWRIE specifications

This type of engine is used mainly to supply tractors. The engine designation indicates the main characteristics of the engine, and they are summed up in Table 1, sometimes the engine designation is simplified to SISU DWI or SISU DWRIE. The specifications of the engine and a section view of the engine are found in Table 2 and Figure 1 respectively.

Table 1: Engine type designation breakdown. Source: (Sisu Diesel, 2022)

4	4 cylinders
20D	Basic type (not ECU)
W	Turbocharged engine equipped with bypass turbo
R	Rotary fuel injection pump
I	Equipped with heat exchanger air to water
E	Emission tested engine (certified) for off-road

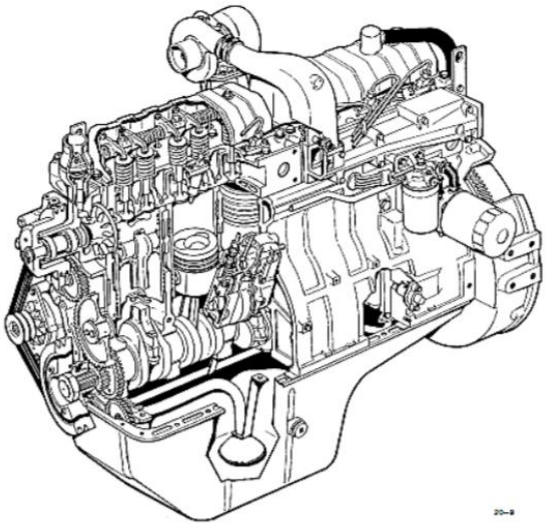

Figure 1: Drawing of Sisudiesel 420 DWRIE. Source: (Sisu Diesel, 2022)

Table 2: SISU diesel 420 DWRIE engine specifications. Source: (Sisu Diesel, 2022)

Manufacturer	SISU Diesel Inc. (FINLAND)
Type	SISU diesel 420 DWRIE
Power	95kW at 2200rpm
Serial nº	J18570
Displacement (dm^3)	4.4
Cylinder bore (mm)	108
Stroke (mm)	120
Compression ratio	16.5
Combustion	Direct injection
Firing order	1-2-4-3
Compression pressure (bar)	24
Weight (kg)	345
Direction of rotation from the engine front	clockwise

It's noted that the compression pressure is the minimum value at operating temperature and starting revs. The maximum permitted difference between cylinders is 3,0 bar. The weight of the engine it's measured without the flywheel and electrical equipment.

As said before, the engine was initially designed as a tractor engine and it was assembled in the laboratory engine for academic purposes. As seen in Table 2, it has direct injection without a common rail. And according to the engine plate, it has an output of 95 kW (approximately 130 hp) at 2200rpm.

3.2 Opel Z16XEP engine

The engine that needs to be tested as well as the SISU engine, is the Opel Z16XEP engine. This engine is also located in the Energy Technology and Automotive Technology laboratory in the basements of Technobothnia, but the engine is not in use at the moment.

3.2.1 Opel Z16XEP engine specifications

This type of engine is used mainly in cars, specifically in Opel Astra. It is a 4-cylinder petrol engine and the specifications of the engine and a section view of the engine are found in Table 3 and Figure 2 respectively.

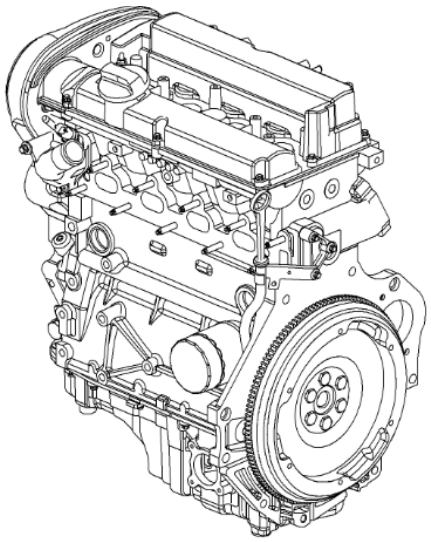

Figure 2: Drawing of Opel Z16XEP engine. Source: (7zap, 2022)

Table 3: Opel Z16XEP specifications. Sources: (Car Repair Manual, 2009; Auto-data, 2009)

Manufacturer	Opel
Type	Opel Z16XEP
Power	77kW at 6000rpm
Serial nº	Z16XEP 20EE9324
Displacement (dm^3)	1.598
Cylinder bore (mm)	79
Stroke (mm)	81.5
Compression ratio	11
Combustion	Multi-point indirect injection
Firing order	1-3-4-2
Compression pressure (bar)	12
Weight (kg)	108
Direction of rotation from the engine front	clockwise

3.3 Engine testing

The main purpose of engine testing is to compare the performance of different states of tune and different types of engines. (Atkins, 2009). Because of the automotive industry's constant development, engine manufacturers constantly perform rigorous engine testing, as part of their research (Martyr & Plint, 2007).

Whenever engine manufacturers develop new technology and implement it on a new engine, an appropriate type of engine test is used to verify the performance of the new engine components. The newly developed technology can then be tested before it is mass-produced (a benefit that reduces the cost of engine development) (Engine Testing Overview). Contrary to road testing, engine testing quantifies and isolates engine performance parameters from vehicle performance. This enables engine developers to determine exactly what engine modifications lead to improvements in the performance, resulting in considerably less testing time (Power Test Dynamometer, 2022). Some form of engine testing always forms part of the engine manufacturing process, where engine testing is primarily implemented in the form of either a hot or a cold test. A hot test is generally performed within an engine production test cell and on a complete engine. The aim is to establish if the engine is complete and runs. However, a cold test is performed on a near-complete engine and employs a cold test rig situated within the assembly line. The purpose of the cold test is to confirm the satisfactory performance of a specific subassembly of the complete engine (Grobbelaar et al., 2017).

Apart from the types of engine testing mentioned above, there are numerous other applications of engine testing. Some of the most common types of engine testing include durability testing, engine performance testing, fuel and lubrication testing, engine emissions testing and exhaust system testing (Atkins, 2009).

3.4 Engine bench tests

The primary function of the test bench is to facilitate the mounting of the unit under test, as well as to support all other equipment required to perform the relevant tests. Generally, the design of the test bench varies according to the type of engine test being performed. General-purpose automotive engine test cells often employ a common tee-slotted bedplate design, which offers maximum flexibility in that it allows both the position of the dynamometer and the engine to be adjusted. When performing hot and cold tests in an engine production environment, the primary concern is that the test bench used must permit fast engine changeovers. Such a test bench only needs to offer limited flexibility in terms of the mounting arrangements that it supports. For research and development purposes, it is also often required that the test bench makes special provisions for the mounting of additional equipment also included in the test procedure (Martyr & Plint, 2007).

In addition, the test bench must be able to withstand the forces exerted by the equipment it supports. This comprises both static, which appears due to the weight of the equipment, and dynamic forces generated throughout the engine test procedure. As a result of this, test benches are typically built to be robust and stiff. However, equipment must be provided for the test bench to absorb as much engine vibration as feasible (Martyr & Rogers, 2021). This is especially important when employing instrumentation that is directly mounted to the test bench because any vibration present at the measurement point would appear as noise in the measured data (Grobbelaar et al., 2017). Therefore, special precautions must be taken to guarantee that the measurement equipment is not subjected to excessive vibration. In most cases, this is accomplished by mounting the engine or measurement equipment on anti-vibration mountings. In addition, the test bench must include the appropriate safety features to ensure that the engine testing operation is carried out safely. If enclosing the test setup is not possible, all components that represent a danger of injury should be covered by a safety enclosure or properly marked with a warning sign. These safety coverings must be sturdy enough to contain the mechanical components of the test setup in the event of a catastrophic breakdown during the testing process, in addition to limiting access to the danger zone (Australian Government, 2012).

The dynamometer is the most critical piece of equipment used in the engine testing operation, second only to the engine being evaluated. The dynamometer's job is to resist and measure the torque created by the primary mover it is attached to. The dynamometer should, in theory, be able to apply varying loads to the engine while it is running at its maximum speed and torque (Atkins, 2009). Furthermore, the accuracy with which the dynamometer measures both the speed and torque of the engine being tested is vital to all other derived measurements made during the engine testing procedure (Martyr & Plint, 2007). To obtain satisfactory results, an appropriate dynamometer must thus be selected that best suits the type of engine testing to be performed.

The dynamometer must be connected to the test engine through a driveshaft to measure the power output. Depending on the dynamic characteristics of the engine-dynamometer setup being employed, there are several ways to achieve this task. The selection of the appropriate shaft and couplings for the driveshaft is not an easy undertaking. A multitude of issues can arise if the driveshaft components are chosen incorrectly or the system is designed incorrectly (Hasnun & Bin, 2012).

3.5 Dynamometers: Measure of torque, speed and power

An engine dynamometer is servicing equipment that allows the operator to safely load an engine with a regulated load. The only way to evaluate engine capabilities is to run it through a loaded engine dynamometer test. An engine may be adequately driven across its power range without being brought into service using a dyno. Before the engine is

fitted into a chassis, defects in the assembly can be discovered, and a real evaluation of the engine's running condition can be done. Also, before an engine is installed, it must pass a final quality test on the dynamometer (Fahad, 2015). The engine dynamometer is the most significant piece of equipment utilized in the engine testing process. The dynamometer's job is to resist and measure the torque created by the primary mover it is linked to. The dynamometer should ideally be able to apply varying loads to the engine while it is running at its maximum speed and torque (Atkins, 2009). The selection of the dynamometer is one of the most important aspects of the entire engine test bench for achieving good speed, torque and power measurements.

This said dynamometers can be classified into two big groups depending on the applications that are going to cover. Engine dynamometers and chassis dynamometers are the two primary types of dynamometers used in engine testing. An engine dynamometer is a device that attaches to an engine's crankshaft and measures the torque generated only by the engine. A chassis dynamometer, on the other hand, is made up of rollers that are driven by the wheels of the vehicle under test, and it measures the torque available at the wheels (Fuller, 2012). Regarding the construction of the engine laboratory and the type of testing that is carried on, the analysis will focus on engine dynamometers. Among engine dynamometers, there is a wide range of options that can be considered. The differential aspect for these refers to the way that the engine torque is absorbed, however, the big majority can be split into two groups. The first group for the ones that absorb torque electrically, and the second group regards the hydraulic absorbed torque (Atkins, 2009).

3.5.1 Eddy current dynamometers

Eddy current brakes leave aside friction and kinetic energy to stop moving elements, in this case, electromagnetism is the basic aspect that carries on this action. When a conductor travels through a magnetic field, opposing forces rotate inside the conductor, resulting in eddy currents (AZoM, 2019). According to Lenz's law, eddy currents are caused when a conductor is exposed to a changing magnetic field due to the relative motion of the field source and the conductor, or, on the other hand, due to variation of the field with time, which causes circulating currents that lead to magnetic fields that oppose the change of the original magnetic field. This interaction of electromagnetic forces is optimal for smooth deceleration. Thus, the basic idea behind this principle is the metal is not leaving the magnetic field where it is originating a change in the magnetic flux due to its movement (Ling et al., 2016). This principle is presented schematically (see Figure 3), where a metal disk is rotating inside an induced magnetic field.

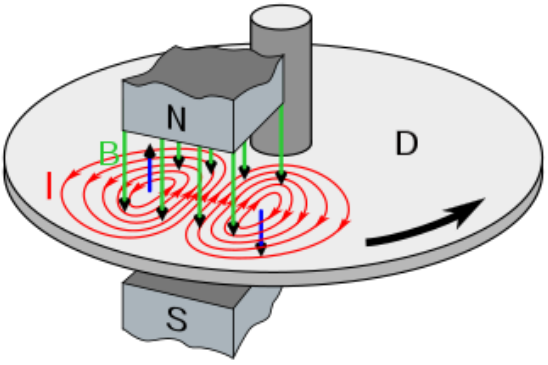

Figure 3: Eddy currents formed in a rotating metal disk inserted on a magnetic flux between magnets. In red, induction lines are shown, as for the magnetic fields B, they are identified with green arrows. Source: (MAGCRAFT Brand Rare Earth Magnets, 2015)

This principle can be helpful in innumerable applications, as far as this study is concerned, the eddy currents can be used to achieve the required braking conditions.

Focusing on the application of the principle in dynamometers, this is used to produce torque and power absorption of the engine that they are attached to by using electromagnetic induction as mentioned before. A toothed rotor made of high magnetic permeability steel revolves between water-cooled steel loss plates with a fine clearance in the most popular variant. One or two annular coils (depending on the arrangement) provide a magnetic field parallel to the machine axis, and rotor motion (see Figure 4) generates variations in magnetic flux distribution in the loss plates (Martyr & Plint, 2007). This variation in the amount of current flowing through the coils varies the amount of magnetic flow generation.

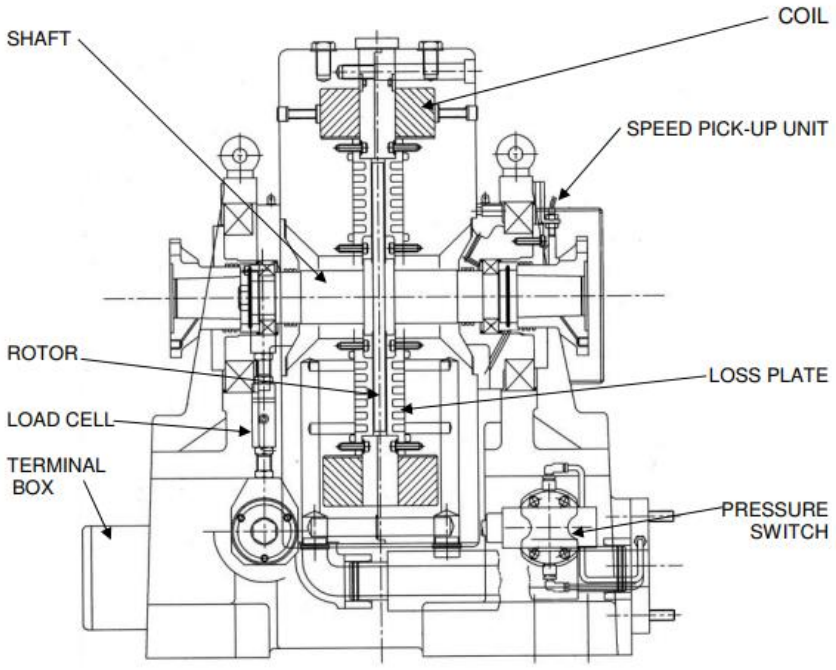

Figure 4: Cross-section view of an eddy current dynamometer produced by Froude company, model AG250HS. Source: (Froude, 1994)

Then, when the shaft of the dynamometer starts the rotation movement, the rotor cuts the magnetic field, generating eddy currents, which generate resistance to the shaft rotation (Killedar, 2012). Heat is delivered to cooling water moving via passageways in the loss plates, with some cooling provided by radial air movement in the gaps between the rotor and the plates. The current provided to the annular stimulating coils is varied to regulate power, and quick load changes are feasible (Coxon, 2011). Eddy-current machines (see Figure 5) are simple and reliable as long as enough cooling water flow is maintained; the control system is straightforward, and they can provide significant braking torque at low speeds. However, eddy current brakes are unable to bring the motion to a complete halt since the braking force provided reduces as the speed is lowered (Ling et al., 2016).

Figure 5: Eddy current dynamometer manufactured by Application Systems, model APPSYS MT. Source: (IndiaMART, 2022)

Following the cooling aspects, leads the study to split eddy current brakes into two big groups, dry gap and wet gap dynamometers. In the first case, the cooling of the machine is an indirect process where the rotating shaft working inside of the magnetic field, is separated from the coolant, normally water. On the other hand, in wet gap brakes, the space between the rotor and the loss plate (inside where it rotates) contains the coolant the rotor is partially submerged (Killedar, 2012).

3.5.2 Magnetic powder dynamometers

Another example, also feasible for the desired application is a powder dynamometer. This kind of brake has similarities with eddy current in terms that the force that decelerates the shaft is induced by a magnetic field (Martyr & Rogers, 2021). In this case, as the name indicates, magnetic powder is placed in the gap between the rotator and the coil (see Figure 6). The working principle is based on using the magnetic powder to generate friction and smoothly decelerate the shaft. Precisely, a coil is used to drive an electrical direct current through it, thus, a magnetic field is induced on the powder (Magtrol, 2017).

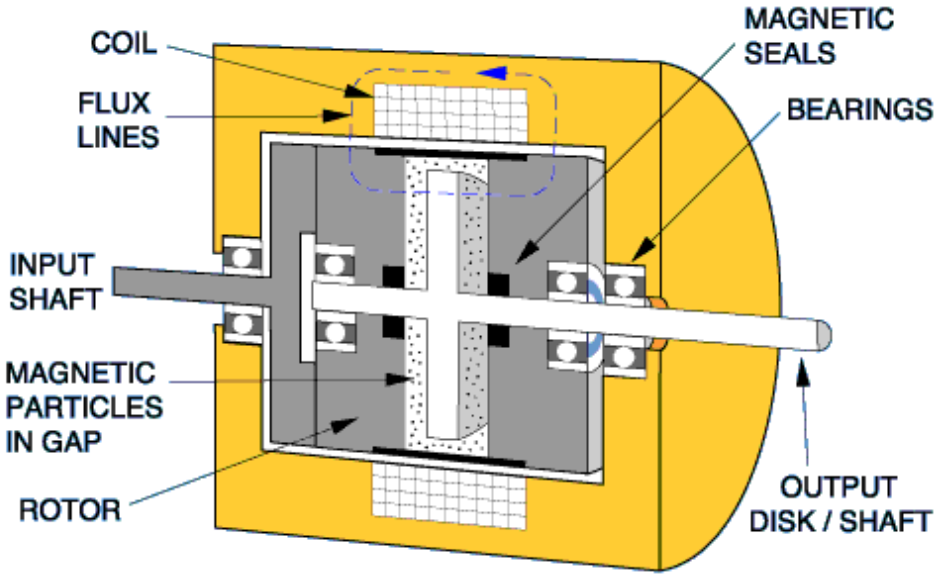

Figure 6: Magnetic powder brake cross-section. Source: (Placid Industries, 2020)

These particles follow the resulting flux lines leading to the formation of chains that are constantly built and broken as the shaft turns and changes the magnetic field, the friction developed by such particles generates a big opposing force to the rotation, i.e. torque (Killedar, 2012). It is important to remark that in this variant to eddy current dynamometers, the generated field is proportional to the applied DC input. Besides that, friction brings heat dissipation problems that typically limit the rotational speed of the shaft and possible data gathering (Placid Industries, 2020).

3.5.3 Hysteresis dynamometers

Hysteresis brakes follow the line of eddy current brakes and powder dynamometers for torque production, these also undergo magnetic forces for the standstill of the shaft. In this case, no friction nor shear forces are involved in the functioning, thus, magnetic hysteresis is the basic effect behind the functioning. As the main components that stand out are a reticulated pole and the rotor-shaft (Dspmindustria, 2021). Figure 7 shows an inner view of the main involved elements of this typology of brakes, which share a lot of similarities with the ones introduced before.

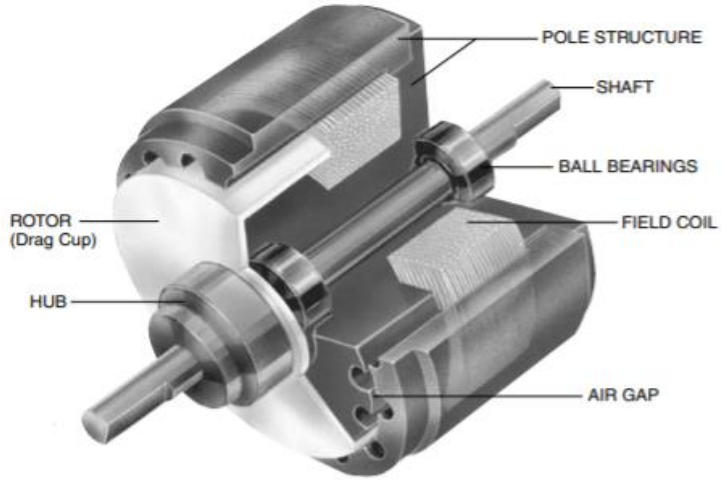

Figure 7: Hysteresis dynamometer sectioned 3D view. Source: (Killedar, 2012)

The air gap creates a flux field when a magnetizing force from a field coil or magnet is applied to the pole structure. The rotor is magnetically restrained, allowing the pole structure and rotor to break together. Focusing on structure differences in comparison to eddy current dynos (to who most resemble), a hysteresis dynamometer is an eddy current absorber that, unlike other "disk-type" eddy current absorbers, houses the magnetic coils inside a vented and ribbed cylinder and rotates it rather than a disk between the electromagnets. The hysteresis absorber's potential benefit is that its diameter may be reduced while its working rpm can be raised. The control of torque in these dynamometers is provided by a field coil, likewise, magnetic powder brakes allow the control of torque by adjusting the DC passing through the said coil (Killedar, 2012).

3.5.4 Water brake dynamometers

Hydraulic dynamometers have the potential to withstand extremely huge quantities of power as well as power at extremely fast speeds. The hydraulic dynamometer (also known as a water-brake dynamometer) is made up of a rotor (connected to a spinning driveshaft) with machined semi-elliptical pockets that are placed inside of a watertight casing. Figure 8 introduces these details and gives a schematic view of the concepts that will be introduced below in this section.

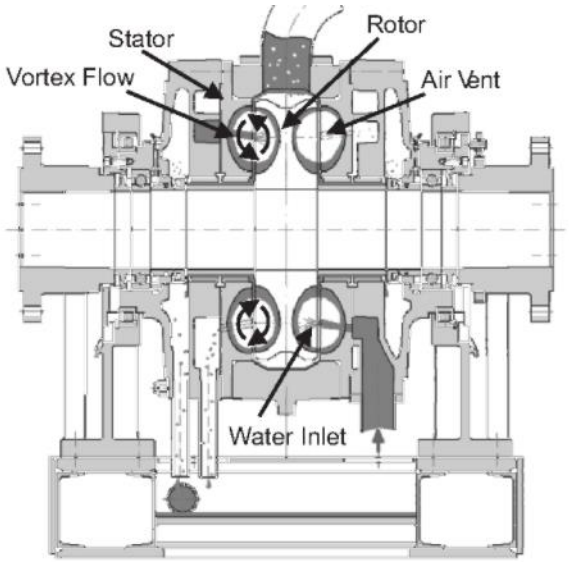

Figure 8: Sectioned view of the water brake dynamometer showing the interaction between the rotor and the fixed casing. Elliptical pockets (gaps in the blank between the rotor and the fixed casing) with the corresponding toroidal flow of water are also represented. Source: (M. Vetr et al., 2017)

The waterproof enclosure has also been machined with similar pockets leading to elliptical enclosures when both elements are combined. The rotor's pockets, as well as those in the casing, are separated by radial vanes (see Figure 9), which are positioned at an angle separating the dynamometer from each other (Martyr & Plint, 2007).

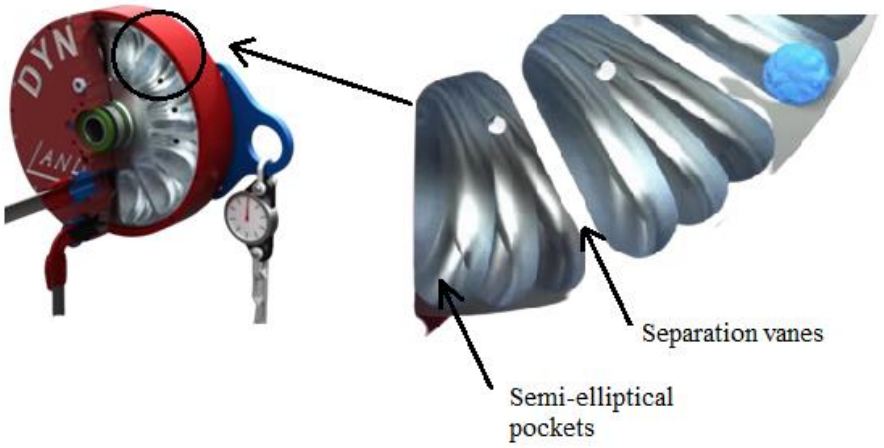

Figure 9: Water brake dynamometer model with detail on the semi-elliptical pockets that lead water particles to flow between the rotor and the casing producing torque. Source: (Adapted from DYNOmite Dynamometer, 2020)

The rotor shaft is held in place by bearings that support it in the dynamometer housing, which is itself supported by trunnion bearings. This implies that the dynamometer's case may freely spin around the same axis as the rotor shaft (Atkins, 2009).

Focusing now on the way that water flows into the dynamometer and also how torque is produced, the rotor shaft is attached to the engine's crankshaft during operation, and the dynamometer's housing is filled with water. Water is released from the rotor

pockets into the pockets in the dynamometer's casing when the rotor rotates in the water-filled casing, this rotation, as shown in Figure 10 a, generates a centrifugal force that sets up a toroidal water stream through the pockets.

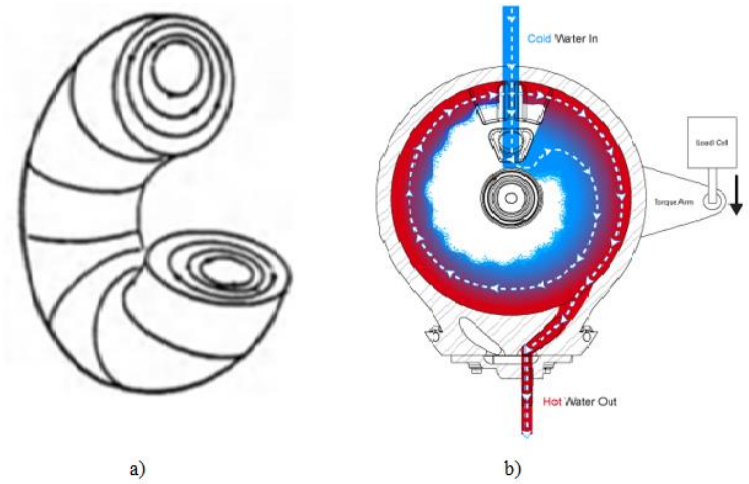

Figure 10: a) Representation of the toroidal flow followed by water particles while circulating on the elliptical enclosures. Source: (Atkins, 2009). b) Representation of the water flow temperature after entering the rotor and circulating on the fixed enclosure. It can be seen how the stream of water enters at low temperature (represented in blue) and after the corresponding friction leaves the enclosure at high temperature. Source: (Stuska Dyno, 2022)

The water is then returned at a slower speed to re-enter the pockets in the rotor, the shearing of the water causes the rotor to have a resistance to rotation, causing the dynamometer casing to suffer a torque reaction. The dynamometer shell pivots on its trunnion bearings as a result of the torque reaction (Atkins, 2009).

The dynamometer's torque response may then be estimated using the formula connecting a lever arm of a specified length to the dynamometer's housing. The force at the end of this lever arm is being measured. Aside from providing rotational resistance, water running through the dynamometer also transports away the heat created during the dissipation of energy within the dynamometer, keeping the dynamometer from overheating (Killedar, 2012). The water causes the rotor to have a resistance to spin, causing the dynamometer case to suffer a torque reaction. The dynamometer shell pivots on its trunnion bearings as a result of the torque reaction (Atkins, 2009).

3.5.5 Oil-shear friction dynamometers

The usage and management of transmission fluid in a friction device consisting of several friction discs and drive plates are known as Oil Shear Technology. This friction stack may function as a clutch or a brake. Fluid may flow through the stack, over the contact surfaces, and out to the housing or an external cooling system thanks to a specialized recirculation mechanism integrated into the hub. As a result, heat that has built up inside the friction stack is taken out of the stack and cooled decreasing friction material

wear and deterioration (powderbulksolids, 2019). A boundary film of transmission fluid is pushed into a shear state between the friction surface and drive plates as the stack is compressed, either by pressure (air or hydraulics) or springs. Torque is conveyed between the two surfaces via this sharing phenomenon of the precisely designed fluid, accelerating or decelerating the other component (KRemington, 2021). Two things are going on. Firstly, because much of the work is done by shearing the fluid, the heat is created inside the fluid rather than in the friction stack, after that, the fluid film isolates the friction disc from the drive plates as shown in Figure 11, which reduces the friction material's mechanical wear (ForceBwU, 2021).

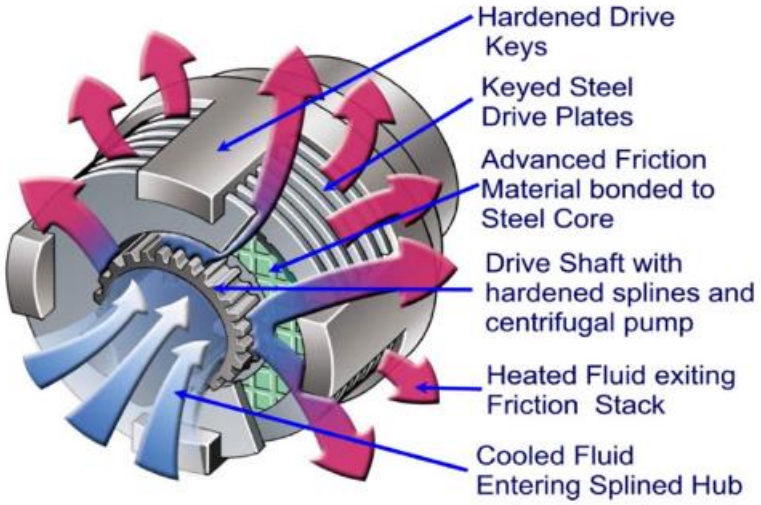

Figure 11: Main parts of the dynamometer applying oil-shear technology and an indication of the flowing heated fluid that excites the friction stack. Source: (ForceBwU, 2021)

As the clamping pressure rises, the transmission fluid in shear passes torque between the two components, rising until mechanical lock-up occurs. A large improvement in thermal capacity and overall cycle life can be achieved by cooling the friction surfaces and minimizing mechanical wear (ForceBwU, 2021). To transmit torque, many competitive clutches and brakes rely on friction between dry surfaces surrounded by air. The high heat generated by skidding on dry surfaces is difficult to disperse fast, resulting in wear, glazing, and friction material deterioration. As a result, there is inaccuracy in positioning, a short service life, and potential safety concerns. Oil Shear Technology also has several additional advantages. The transmission fluid also lubricates the bearings, splines, and driving pins, decreasing wear and extending the life of those components. And the housing itself has several advantages. It is a high-efficiency heat exchanger that extracts heat from a fluid and dissipates it to the outside. Because the transmission fluid must be retained within the brake, the housing is completely encased and sealed, preventing dirt, dust, chips, food, moisture, or chemicals from entering (powderbulksolids, 2019). It also keeps contaminants within, preventing friction material dust, which is a major problem with dry friction goods.

The provision of a transmission film between the friction material and the corresponding steel disc is a key component of Oil Shear Technology. The drive plate rotates with the input power source (usually a motor), while the splined friction disc is linked to the output or indexing shaft in a clutch. The output shaft is accelerated to the input speed when it is engaged (ForceBwU, 2021). The drive plates are secured to the housing and the friction discs rotate with the output shaft in a brake. When the output shaft is engaged, it is decelerated until it comes to a complete halt. The friction disc and driving plate are squeezed together during the engagement. A piston propelled by pneumatic or hydraulic pressure, or springs through a pressure plate can do this (powderbulksolids, 2019).

The more torque is delivered, the higher the engagement pressure. Maintaining a fluid layer between the friction disc and the driving plate is the Oil Shear principle. The fluid film is sheared when they are forced together at various speeds, imparting torque between the two components, moreover, it separates the two sections during this dynamic period of acceleration or deceleration, essentially reducing mechanical wear (see Figures 10a and 10b). The film is shattered when they come together, and the portions mechanically lock together (static torque). This, on the other hand, occurs at a low differential speed, resulting in minimum wear (KRemington, 2021).

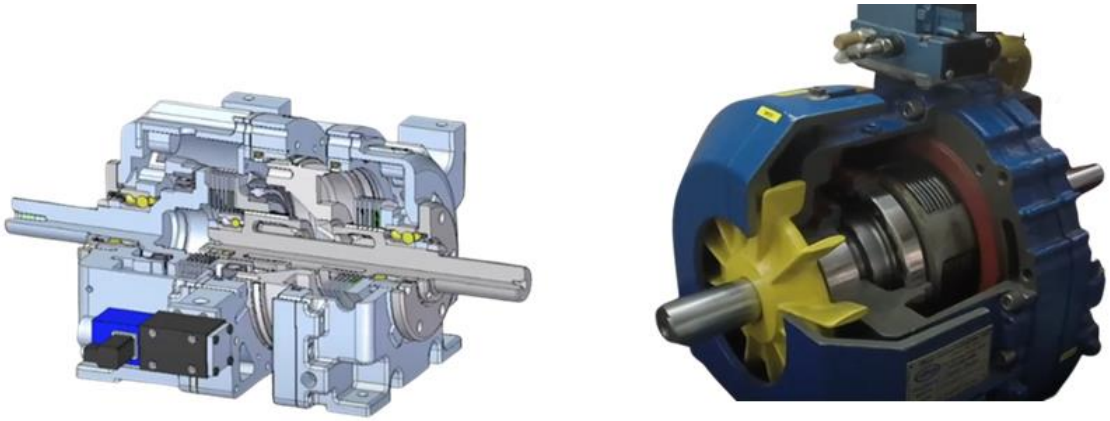

Figure 12: a) 3D model of the oil shear brake represented with a sectioned view. Source: (Globalspec.com, 2022). b) Real model of an oil shear brake with an extracted section of the external enclosure (in blue). Source: (ForceBwU, 2022)

3.6 Coupling and mounting of engine test benches

In this section the coupling of the engine and dynamometer is going to be introduced, focusing on all aspects that have to be considered for achieving a satisfactory design. At the same time, regarding the mounting, design techniques for this aspect are going to be introduced in a way that its design can be carried out. However, before introducing this literature it is important to focus on the study of vibrations that appear during the testing of engines. This is an aspect that requires the dedication of entire departments for its complexity and importance for extending the lifetime of all the setup. Thus, before

diving into design aspects, the most important details regarding vibrations in engine testing are going to be introduced, types of vibrations, their origin, physical aspects and the potential effects on the whole mounting.

3.6.1 Vibration study

Vibrations have a big impact on the operation of the coupling of the engine and also on its mounting, starting with the mounting, for isolating the engine and other important parts from being damaged and for the coupling, for controlling the appearance of torsional vibration to ensure critical frequencies lie outside the normal operating of the engine. In almost every engine test cell, the engine is the sole significant source of vibration and noise. Secondary sources, such as the ventilation system, pumps, circulation systems, and dynamometer, are frequently overwhelmed by the impacts of the primary sources. To deal with these impacts, there are several facets to this issue, firstly, the engine, as well as any connections to it, must be positioned in such a way that neither it nor the connections to it are damaged. Thus, these vibrations caused by the engine should be transmitted to other structures (Martyr & Plint, 2007).

Firstly, focusing on the reason why vibrations are formed inside the engine, the reason is hidden behind the mechanism that transforms the heat energy released during the combustion process into mechanical energy, the connecting rod together to the crank. This system is formed by the piston and the crankshaft too, what difficulties the operating due to the different trajectories that are described by the different members, i.e. while the piston describes a linear movement, the crankshaft has a circular movement that varies with the rotative speed, regarding the connecting rod, it has a combined movement, as it accompanies the piston, it has some linear displacement but at the same time, as it also works together with the crankshaft, it also describes some rotatory trajectory. This combination of different trajectories between elements and the appearance of accelerations and decelerations of the piston while covering the distance between the top dead centre and the bottom dead centre becomes a source of vibrations (Raúl & Maderna, n.d.).

To analyse this kind of vibrations, the natural frequency f_n and the interfering frequency f_{int} are determinant. Starting with the natural frequency, it is known as the rate at which an object vibrates when it is disturbed (and, 2022). For calculating it (it will be used in Section 5 for calculations related to the mountings), the following expression can be used:

$$f_n = \frac{1}{2 \cdot \pi} \cdot \sqrt{\frac{k_d}{W}} \qquad [3.1]$$

In this case k_d refers to the dynamic stiffness constant (dynamic stiffness is considered as the existing load is oscillatory) of the element and W the weight supported.

As for the interfering frequency, it is described as any kind of undesired vibrations for the system (Steffka & Trzcinski, 2007), relating that in the context of the project, the source of vibrations with higher amplitude is going to be the engines rotating at idle speed N_{idle}. In this way, f_{int} will be calculated as:

$$f_{int} = \frac{N_{idle}}{60} \quad [3.2]$$

3.6.1.1 Vibrations originated in the engine that is transmitted to the basement

To study the origin of this, the study has to focus on the connecting rod crank mechanism (see Figure 13) that was mentioned before, in this case, the variability in speed and acceleration originates from periodic forces, the main force considered can be expressed as an approximation in the form:

$$F = m_p \omega_c^2 r cos\theta + \frac{m_p \omega_c^2 r cos2\theta}{n} \quad [3.3]$$

This equation shows the most important terms to consider in the force F that represents the generation of dangerous vibrations. On it, m_p represents the sum of the mass of the piston plus, by convention, one-third of the mass of the connecting rod, ω_c represents the rotational speed of the crankshaft, r represents the length of the connecting rod, θ represents the angle that the crankshaft has rotated with respect to the vertical and finally, n represents the length of the rod l divided by r.

In this equation, the only periodic forces that appear once or twice for each rotation of the crankshaft are being considered. Starting with the first member of the equation, it represents first-order inertia force which is equivalent to centrifugal force (Raúl & Maderna, n.d.). A first-order force is the one that is repeated once every time the crankshaft turns once (Martyr & Plint, 2007).

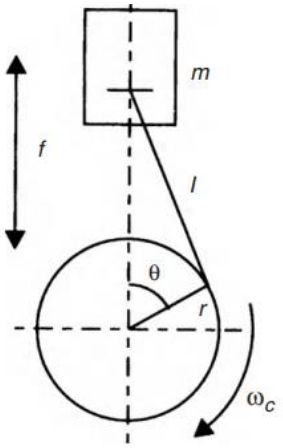

Figure 13: Connecting rod crank mechanism simplification in one plane. Source: (Raúl & Maderna, n.d.)

Following, the second term of the equation represents the component of a force that is rotating at twice the engine speed generated at the crankpin radius, thus, this force is

appearing twice each time the crankshaft completes a rotation, which means that it is a second-order force, other forces of higher order are not considered due to the small effect in comparison to the introduced ones (Raúl & Maderna, n.d.).

It is important to remark that the number of unbalanced forces that appear on the mechanism is mentioned but to have a more accurate study, each of the members should be isolated in this analysis to consider all the effects more precisely. Also, in this case, these forces have been presented for a single-cylinder engine, however, this number and also the geometry of the engine cylinders influence the balancing of these forces, for instance, for larger engines, the first order forces are balanced, for two and four-cylinder engines, the second-order forces are unbalanced and they get increased. Now, having presented all the forces, the origin of vibration can be better understood due to the existing unbalanced forces (Martyr & Plint, 2007).

3.6.1.2 Torsional oscillation originated in the crankshaft

The rapid impulses from combustion gases and the inertia of the crank revolving geometry are the main sources of these torsional vibrations. The crankshaft twists and then rebounds like an elastic band after each combustion event, during one crankshaft rotation, a succession of these powerful twisting actions happen several times, torsional vibration is the term for this twisting action (ATA, 2018). Such vibrations are created by the pulsing torque imparted to the crankshaft by each cylinder firing, something that affects all engines. With each stroke, the crankshaft twists slightly back and forth, due to their high compression ratios, diesel engines are particularly prone to vibration. The engine's pulsing output may be computed as a frequency that varies with rpm. The frequency increases as the rpm rise. As the engine's firing frequency approaches the inherent frequency of the driven equipment, problems begin to emerge. The driven equipment's inherent frequency is typically significantly higher than the engine's, thus this is not an issue. With quicker rotating engines, though, it becomes a worry (MER Equipment, 2014).

3.6.2 Engine mounting and test-bed attenuation systems

Before introducing the design basics, the study will focus on what is defined exactly as an engine mount, this part of the engine test setup refers to vibration dampeners, which have the function of absorbing the energy and vibrations of the system and converting it into heat (Rpmrubberparts, 2015). Thus, this system provides the needed isolation for minimizing the transmitted forces from the engine to the bed, avoiding the engine bounce and creating a rubber break between the engine and the chassis or in the case of engine testing, the frame. For doing so the dynamic stiffness and damping of the mounting have to be frequency and amplitude-dependent (Alkhatib, 2013).

The fundamental challenge in engine mounting design is to keep the engine's movements and forces transferred to the environment to tolerable levels as a result of the inevitable forces and couplings briefly discussed above. When it comes to car

engines, it is common practice to employ the same flexible mounts and positioning points as in the vehicle; nevertheless, this does not always result in a good solution. The mountings are carried on a very light structure in the vehicle, but they may be coupled to a fairly hefty pallet or even a seismic block in the test cell (Martyr & Plint, 2007). The engine may also be installed with extra equipment and numerous service connections in the test cell, all of these elements change the dynamics of the system as compared to the state of the engine in operation, and can lead to fatigue failures of the engine support brackets as well as auxiliary devices like the alternator. In most circumstances, stationary engines will be mounted in a single plane on four or more flexible mountings at or near the horizontal centreline of the crankshaft.

Focusing on the basic design factors for the isolation and control of vibrations, Wegetit (2022) suggest the following checklist criteria:

- Specification of force isolation.
- Natural frequency range to achieve the level of isolation required.
- Total applied load and operating conditions.
    - Engine type.
    - Maximum output torque.
    - Idle and operating speeds
- Load distribution of the machine.
    - Mount locations.
    - Equitable sharing on each mounting.
    - Position of the centre of gravity to achieve desired stability.
- Vibration amplitudes.
    - Start and stop conditions (out of steady-state).
    - Normal operation.
    - Need of sub-basement.

Having presented that list, the most important thing is to avoid “coupled” vibrations, for instance, pitching generated forces due to the existing unbalance in the vertical direction or rolling moments generated by torque reaction forces are possible origins of this issue, which can lead to resonance effects (much higher frequencies than the existing ones).

Following, different solutions for attenuating vibrations on engine test beds are going to be presented, however, before doing so, as this is a widely studied field, it is important to highlight that countless forms have been used for dealing with vibrations which means that they can be classified in different ways, even though they are most commonly defined as elastomeric mounts, passive hydraulic engine mounts and finally, active engine mounts.

3.6.2.1 Elastomeric engine mounts

Rubber is used to make elastomeric mounts. Elastomeric mounts are built for the required elastic stiffness rate characteristics in all directions for adequate vibration isolation. They are low-maintenance, cost-effective, and small. A Voigt model, which comprises spring and viscous damping as shown in Figure 14, may be used to simulate the elastomeric mounts.

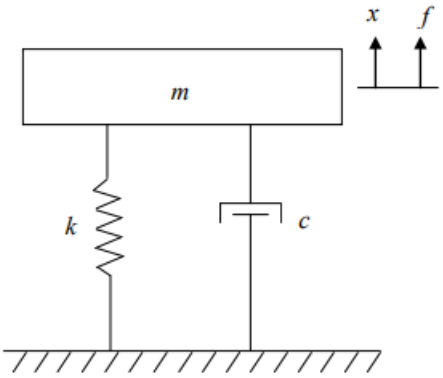

Figure 14: Mechanic Voigt model for simulating an elastomeric mount. A spring and a damper are the devices that simulate the damping system. *k* indicates the stiffness of the spring, *c* defines the damping coefficient and *m* the mass of the system. Source (Alkhatib, 2013)

Designing a mounting system that meets a wide range of design criteria is tough. At low frequencies, amounts with high rigidity or damping rates can produce low vibration transmission, but its performance at high frequencies may be poor (GMT Rubber, 2021). Low rigidity and damping, on the other hand, will result in low noise levels but excessive vibration transmission. To achieve a balance between engine isolation and engine bounce, a compromise is required. The mount rigidity must be as low as feasible to produce minimal vibration transmissibility. However, higher static deflection results as a result of this. For decreased transmissibility across a wider frequency band, lower damping is also desired. The maximum stiffness, on the other hand, improves handling and manoeuvrability. Elastomeric mounts offer a compromise between the opposing demands of reduced static deflection and improved vibration isolation (Alkhatib, 2013). Having said that, different examples can be used in the function of the requirements that are needed, firstly, centre bonded mounts are a good option that works to isolate shock (see Figure 15). They have a simple design that makes installation simple and uncomplicated. They can be used in a variety of applications that need isolation in a single direction.

Figure 15: Elastomeric centre bonded mount. The figure shows how this mounting would work with the connection of one bolt to the vibrational body and offers the possibility of attaching this to another structure with four more bolts. Source: (GMT Rubber, 2021)

Also, heavy shock loads may be supported by centre bonded mounts, which provide comfort for the operator and reduces wear and tear on the machinery. Another solution (see Figure 16) that could be considered for this application is two-piece mounts, its key distinction from centre bonded mounts is that they can tolerate vibration inputs from both directions (think rebound loading), making them excellent for tough or off-highway applications.

Figure 16: Elastomeric two-piece mount isolators. Source (Rubberpartscatalog, 2022)

Its basic form may be manufactured from several energy-absorbing elastomers, giving it a lot of functionality and application versatility. The noise and vibration of dynamic forces are absorbed by a two-piece motor mount from both sides. The mount is intended to focus pressures on both sides of it rather than all around it.

3.6.2.2 Passive hydraulic engine mounts

These mounts may be set to have a lot of damping at the shock excitation frequency, which helps to decrease vibration. These mounts often have higher dynamic rigidity than elastomeric mounts. The isolation in these mounts is decreased at higher frequencies, even though the damping is good at low frequencies. How it can be seen in Figure 17, the solution is to add a decoupler to the hydraulic mount that acts as an amplitude-

restricted floating piston. It enables the mount to function like an elastomeric mount, resulting in excellent vibration isolation at high displacements (Alkhatib, 2013).

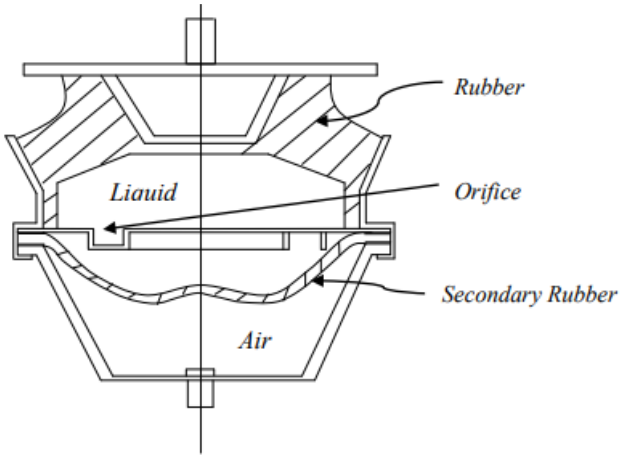

Figure 17: Passive hydraulic engine mounting scheme. It can be seen how the rubber isolator is complemented by a liquid chamber and an air gap to conform to a complete isolation system. Source: (Alkhatib, 2013)

As an example of the passive hydraulic system, centre bonded mounts are highlighted because of the benefits that provide, offering a much more specific damping profile for application as the fluid chamber can be tuned to the application.

3.6.2.3 Active engine mounts

In this case, one or more actuators provide a counteracting dynamic force to inhibit the propagation of the system disturbance force in active vibration control. A general active mount consists of an elastomeric or hydraulic passive mount, as well as a force mount. Passive mounts have constraints that active mounts can overcome. At low frequencies, active elastomeric mounts can be highly rigid, while at high frequencies, they can be very soft. Meanwhile, the active hydraulic mounts may be set to provide enough damping at engine bounce frequency while maintaining very low dynamic stiffness at high frequencies. Active engine mounts enable high engine vibration levels by offering improved isolation. This may decrease the need for a balancing shaft and allow the frame to be lighter (Rpmrubberparts, 2015). Anyway, this solution is more implemented for vehicles or machinery that is not static, for this reason, the study is not going to give specific details as this solution will not be applied in this work.

3.6.3 Driveshaft and safety guard design

To measure the power output of the test engine, the dynamometer must be coupled to the engine using a driveshaft. There are various ways of accomplishing this task, depending on the characteristics of the engine-dynamometer setup being used. However, the selection of suitable couplings and shafts for the connection of the engine to the dynamometer is by no means a simple task. Incorrect choice or faulty system design may give rise to several problems (Martyr & Plint, 2007).

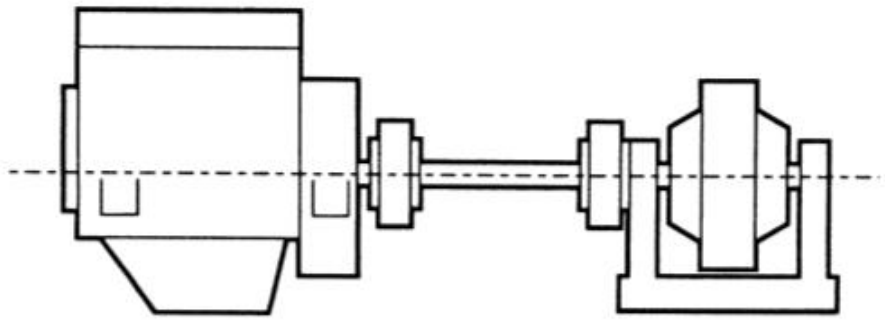

Figure 18: Simple form of a dynamometer-engine line. Source:(Martyr & Plint, 2007)

In general, dynamometer shafts are not designed to withstand heavy bending moments, which can be caused by the use of heavy couplings or by misalignment between the dynamometer and the engine. For this reason, flexible couplings should be used in the lightest possible construction and perfect dynamic balance (Atkins, 2009).

One of the most common problems associated with driveshaft design is the appearance of torsional oscillations during the engine testing procedure as introduced in Section 3.6.1. These oscillations are excited by the variation in engine torque, which in turn is a product of the variation in the pressure of the engine's cylinder between different cycles.

In its simplest form, the engine–dynamometer system may be regarded as equivalent to two rotating masses connected by a flexible shaft. Such a system has an inherent tendency to develop torsional oscillations. The two masses can vibrate 180 degrees out of phase about a node located at some point along the shaft between them (Morris, 1964). The resonant or critical frequency of torsional oscillation of this system is given by:

$$n_c = \frac{60}{2\pi} \cdot \sqrt{\frac{C_c \cdot (I_e + I_b)}{I_e \cdot I_b}} \qquad [3.4]$$

If this system is excited by a constant torque (T_{ex}) at a constant frequency (n), then the relation between the amplitude of the oscillation (θ) and the frequency ratio is represented in Figure 19.

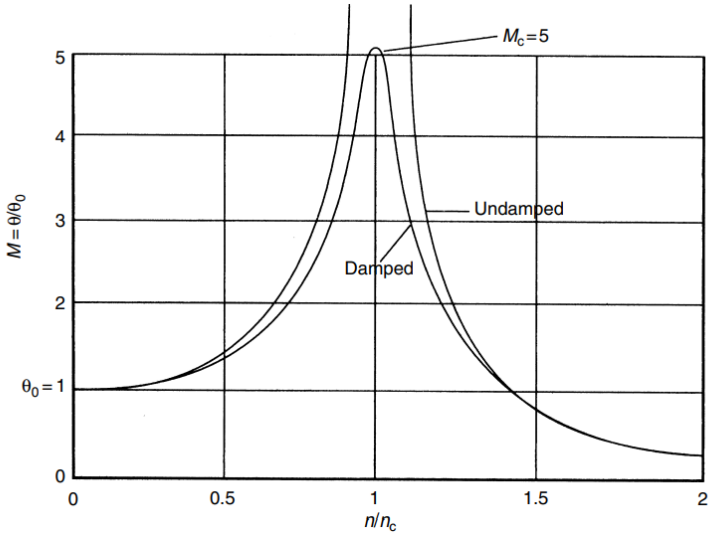

Figure 19: Relationship between frequency ratio, amplitude and the other dynamic amplifier M_c. Source: (Martyr & Plint, 2007)

From the figure above, it can be seen that at low frequencies, the combined amplitude of the two masses is equal to the static deflection of the shaft under the influence of the exciting torque, being $\theta_o = \frac{T_{ex}}{C_s}$ and C_s the stiffness of the shaft. As the exciting frequency increases, the oscillation amplitude increases and at $n = n_c$ it becomes theoretically infinite, meaning that the shaft would fracture (Martyr & Plint, 2007). Beyond this point, the amplitude of oscillations decreases with increasing frequency.

Figure 19 also shows the behaviour of a damped system, showing that the value of the dynamic amplifier (θ / θ_o) increases when increasing the frequency to reach, in this case, a maximum of 5, being that frequency the critical frequency, as opposed to becoming theoretically infinite as for the undamped case. After that, same as for the undamped system, at higher frequencies, the amplitude of the torsional oscillations decreases with an increase in frequency.

It is well known that any periodic curve of this kind may be created from a series of harmonic components, each a pure sine wave of a different amplitude having a frequency corresponding to a multiple or submultiple of the engine speed. In the case of a four-cylinder four-stroke engine, there are two firing strokes per revolution of the crankshaft and the rotating moment curve is repeated at intervals of 180º (Martyr & Plint, 2007). The major critical speed for a multi-cylinder, in-line engine is of order:

$$N_0 = \frac{N_{CYL}}{2} \qquad [3.5]$$

Thus, in the case of a four-cylinder, four-stroke engine the major critical speeds are of order 2, 4,6, etc.

The first harmonic is generally of most significance in the excitation of torsional oscillations, and generally, it is sufficient to calculate the critical frequency from equation [3.4] and then calculate the corresponding engine speed from:

$$N_c = \frac{n_c}{N_0} \quad [3.6]$$

As consequence, the driveshaft needs to be designed such that it has an appropriate stiffness to ensure that the critical frequency of the shaft is outside the normal operating range of the engine being tested. Also, the shaft must have an adequate amount of damping to allow the engine to be run through the critical speed without resulting in unwanted torsional oscillations that may lead to the failure of the shaft (Martyr & Rogers, 2020).

Also, the shear stress that the shaft takes needs to be considered. The maximum shear stress induced in a shaft with a diameter *D*, by a torque *T* is given by:

$$\tau = 16 \cdot \frac{T}{\pi \cdot D^3} \quad [3.7]$$

The torsional stiffness of a solid shaft of diameter *D* and length *L* is:

$$C_s = \frac{\pi \cdot D^4 \cdot G}{32 \cdot L} \quad [3.8]$$

Being *G* the modulus of rigidity of the selected shaft material.

When a shaft rotates, it may well go into transverse oscillations. If the shaft is out of balance, the resulting centrifugal force will induce the shaft to vibrate. When the shaft rotates at a speed equal to the natural frequency of the transverse oscillations, the vibrations become large and show up like a whirling of the shaft (freestudy, n.d.). The coupling shaft is usually supported at each end by a universal joint or a flexible coupling, then the whirling speed of a solid shaft of length L, modulus of elasticity$E$ and mass W_s is given by:

$$N_w = 30 \cdot \frac{\pi}{L^2} \cdot \sqrt{\frac{E \cdot \pi \cdot D^4}{64 \cdot W_s}} \quad [3.9]$$

It is known that the whirling speed of a shaft is identical to its natural frequency of transverse oscillation. To allow for the effect of transverse coupling flexibility the simplest procedure is to calculate the transverse critical frequency of the shaft plus two half couplings from the equation:

$$N_t = \frac{30}{\pi} \cdot \sqrt{\frac{k}{W}} \quad [3.10]$$

Where now W is the mass of the shaft plus half couplings and k is the combined radial stiffness of the two couplings.

Then the whirling speed *N* taking this effect into account is given by:

$$\left(\frac{1}{N}\right)^2 = \left(\frac{1}{N_w}\right)^2 + \left(\frac{1}{N_t}\right)^2 \quad [3.11]$$

Special effort must be taken to ensure accurate alignment of the engine and the dynamometer, to avoid generating out of balance forces that place unnecessary stress on the engine and dynamometer shaft (Atkins, 2009). Generally, a Cardan shaft with a universal joint at each end is a favoured choice of automotive test engineers.

Figure 20: Cardan shaft. Source:(Cardanshaftsindia, 2015)

These shafts are installed with a certain misalignment to prevent the brinelling of the bearings installed at each end of the shaft (Atkins, 2009). In addition, to avoid induced torsional oscillations, the two yokes of the intermediate shaft joints should lie in the same plane (Martyr & Plint, 2007).

In the absence of a Cardan shaft, alignment between the engine and dynamometer must be carried out with a high degree of accuracy. However, it should be taken in a place where the engine mounts will tend to move and settle after the initial installation, and the alignment will need to be checked regularly over the first few days of testing. Poor attention to prop shaft selection and installation are potentially dangerous to test cell personnel due to the high speeds and high inertia forces (Atkins, 2009).

Because the kinetic energy in a spinning broken propeller shaft is considerable, it is always a good idea to install a sturdy safety containment device in case of an unforeseen catastrophic coupling failure (Atkins, 2009). Preferably, the guard should be steel not less than 6 mm thick, split and hinged in the horizontal plane for shaft access (Martyr & Plint, 2007).

In the case of the SISU engine, a large multi-cylinder engine, the wind-up of the crankshaft as a result of torsional oscillations can be very significant and the two-mass approximation is not adequate more elaborate analysis is needed. The amplitude of the various harmonic excitation forces is given by the multiplication of the p factors shown in Table 4, and the mean turning moment.

$$T_{ex} = p \cdot M_{mean} \quad [3.12]$$

Table 4: p factors. Source: (Den Hartog, 1956)

Order	½	1	1 ½	2	2 ½	3…	8
p factor	2.16	2.32	2.23	1.91	1.57	1.28	0.08

The mean turning moment developed by the cylinder can be calculated using the following equation:

$$M_{mean} = IMEP \cdot \frac{B^2 \cdot S}{16} \cdot 10^{-4} \quad [3.13]$$

Being *B* and *S,* the bore and the stroke are given by the engine manufacturers.

The amplitude of the vibratory torque T_v induced in the connecting shaft by the sum of the exciting torques for all the cylinders is given by:

$$T_v = \frac{\sum T_{ex} \cdot M_c}{1 + \frac{I_e}{I_b}} \quad [3.14]$$

Where M_c is the dynamic magnifier, dependent on the coupling material.

The complete analysis of the torsional behaviour of a multi-cylinder engine is a substantial task, as computer programmes are available which reduce the effort required. However, in this part, the calculations will be done in Section 0.

3.6.4 Flexible couplings

The choice of the appropriate coupling for a given application is not easy: the majority of driveline problems probably have their origin in an incorrect choice of components for the driveline and are often cured by changes in this region (Martyr & Plint, 2007).

As discussed before, the driveline is highly susceptible to torsional vibrations, and internal combustion engines are prone to excite such oscillations. The magnitude of these disturbances is a function of the damping capacities of various elements, mainly the shaft, the couplings, the dynamometer, and the engine itself. From the previous list, the couplings are the only element from the system in which the damping capacity may be changed, and in many cases, the damping capacity of the other parts of the system may be neglected.

According to (Atkins, 2009), the suitability of the coupling should include the following considerations:

- The ability to handle the peak instantaneous cyclical torque due to the engine under consideration.
- The effect of the torsional stiffness of the coupling proposed, usually as a result of natural torsional frequencies of the installation in which the coupling is fitted.
- The effect of the first two considerations on the amount of heat generated in the coupling. This is highly important when rubber in shear or direct tension or compression type couplings are chosen.

- The effect of the coupling so far selected on the whirling characteristics of the whole coupling shaft.
- Possible detrimental effects due to the inability of the coupling to deal with reasonable runout. The effect of the coupling so far selected on the whirling characteristics of the whole coupling misalignment or, in certain cases, the effect of end loading produced as a direct result of a torsional twist on the bearings and so forth of the engine and dynamometer.

4 Selection of a new dynamometer

After the review of the literature, the required background in all the involved aspects in the thesis has been acquired, leading the project to focus on achieving the objectives that were set in Section 2, which would correspond to the most practical part. Respecting the order previously determined, the first stage refers to the evaluation of the existing equipment for the test bench the selection of a new dynamometer has to be the first stage, and then, after that, its adaptation to the engine laboratory facility (engines, engine bed…) will be the next stage. Thus, as said before, the following sections (from 4.1 to 4.3) will be focused on the research of a new dynamometer.

4.1 Current options analysis

The start point will be the analysis of the current water brake, which is the current solution implemented in the laboratory and has been the motivation for doing this project. Once this will be studied (see Section 4.1.1), finding and justifying the reasons why it is not a good solution, the research of alternatives will be the matter of study. As it is known, the Novia UAS owns an eddy current dynamometer that has been used in the past for other projects and could be a good solution for the requirements that have been set. In this way, Section 4.1.2, is going to be oriented in studying the feasibility of this regarding the conditions that the engines require for having good test results. For proceeding with the study, it is required to have the values of torque and power in all the range of speeds of the SISU engine and the Opel engine, this data is accessible in Appendix I and Appendix II, respectively.

4.1.1 Study of the current water brake

As it was known, and also motivated the start of the project, the current water dynamometer, as can be seen in Figure 21, cannot offer enough torque to break the engine at low speeds.

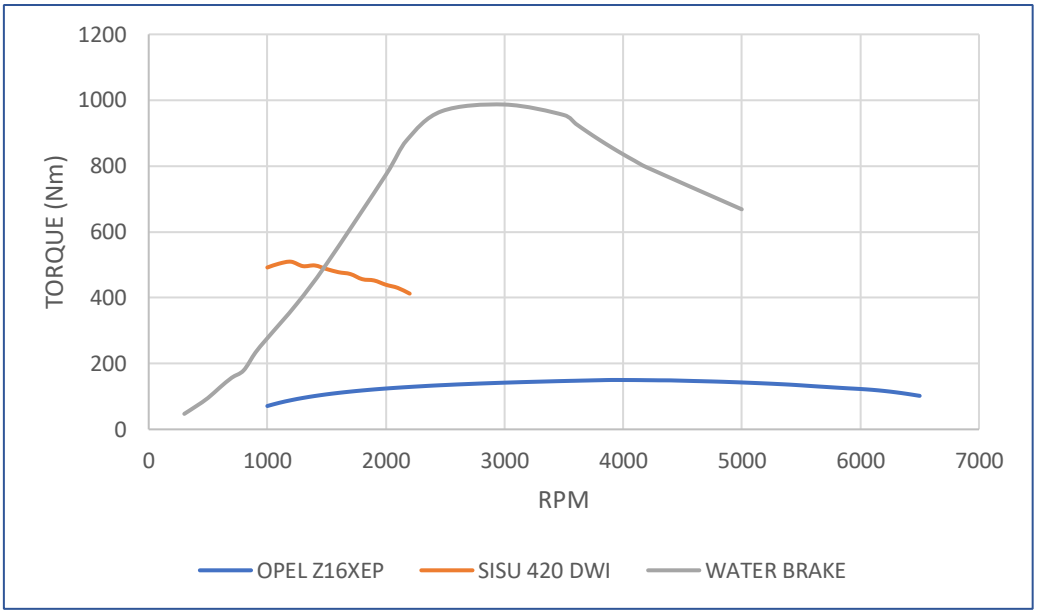

Figure 21: Torque comparison (Nm) of the tested engines and the available water brake. Numerical data of the water brake is accessible in Appendix III.

When studying if a dynamometer can brake an engine, it can be done by comparing the torque of both machines. As the dynamometer is the element that has to stop the rotation of the engine, its torque needs to be bigger. Moreover, the difference between both at all speeds has to consider a safety margin to avoid the dynamometer reducing its lifetime. Having said that, an engine will suit with a certain dynamometer in case its torque curve remains under the curve of the dynamometer all the time, which means that at a certain speed, the dynamometer will always offer a bigger torque than the mentioned engine. In this case, comparing the toque curve for the SISU 420 DWRIE engine and the water brake, it can be seen how at speeds under 1500rpm, the torque produced by the SISU engine (487.014Nm) is very close to the value that the water brake could absorb (502.93Nm), what means that at speeds lower than this value, the dynamometer will not be able to brake the engine. To get a fast picture of if the dynamometer can brake the engine or not, it is as simple as comparing if the curve of the engine torque crosses at some point the dynamometer one.

This, translated to the laboratory causes the following situation: The engine test starts, with the motor increasing its speed until the maximum achievable value, once this is reached, the dynamometer starts braking the engine, however, when the rotatory speed falls to 150rpm, the dynamometer cannot offer enough torque to keep braking the engine, what is translated to a situation where the engine would keep working, so there is no way to record data at lower speeds. Is for that that the way of testing requires reducing the speed of the engine directly from its control instead of using the dynamometer for doing so, thus this model of the dynamometer, is not a good option as it was known.

4.1.2 Study of the eddy current EC50TC dynamometer:

Knowing now how to check fast if the dynamometer can brake the engine, analysing Figure 22, it can be observed how in this case, the torque curve for the SISU 420 DWRIE stays behind the EC50TC dynamometer, which means that at every point, the brake offers a bigger torque than the engine, being this able to be stopped.

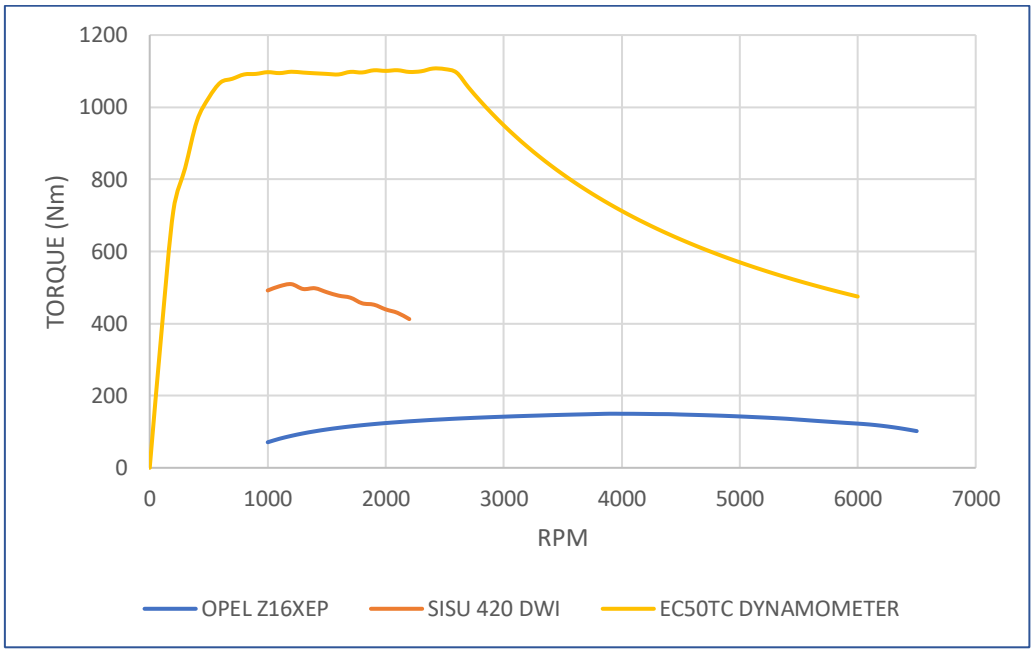

Figure 22: Torque comparison (Nm) of the tested engines and the available Eddy current dynamometer. Numerical data of the eddy current dynamometer is accessible in Appendix IV.

However, even if before the Opel Z16XEP was not considered while analysing the water dynamometer as it was not a good solution for testing the SISU engine, now, it is required to check if the Opel engine can be working with it. In terms of torque, there is no limitation this dynamometer is quite over-dimensioned for this engine regarding the load percentage requirements that will be introduced in Section 4.2. Moreover, this would offer a good characteristic as when it would be working with the SISU engine, the torque offered by the dynamometer is quite constant (see Figure 22 yellow curve in the range of speeds between 600rpm and 2500rpm approximately), a factor that would pay a big role in the stability of the whole setup and a reduction in the generation of vibrations. Having said that, the torque would not be a problem in this case (with any of the engines), however, the issue would be related to the rpm. Checking the grey curve (from Figure 22) referent to the Opel engine, it can turn up until 6700rpm, while the dynamometer can only work up to 6000rpm. This brings a new limitation that would be a negative aspect of the testing process as no data could be obtained at high speeds for the Opel engine. For this reason, the eddy current dynamometer is also limited in terms of testing and a different option should be considered.

4.2 Research and analysis of alternatives

After analysing the different available dynamometers, it has been proved that all the solutions present at some point some kind of limitation, for this reason, it has been required to look for alternatives in the market.

Before the start of the research, some previous requirements have been set to narrow down all the possibilities that could suit them. Firstly, to enlarge the life of the dynamometer as much as possible and avoid any bad functioning during the testing, it has been considered to establish a maximum workload for the brake, thus instead of requiring it to work to its maximum capacity, establishing a security factor could help on reducing the possibilities of issues appearing in the dynamometer. Thus, the brake will be set to be working at a maximum of 80% of its capacity, which means that the dynamometer would always be able to offer a 20% bigger torque than what the engine needs to be braked at that rpm. This has been the first requirement as conditions that need to be matched, the peak of torque and power will be the biggest limitations for the selection.

Also, some measurements have been taken in the laboratory to check if the dynamometer could fit in the existing infrastructure without requiring any big modifications to the disposition of the laboratory, which would save a lot of time and money in terms of rebuilding all the facility instead of taking profit of the existing one.

Moreover, as with all projects, the importance of the budget is capital, which means that before starting with any research, a maximum value for completing all the stages of the project should be considered. For this reason, the selection of it is another requirement that could narrow down even more the research and feasible solutions. As for the value it has to be something that Novia UAS could afford and could assign for a project of this magnitude, thus, after some discussion with the supervisors of the project the total amount that could be destined for this should not surpass the 30000€.

Finally, before the final options are going to be presented, it has to be highlighted that during the process of research a big number of different options were studied, considering different types of dynamometers as the ones that were presented in previous sections of the project in the literature study (see Section 3.5) however when two engines have to be tested, the feasible solutions get reduced as the requirements increase as it has been shown. Thus, it has been possible to verify how out of the different models introduced the testing of Diesel engines (SISU DWRIE 420) is normally done by eddy current dynamometers for the combination of high torque and power absorption and reduced size. As introduced below, these reasons play a big role in which are going to be the most important considered options.

Starting with the magnetic powder dynamometers, during the research between different companies that produce them, it has been found that they have a big limitation in terms of the power that provide, in general terms, the most powerful models can

offer up to 48kW, what is a big limitation as for the SISU engine, the needed power has to be at least around 140kW for having a safe margin. Moreover, the fact of working with magnetic powder increases the level of required maintenance and overheating at high speeds due to the friction produced, in this way, testing of the Opel engine could cause heat close to its maximum speeds. However, in the literature study (view Section 3.5.2), it was important to consider them and introduce their working principles for having a better background in the field and understanding why now they can be considered as a feasible alternative.

Following, hysteresis dynamometers which were also introduced previously (see Section 3.5.3) avoid the issue regarding the lack of power that appeared with magnetic powder dynamometers. For instance, according to (Atkins, 2009), the range of power where these dynamometers can work is up to 150kW, which could be a good solution for matching the requirements, anyway, in this case, the issue appears with the torque capacity when different options were researched, it has been found that this kind of dynamometers offers high-speed working ranges, which can surpass 30000rpm, however, this limits the torque to values under the 60Nm, for this research, the information provided by the companies JAD systems and Magtrol (which have an important role in the market) has helped to conclude that this option cannot be as competent as the eddy current types.

Finally, water dynamometers were also an object of study and research because of the capacity for working with Diesel engines and also because the previous solution (even if it was not efficient) was a water brake, for this reason, finding a model that could improve the tests characteristics of the current water brake, could be considered as an option. Anyway, similar issues appear again in this case, the problem is that generally, water brakes cannot offer the higher-rated torque at low speeds, a big issue regarding Diesel engines as they offer big torque values at low speeds (see Appendix V), in this way, the solution for using a water brake would require to consider a very over-dimensioned dynamometer which could offer the required torque at low speeds but then at higher speed, it would be working at values of 20 to 30% of its capacity. Furthermore, water brakes usually work at lower speeds, which could also present problems for working with the Opel engine. Is for that that this option was turned down as not many options found in the market were efficient enough.

To conclude before heading to the considered alternatives, during the analysis it has been demonstrated how the eddy current dynamometers are the most suitable ones for the required testing conditions, which generally avoid all the issues present in the other remarked models. Thus, two eddy current dynamometers were selected for testing, the initial selection of both was based on company-supplied performance criteria, price, and availability. These alternatives will be introduced, analysed (see Sections 4.2.1 and 4.2.2), and finally discussed in the form of a matrix of decisions (see Section 4.3) below.

4.2.1 DW250 Jiangsu Lanmec

This is the first option that has been considered in the research, the major motivation is the price that this company offers to customers, which can be considered one of the most competitive ones. Also, the fact that its specifications are quite close to the demanded requirements, makes it a very attractive solution (see Figure 23).

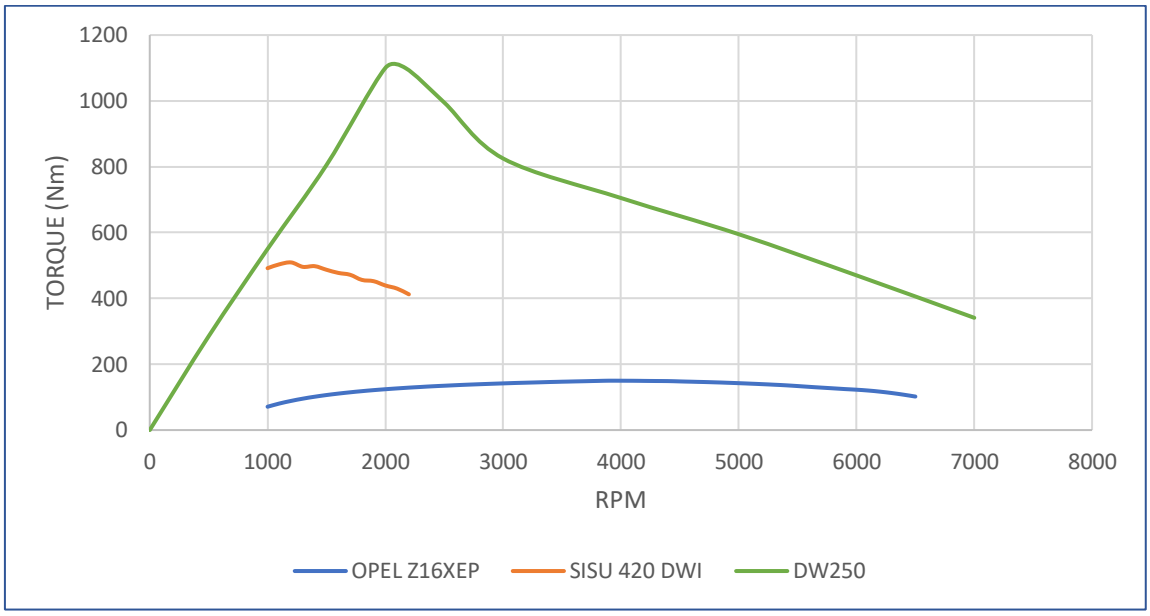

Figure 23: Torque comparison (Nm) of the tested engines and the alternative dynamometer DW250 manufactured by Jiangsu Lanmec. Numerical data of the dynamometer is accessible in Appendix VI.

Firstly, regarding torque, it can be observed how the most limiting engine that has to be tested, the SISU 420 DWRIE, stays all the time under the dynamometer curve, which means that during the whole study, it could be braked providing valuable data at all speeds. However, some aspects have to be highlighted. In the first case, analysing the couple at low speeds, specifically at the lowest, when the SISU would be rotating at idle speed (1000rpm), the margin between the torque of both elements is quite small while the SISU engine would be producing a total of 491.79Nm, the maximum torque that the DW250 dynamometer could absorb would be 550Nm, what means that the brake would be working at an 89.3% of its maximum capacity at this point. It has to be mentioned that this exceeds the pre-established limit of the 80%. Anyway, this situation is not a big setback as it takes place at idle speed when not much information or data is being compilated.

At the same time, with a quick look at Figure 23, it is possible to detect that after low speeds, the torque that is offered by the DW250 exceeds the torque required by the SISU engine by a very big margin. For instance, at 2000rpm, the torque offered by the engine is 439.27Nm, the point at which the dynamometer could offer up to 1100Nm, a value that would let the brake work under 50% of its maximum capacity.

Regarding power, observing Figure 24, the required power to brake the SISU engine (also the most restrictive in this case) would be available on the DW250.

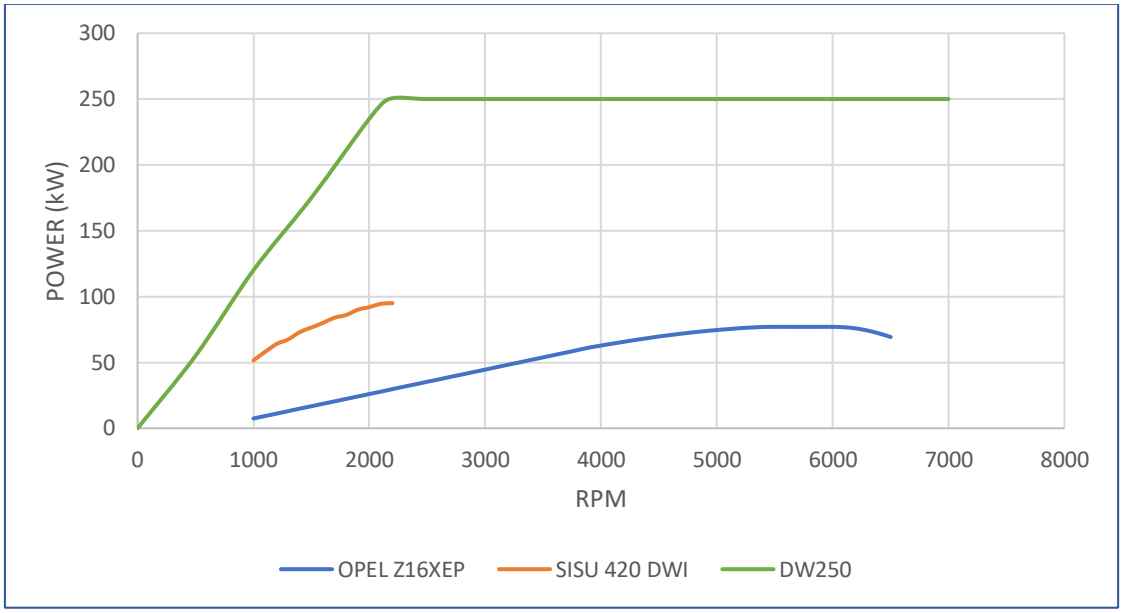

Figure 24: Power comparison (kW) of the tested engines and the alternative dynamometer DW250 manufactured by Jiangsu Lanmec. Numerical data is accessible in Appendix VI.

The worst conditions, as it happened when studying the torque curves take place at idle speed, however, in this case, the margin is bigger as the engine produces a total power of 51.5kW, while the dynamometer could brake up to 120kW. Likewise, there is quite over-dimensioning in terms of power as the engine never gets over 95kW and the brake could absorb a total of 250kW, which secures the dynamometer to be working at 38% of its total capacity when the engine is offering the maximum power.

Finally, in terms of dimensions, regarding the sketch provided by the manufacturer and the available space in the laboratory, the DW250, shown in Figure 25 could be a good option to consider.

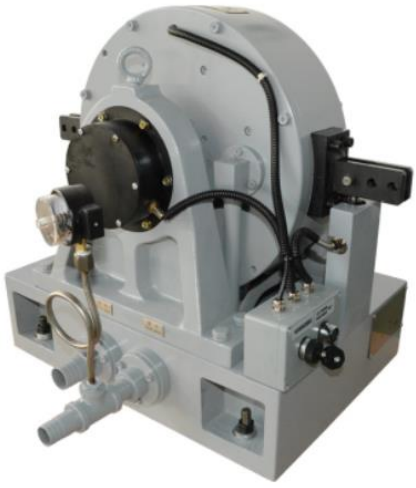

Figure 25: Lanmec DW250 real model. Source: (Lanmec, 2022)

Especially, its lower price in comparison to other alternatives, see Appendix VI. (The price is about 17500€ considering the dynamometer and all the required elements for using it).

4.2.2 DE200 Taylordyno

For this dynamometer, the study is going to be made in the same way. Starting with the torque, it can be analysed how when the engine produces the maximum value (see Figure 26), it comes parallel to the maximum torque that the dynamometer can provide (a similar situation that appeared when studying the ECTC50 dynamometer), what is a very positive aspect because the brake could be working close to constant torque when braking the engine, reducing in a big way the vibrations that would appear in this operation.

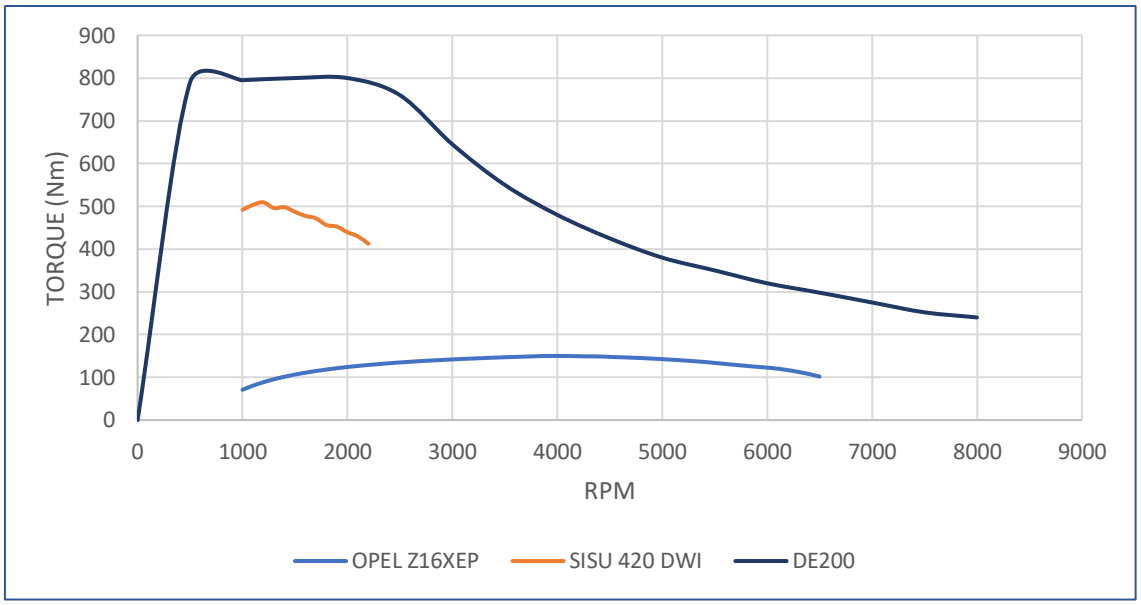

Figure 26: Torque comparison (Nm) of the tested engines and the alternative dynamometer DE200 manufactured by Taylordyno. Numerical data of the dynamometer is accessible in Appendix VII.

The most adverse conditions would appear at 1200rpm, where the engine produces a maximum torque of 509.3Nm, anyway, at this point the brake could absorb until 800Nm, leaving it to a 63.7% of its total capacity, which in comparison to the DW250, avoids working at some point close to the maximum demand and also, studying the rest of the curve, it can be seen how it is not over-dimensioned as this is also the maximum margin between the torque of both elements, what means that in this aspect, the DE200 dynamometer offers much better working conditions in terms of torque. On the other hand, even if it is not mentioned, the Opel engine would always be matching the working conditions.

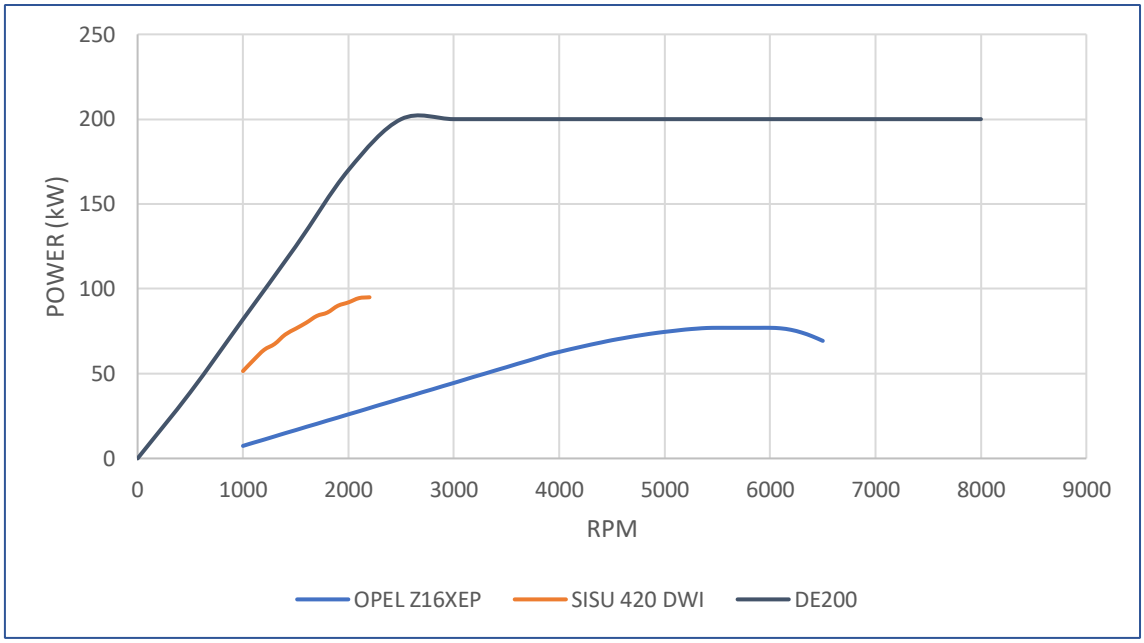

Figure 27: Power comparison (kW) of the tested engines and the alternative dynamometer DE200 manufactured by Taylordyno. Numerical data of the dynamometer is accessible in Appendix VII.

In terms of power, the situation, in this case, is very similar to the DW250, but in this case, as can be observed above (see Figure 27), the maximum power that can be absorbed reaches 200kW, being better adapted to the requirements of the engines and avoiding the previous over dimensioning. However, when leaving aside the technical aspects, the DE200 (see Figure 28) becomes an option that requires much more budget.

Figure 28: Taylordyno DE200 real model. Source: (Taylordyno, 2022)

In this case, just considering the dynamometer, the price would be around 68000€, which goes over the budget maximum by double.

4.3 Matrix of decision

Once the options have been presented and analysed, it is possible to make some conclusions about which of the alternatives suits the best overall. For the final decision making, some crucial parameters are going to be assessed for each of the alternatives, thus, after that, the dynamometer that gives a better general result is going to be taken. The defined parameters to assess are:

- Adaptation to the budget
- Adaptation to technical requirements
    - Normal working conditions
    - Workload
    - Over-dimensioning
- Adaptation to existing infrastructure
- Company customer service

Table 5: Matrix of decision grading the most important factors considered for the dynamometer selection. Grades go from 0 to 5, which refers to poor and perfect, respectively.

Parameters	Purchase cost	Normal working conditions	Workload	Over-dimensioning	Infrastructure adaptation	Company customer service
DW250	5	5	3	3	4	4
DE200	0	5	5	5	4	5

Finally, comparing the given results for each field to both options, even if in terms of technical aspects, the DE200 is the best option the fact of having a reduced budget and the price difference is the aspect that makes the difference for the decision making. After assessing every single aspect, the final result for the DW250 is 24 out of 30 while the DE200 receives a total of 24 too, however, what has just been mentioned about the budget makes the balance fall in favour of the cheapest option, the DW250.

5 Mounting selection

The next step of the remodelling process is selecting the right mountings for the setup. It is important to remark that this part is not based on designing new mountings from scratch that would be optimal for our facility. In this case, the idea is similar to the process that was done for selecting the new dynamometer, starting with the analysis of the current material and in case it is needed, finding better alternatives.

The current bench test owes a total of four mountings that isolate the vibrations that come out from the SISU 420 DWRIE engine. The same with the Opel Z16XEP engine, which has its corresponding mountings too. In this way, knowing in advance that the mountings for the Open engine will not suit the SISU engine (because of the difference in weights, see Section 5.1) it will be verified if it could suit the existing ones. For this reason, the study has to check which are the current operating conditions.

For these verifications, two paths can be followed in this section, on the one hand, a more numerical way for finding a solution with the back of vibration theory, and on the other hand, a more practical solution that is based on working with graphic information provided by different manufacturers. For this section, it is thought that working with diagrams provided by the different suppliers in the market can be the most efficient way to get a solution, even if some calculations are required for doing so too.

5.1 Verification of the current mountings

As said in Section 5, even if the current setup seems to be working properly with the current mountings, it is known that at low speeds, the current engines present certain vibration levels that could be reduced (referring to the SISU engine). Also, the idea of testing more than one engine requires the mountings to verify new requirements. It is important to remark that the Opel engine has also four mountings that could be kept in case they were a good solution.

For starting the process, it is required to find trusted catalogues that can help to get an optimal solution, different companies have a good reputation in the market. The first will be the one that provided the current mountings (for both engines), Trelleborg AB. Then, companies such as Vulkan Group will also be used to complement the study.

The current mounting models are:

SISU 420 DWRIE: RA100/M16 40 deg IRH
OPEL Z16XEP: RA125 EMA

The first required information is the load that the mountings will have to hold, in this case, the engine weights (see Appendix I) and other elements like wiring, filters, flywheel and in the case of the Opel engine, a structure where it is contained, which is introduced in detail in section 7 (see Figure 42)

Starting with the SISU 420 DWRIE, the listed weight, W_{engine} is 345kg. However, it is specified that in this case, the flywheel, its casing and the wiring have not been considered in this value. This information can be found with the NX software defining the material of the part in question. Thus, with the 3D models of these parts, this information can be accessed, resulting in:

$$W_{housing} = 21.60kg$$
$$W_{flywheel} = 18.50kg$$

Thus, considering a total of 10kg for the wiring (leaving a certain margin), the total weight, W_{total} to consider will be:

$$W_{t_{SISU}} = W_{engine} + W_{flywheel} + W_{housing} + W_{wiring} = 345 + 18.496 + 21.6 + 10 = 395{,}096Kg$$

To leave a security margin for the previous value, the weight that will be considered $W_{t_{SISU}} = 400Kg$. Following, as introduced before, the idea is to keep the facility the most similar as possible so, the total number of mountings that will be used is 4, for this reason, considering that every mount will hold a quarter part of the previous value, $W_{m_{SISU}} = 100Kg$.

Secondly, the Opel weight is needed, in this case, it has not been able to access the information accurately as it was done with the SISU, however, after some research, for similar engines in the market, precisely, a Vauxhall engine with the same number of valves and similar volume, it has been found a total weight of 108kg (Gomog, 2022). Considering other elements, especially the structure that contains the engine which is planned to be kept, the heat exchanger, etcetera. It has been considered that a total weight, $W_{t_{OPEL}}$ of 200kg is a good approximation with also some room for manoeuvre.

In this way, for the Opel engine, the mountings would hold $W_{m_{OPEL}}$:

$$W_{m_{OPEL}} = \frac{200}{4} = 50kg$$

The next step of the process refers to the calculation of the required parameters to check which are the vibration levels with the back of the graphs provided by the manufacturers (see Following, the geometrical data about the DE200 dynamometer and other specifications is presented.). The way to work with these graphs is very similar to how it was introduced before in Section 3.6.2, remarking that the calculation of the loads and their distribution has already been introduced, and also, in this case, it is explained how to work with the diagrams provided by the manufacturer in points 3, 4 and 5. Thus, as (Trelelborg, 2022) indicates:

1. Determine the load per mounting (kg). Just determined above.
2. Determine the interfering frequency (Hz).
3. Start with diagram 1 (see Figure 29, the diagram on top-left), enter it with the value of the load and intersect horizontally the desired mounting model (inclined lines).

4. Connect the intersection point vertically down to the interference line with the Interfering frequency value in diagram 3 (see Figure 29, the diagram on the bottom). Step 4 allows verifying if the resonance zone is avoided.
5. Finally, the static deflection can be determined by extending the horizontal line made in the diagram until intersecting the model in diagram 2 (see Figure 29, the diagram on the top-right) and the degree of isolation, which determines how good are the vibrations originated on the engines isolated can be determined by extending horizontally the Interfering frequency value from the diagram 2.

Following step 2, the interfering frequency, f_{int} can be calculated using the idle speed (accessible in Appendix I and Appendix II), N_{idle} of the engine:

$$f_{int} = \frac{N_{idle}}{60}$$

$$f_{int_{SISU}} = \frac{1000}{60} = 16.67Hz$$

$$f_{int_{OPEL}} = \frac{770}{60} = 12.83Hz$$

(Idle speed for Opel engine is given in a range from 770 to 930rpm, for the calculations, it is going to be considered the less favourable in terms of interfering frequency).

With this calculated, it is possible to determine in what zone will the mountings be working (see Figure 29).

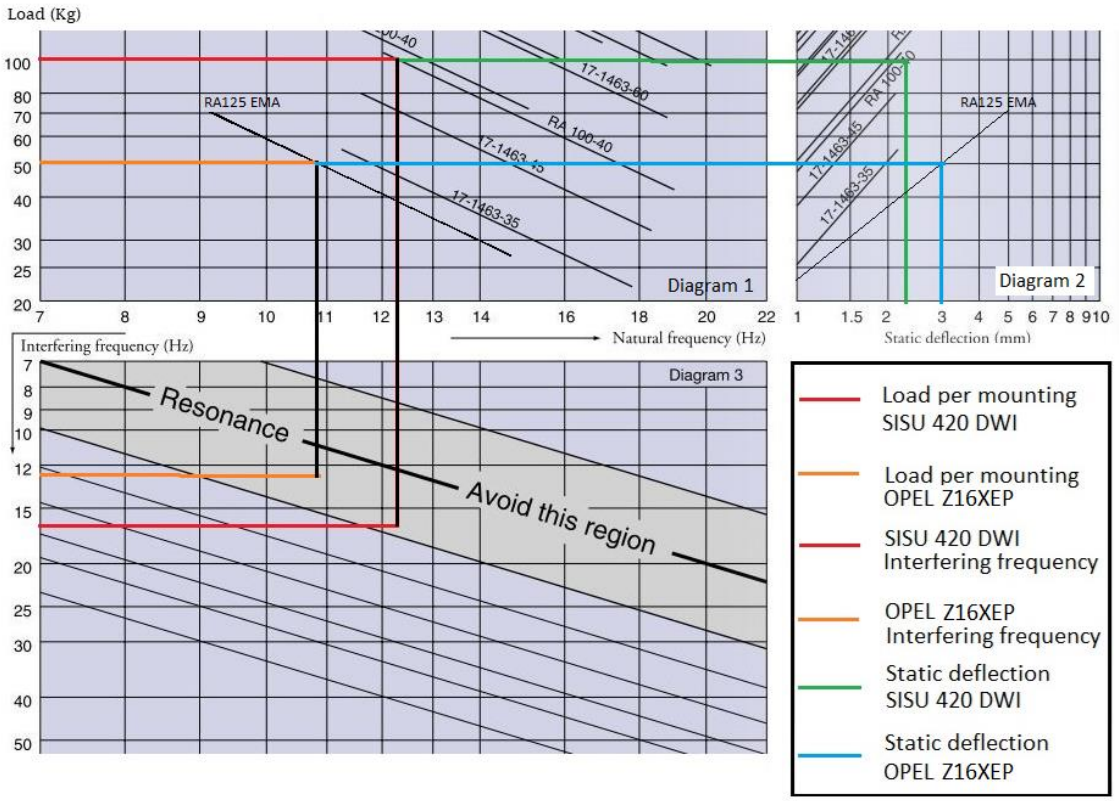

Figure 29: Trelleborg catalogue diagrams for determining the vibrational status of the mountings. Diagram 1 (on top left), diagram 2(on the bottom) and diagram 3 (on top right). Source: Adapted from (Trelleborg, 2022)

In this case, both of the engines fall into the resonance zone, especially the Opel engine, which at idle speed is very close to the resonance line. In the case of the SISU engine, it has a similar situation, also falling in the resonance zone but not as close as the Opel. Even if this could be seen as a bad solution, it has to be said that when the engines would be tested at speeds higher than the idle, the interfering frequency would grow, which means that the vibrations would start to be. Anyway, for improving the functioning of the whole setup, it is required to find alternatives in terms of mountings for both engines.

5.2 Research of alternatives

While looking for an alternative to the product offered in this catalogue (see Appendix VIII) there is some limitation. For the SISU 420 DWRIE, the best option is the existing one. There is no accurate information on the diagrams for other models because the needed requirements are out of range. Thus, for improving the bench test, it is required to work with a different supplier in the case that it was desired to work with the same mountings for both engines, as mentioned at the beginning of this section (Vulkan Group).

Firstly, the first aspect to cover before finding alternatives is the types of mountings that would suit better the required conditions, not based on the model but focusing on their

general design. As introduced before in section 3.6.2, there are different types of engine mountings: Elastomeric mounts, passive hydraulic engine mounts, and active engine mounts. For the remodelling of the current set, it has been found in the market that the best option is the elastomeric engine mounts. When comparing the different examples, some aspects have led the study on turning down the other two types. Firstly, passive and active mounts are more orientated to a sector where the engines are not tested but are used for the mobility of passengers, which requires the maximum level of isolation for the vibrations all the time, something that is more focused on the comfort than in the security as low levels of vibrations can always be accepted. This requires more complex systems, in fact, elastomeric mounts are much more simple than active and passive mounts, thus, higher complexity involves a higher probability of issues, less reliability, and a bigger budget. In this way, these reasons have tipped the balance in favour of elastomeric engine mounts.

Leaving aside the types and focusing on more numerical aspects, before the research starts, it is required to determine the minimum natural frequency (see Figure 30) to avoid the resonance zone for each engine (For working with the previously introduced diagrams). A value that will help select the right model.

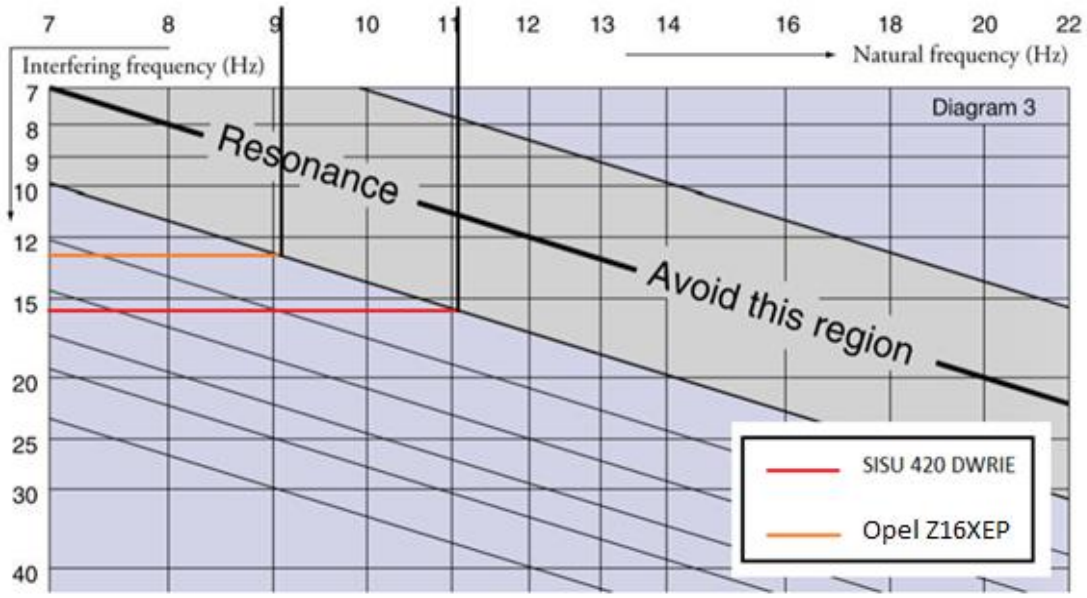

Figure 30: Maximum required natural frequency for the selection of the mountings of each engine. Source: Adapted from (Trelleborg, 2022)

Graphically, the maximum natural frequency that the new mountings should provide can be estimated, even if the value is not accurate, it is easy to determine that for the SISU 420 DWRIE, the frequency will have to be lower than 11Hz and for the Opel Z16XEP, it will have to remain under the 9Hz.

As was introduced before in this section, this project is focused on remodelling the laboratory most efficiently, is for that that, in case it was possible, having the same

mountings for both engines would be the most desired solution. In case it was not possible, it would be required to find different mountings for each one.

5.2.1 Alternative 1: Working with the same mountings

Knowing beforehand that there are no models similar to the existing ones provided by Trelleborg AB that could suit the SISU engine at low speeds, Vulkan group (see Appendix IX) is the alternative considered. In this case, the company gives the vertical nominal load in kN and the vertical static stiffness at nominal load. However, it does not provide any diagrams like the Trelleborg company (Which will also be used in this section). In this way, the natural frequency of the material will be the variable that will allow using the previous diagrams (see Figure 29) but without working with the models that are represented on them (As they refer to the Trelleborg solutions). This process will allow verifying if the selected mounting is in the resonance zone inversely that it was done before.

To start, the load has to be calculated in kN:

$$W_{m_{SISU}} = 100 \cdot 9.81 = 981\ N = 0.98kN$$
$$W_{m_{OPEL}} = 50 \cdot 9.81 = 490.5\ N = 0.49kN$$

Using this value, the catalogue of the Vulkan group provides different models of mountings that could offer a feasible solution for our requirements. The first selection is done by the load that can be held, thus the models are the VDM and VD (see figure Figure 31). Anyway, for the desired requirements, the VD series offers lower vertical stiffness, which results in a smaller natural frequency, leading to fewer vibration problems.

		$F_{z,\ Nominal}$ [1]	$C_{z,\ Nominal}$
		[kN]	[kN/mm]
Baugruppe Dimension group	Elementsteifigkeit Element stiffness	Vertikale Nennlast Vertical nominal load	Vertikale statische Steifigkeit bei Nennlast Vertical static stiffness at nominal load
VD 3	22	0,75	0,15
VD 3	24	0,95	0,19
VD 3	26	1,10	0,23
VD 4	22	2,30	0,85
VD 4	24	2,80	1,35
VD 4	26	3,30	1,75

Figure 31: List of available mountings regarding the vertical nominal load to hold and the vertical stiffness at calculated loads. Source: Adapted from (issuu, 2022)

In this case, there is one feasible option, the VD 3 concerning element stiffness 24. In terms of room concerning the maximum allowed vertical load, it is specified that this value refers to 75% of the maximum load that could be held, so there is still a certain margin even if it could seem that the model could not be a good example. It has to be remarked that in this specific aspect, the SISU 420 DWRIE is the most limiting engine as it weighs more, for this reason, selecting the same mountings implies that the vertical

nominal load will be determined by said engine. Thus, the real percentage R_{per} of the maximum load M_{max} for this model would be:

$$M_{max} = \frac{F_Z}{0.75} = \frac{0.95}{0.75} = 1.27$$
$$R_{per} = \frac{W_{m_{SISU}}}{M_{max}} = \frac{0.98}{1.27} = 0.773$$

The previous calculations determine that this mounting would be working at 77.3% of its capacity. What shows a certain margin in respect to the maximum allowed load, a very positive aspect that will help in extending the life of the product.

Following, it has to be verified that the solution avoids the resonance effect. For doing so, it is required to calculate dynamic stiffness k_d of both rubber mounts as it is going to hold the effects of a dynamic force. After that, the natural frequency f_n can be obtained with the value provided in Figure 31 regarding the vertical static stiffness at nominal load C_{vert}:

$$C_{vert} = 0.19 \frac{kN}{mm}$$

(Value for nominal load, even if the current requirements surpass a little bit of the nominal load, it is by a very small margin so it is considered to still work with this value)

Adapting the previous values that regard static situations to the equivalent value for dynamic scenarios, according to (Lee et al., 2013) a conservative approach for determining the dynamic stiffness equivalent to rubber k_r can be calculated by multiplying the static stiffness by 1.2~1.5. In this case, it has been considered to work with a value of $k_r = 1.3$; which is close to the middle of the range.

$$k_d = k_r \cdot C_{vert}$$
$$k_d = 1.3 \cdot 0.19 = 0.247 \frac{kN}{mm} = 2.47 \cdot 10^5 \frac{N}{m}$$

Here, to calculate the natural frequency, as it is dependent on the mass of the element that has to be dampened, the study has to differ from the SISU engine and the Opel engine:

SISU 420 DWRIE:

$$f_n = \frac{1}{2 \cdot \pi} \cdot \sqrt{\frac{k_d}{W_{mount}}} = \frac{1}{2 \cdot \pi} \cdot \sqrt{\frac{2.47 \cdot 10^5}{100}} = 7.91 Hz$$

Opel Z16XEP:

$$f_n = \frac{1}{2 \cdot \pi} \cdot \sqrt{\frac{2.47 \cdot 10^5}{50}} = 11.18 Hz$$

In this way, it is verified that this company cannot offer a model of mountings that could work for both engines at the same time since the Opel engine would present resonance. This problem persists among the different companies that have been also considered, the main reason is that the difference in the weight and interfering frequencies for each engine is too big for finding just one model of mountings that could avoid resonance. In this way, the only parameter that could be modified for working with just one model of mountings is the interfering frequency (modifying the idle speed). Increasing this value could help the Opel engine to avoid the resonance zone. Analysing again the used diagrams and knowing the value of the natural frequency for the mounting (11.18Hz), setting the same idle speeds for both engines would provide a feasible solution since both engines would fall out of the resonance zone (see Figure 32).

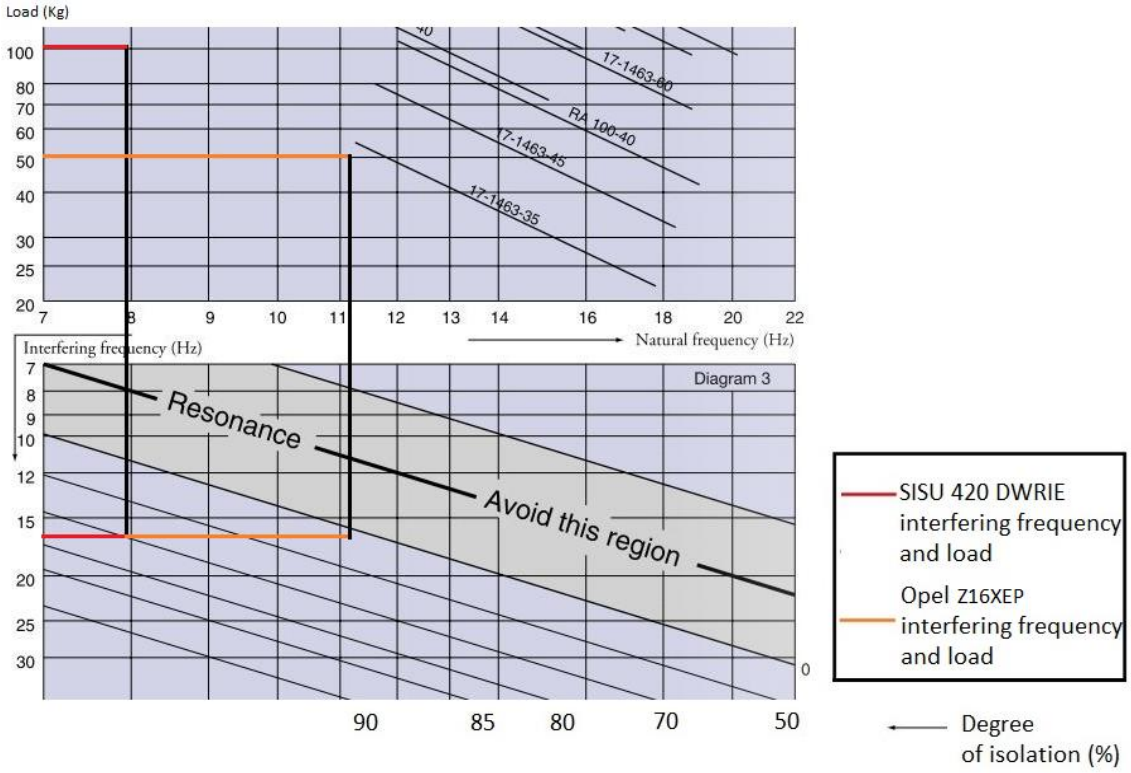

Figure 32: Comprobation of the alternative mountings. Source: Adapted from (Trelleborg, 2022)

Finally, it is checked how the previous issue regarding the Opel engine falling into the resonance zone, would now be avoided, providing also some level of isolation at low speeds, which in comparison to the current operating conditions would be an improvement.

5.2.2 Alternative 2: Finding different mountings for each engine

This alternative would reduce a little bit the modularity of the whole setup but would present more flexibility for the isolation of the vibrations for each engine. Starting with the SISU engine, the previous model from the Vulkan group is considered to be a good option so it will be kept. However, for the Opel engine, if the idle speed remains at its original value, it is required to find a different model. Going back to Trelleborg AB (which

provides solutions for smaller loads), it has been found a different series that could provide a good solution with the help of the diagrams referring to this new series (see Figure 33).

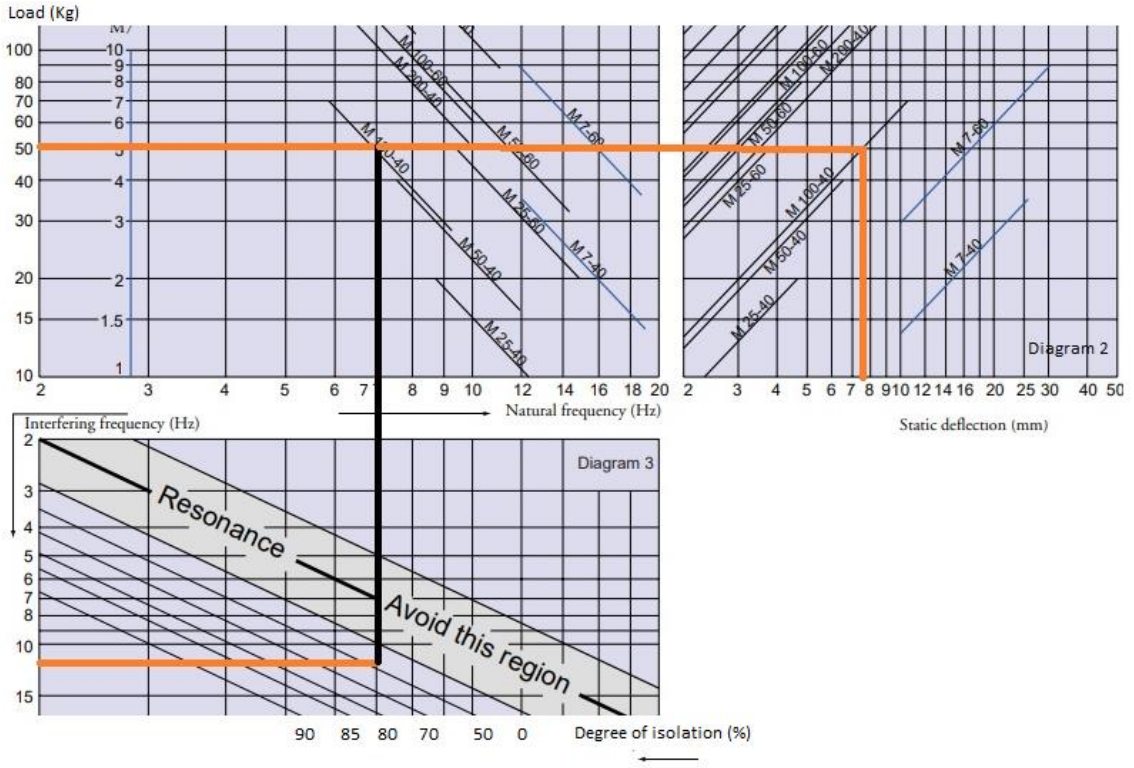

Figure 33: Comprobation of the second alternative mountings for the Opel Z16XEP. Source: Adapted from (Trelleborg, 2022)

After analysing the diagrams, it has been verified how these mountings would provide a feasible solution in the case of the Opel engine, avoiding the resonance zone and providing a degree of isolation of the 50% in the worst conditions. However, in this case, the static deflection would be a bit larger than the previous solutions as it would be close to 8mm. All the detailed information about the selected mountings can be accessed in Appendix X.

5.2.3 Matrix of decision for the mounting selection

Finally, after providing the previous solutions, the same line as for the selection of the dynamometer will be followed, defining first the most influencing parameters for the selection and grading them before making the final decision. In this case, said parameters will be:

- Price of the mountings
- Degree of isolation provided at idle speed
- Static deflection
- Modularity

Modifications required in the current setup Following, Table 6 shows the grades given for each parameter:

Table 6: Matrix of decision grading the most important factors considered for the mountings' selection. Grades go from 0 to 5, which refers to poor and perfect, respectively.

Parameters	*Purchase cost*	*Degree of isolation*	*Static deflection*	*Modularity*	*Required modifications*
Alternative 1	5	3	4	4	1
Alternative 2	3	5	3	3	5

Considering the previous grades, alternative 1 gets a total score of 17 while alternative 2 receives a total score of 19. As it can be seen in Table 6, the required modifications are the parameter that tips the balance in favour of alternative 2 since it would require the Opel engine to have some modification for running at higher speeds at idle, something that would not allow the tests extracting the maximum information from it. In contrast to the previous matrix of decision (see Table 5), in this case, the chosen alternative is the most expensive one as two different types of mountings will be used, however, this is compensated by a better degree of isolation at idle speeds and no modifications of the current equipment would be required.

6 Coupling selection

As reviewed in Chapter 3.6.4, the correct choice of coupling for the driveshaft is very important. The next step of the process is the selection of the correct coupling. This is similar to the other chapters reviewed previously, where the coupling will not be designed from scratch, but the choice of a correct coupling from the market will be done.

As it has been done before, the analysis of the current setup will be done to see if we can keep the current couplings and if it is needed, find new alternatives. The first option will be using the same coupling for both engines, and if that is not possible, different couplings for each engine will be used.

To do this analysis, the calculations mentioned in Section 3.6.4 will be done. For this analysis, it is going to be checked if the current coupling used in the SISU engine is optimal and if it can work as well for the Opel engine.

6.1 Verification of current couplings

The current setup of the driveline for both engines is shown in the next figures.

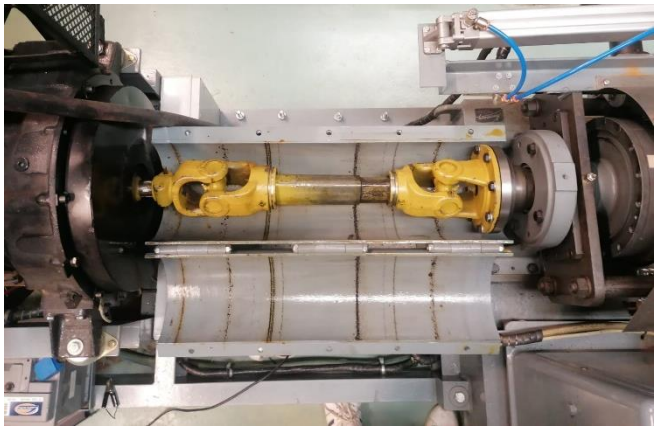

Figure 34: Current driveline of the SISU 420 DWRIE engine. Source (Author's own)

Figure 35: Current driveline of the Opel Z16XEP engine. Source (Author's own)

It can be seen from Figure 34 that the setup used in the SISU engine is the flywheel attached to the coupling which both are inside the casing. Then, the coupling is connected to the Cardan shaft and the shaft is directly connected to the dynamometer.

The setup for the Opel is no different from the SISU. It is seen in Figure 35 that the flywheel (inside the casing) is connected to the coupling, which in this case it's not inside the casing, then connected to the Cardan shaft, and at the end of the line, there is a dynamometer.

As the model of the coupling of the Opel engine is not stated, the calculations will be done based on the coupling of the SISU engine, which is CENTAX-V 35. The properties of this coupling are shown in the following figure.

CENTAX size Größe	Shore-hardness Gummiqualität Shore A	Nominal torque Nenn-drehmoment T_{KN} [Nm]	Max. torque Max. Drehmoment T_{Kmax} [Nm]	Continuous vibr. torque at 10 Hz Zul. Wechseldreh-moment bei 10 Hz T_{KW} [Nm]	Allowable energy loss Zulässige Verlustleistung P_{KV} [W]	Dyn. torsional stiffness Dyn. Dreh-steifigkeit C_{Tdyn} [Nm/rad]	Relative damping Relative Dämpfung Ψ	Flange SAE J620 or DIN 6288 Flansch SAE J620 oder DIN 6288	Max. Speed Max. Drehzahl n_{max} [min^{-1}]
12	45	230	700	58	100	1380	1,2	6,5	5000
	50	250	750	62		1875	1,4	8	4500
	60	280	840	70		2400	1,6		
14	45	330	1000	82	130	2250	1,2	8	4500
	50	360	1080	90		2700	1,4	10	4000
	60	400	1200	100		3400	1,6		
16	45	450	1350	112	150	3000	1,2	8	4500
	50	500	1500	125		3900	1,4	10	4000
	60	560	1680	140		4900	1,6		
20	45	570	1700	140	170	3750	1,2	10	4000
	50	630	1900	158		4800	1,4	11,5	3600
	60	700	2100	200		6000	1,6		
25	45	770	2300	195	200	5100	1,2	10	4000
	50	850	2550	212		6450	1,4	11,5	3600
	[illegible]	[illegible]	[illegible]	[illegible]		[illegible]	[illegible]		
35	45	1100	3300	275	230	7200	1,2	11,5	3600
	50	1200	3600	300		8700	1,4	14	2700
	60	1400	4200	350		11000	1,6		
45	[illegible]	[illegible]	[illegible]	[illegible]	260	[illegible]	[illegible]	11,5	3600
	50	1800	5400	450		12800	1,4	14	2700
	60	2200	6600	550		16000	1,6		
50	45	2250	6750	560	320	15300	1,2	14	2700/2460*
	50	2800	8400	700		18000	1,4		
	60	3000	9000	750		22500	1,6		
55	45	2900	8700	725	360	19500	1,2	14	2700/2460*
	50	3500	10500	875		23000	1,4		
	60	4000	12000	1000		29000	1,6		
65	50	5000	15000	1250	380	33000	1,4	14 16	2700/2460* 2400/2200*
	60	5600	16800	1400		41300	1,6	18	2200/2000*
68	50	7000	21000	1750	420	70500	1,4	18	2200/2000*
	60	8250	24750	2063		87000	1,6		
70	50	11500	34500	2875	540	102000	1,4	21	1870/1700*
	60	12500	37500	3125		127500	1,6		
72	50	15000	45000	3750	600	142000	1,4	21	1870/1700*
	60	16500	49500	4125		177000	1,6	24	1720/1560*
75	50	20000	60000	5000	720	200000	1,4	710 750	1680/1530* 1600/1450*
	60	22000	66000	5500		250000	1,6	850	1420/1300*
78	50	31500	94500	7875	850	285000	1,4	900	1330/1220*
	60	35000	105000	8750		356000	1,6	950	1270/1150*
80	50	40000	120000	10000	1000	400000	1,4	950	1270/1150*
	60	44000	132000	11000		500000	1,6	1060	1140/1040*

* Werte in Klammern für Klassifikation

Figure 36: Properties of the CENTAX-V couplings. Source: (CENTAX, 2022)

It can be seen from the Figure above that the CENTAX-V 35 has a nominal torque varying from 1100 to 1400, which for our purpose is optimal. However, the maximum speed allowed for this model is up to 3600rpm. This is not a problem for the SISU engine, as it can only go up to 2200rpm, but it causes problems for the Opel engine, which can go up to 6500rpm.

This means that this coupling cannot be used for the operation of the Opel engine, so no further calculations are going to be done.

Besides the limitation of the rpm, it exists another limitation, which is the flywheel size. It is known that the Opel flywheel differs from the SISU flywheel. The size of the flywheel comes with the SAE (Society of Automotive Engineers) size. For the SISU flywheel, AGCO power has given out all the information required to do all the calculations and also the SAE measurement (see Appendix XI). However, Opel information is more limited so approximations are needed.

It can be seen in equation [3.4] that the critical frequency of the shaft is dependent on the inertia of the engine and the dynamometer. So before searching for alternatives, it is needed to check if the current coupling of the SISU engine can be used with the new dynamometer.

6.1.1 Verification of the SISU coupling

To do this, equation [3.4] will be used, but instead of calculating the critical frequency as if it was a stiff connection, the calculation will be done assuming that the coupling supports all the torsional stress of the driveline. So instead of using the stiffness of the shaft, the stiffness of the rubber coupling will be used. As mentioned, the values of inertia are given by the providers (see ANNEX XIV and ANNEX VI, respective to the selected dynamometer), as well as for the stiffness is taken from Figure 36.

Having this said, using equation [3.4], the critical frequency is:

$$n_c = \frac{60}{2\pi} \cdot \sqrt{\frac{8700 \cdot (0.624 + 1.8)}{0.624 \cdot 1.8}} = 1308.49cpm$$

Being [cpm] a non SI unit meaning counts per minute.

For a four-cylinder, four-stroke engine, it has been seen in previous chapters that the first major critical harmonic is generally of most significance, and it is sufficient to calculate the critical speed at that harmonic. Using equation [3.6], the corresponding engine speed is:

$$N_c = \frac{1308.49}{2} = 654.24rpm$$

This critical speed is lower than the idle speed of the engine, which means that the coupling can be kept being used with the new dynamometer.

In this case, the critical speed is below the idle speed but is a common practice to arrange for this to lie between the idle speed and the minimum full load speed, which is the minimum speed that power can be extracted from the engine, in this case, it would be 1000rpm and 1300rpm respectively.

6.2 Approximations for the Opel Z16XEP

As said before, Opel does not give a lot of information about their products, so research has been done to get the information needed for the calculations.

The first approximation comes with flywheel sizing. As the access to the flywheel in the Opel engine is very limited (as seen in Figure 35), and all the driveline needs to be removed take measurements, a flywheel model for the engine has been designed based on images of flywheels that can operate in that engine.

Once a good reference has been taken, the flywheel is 3D designed with the program NX, the same program that will be used afterwards for the design of the engine bed. The approximate design of the flywheel can be seen in the following figure.

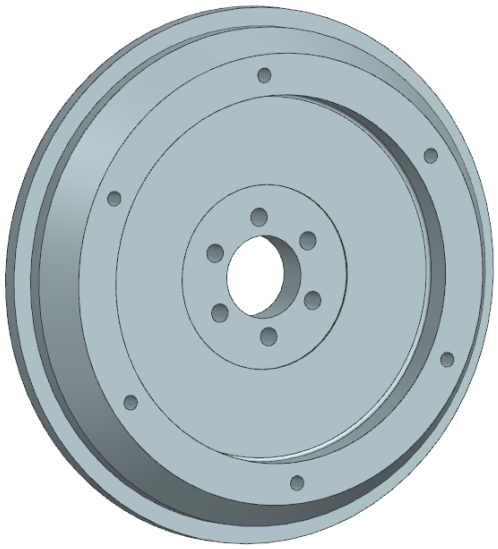

Figure 37: Approximate version of an Opel Z16XEP flywheel. Source (Author's own)

The dimensions of the flywheel can be accessed in Appendix XII. From this approximation, it can be said that the SAE size of the Opel flywheel would be a size 7 ½.

Another approximation made for the project is the material of the flywheel. This is needed to know the moment of inertia of the flywheel, which will come in use in the next approximation. After some research, the selected material is AISI Maraging Steel, a carbon-free iron-nickel blend of steel with a hint of aluminium, titanium, cobalt, and Molybdenum.

NX is a powerful tool to work with, as it gives interesting values without the need for calculations. In this case, the value that is needed is the moment of inertia. The following table gives us the information we need about the designed flywheel.

Table 7: Properties of the designed flywheel. Taken from Siemen NX.

Density	0,000008	kg/mm³
Area	177364,41	mm²
Volume	1695035,55	mm³
Mass	13,5602844	kg
Ixxw	147984,755	kg·mm²
Iyyw	78935,7329	kg·mm²
Izzw	78935,7329	kg·mm²

The inertia value that will be used in the calculations will be Ixxw.

The last approximation that will be done is the total inertia of the engine. As seen in equation [3.4], the critical speed is dependent on the inertia of the engine and the inertia of the dynamometer. As said previously, AGCO power has given the value of the engine inertia as well as Jiangsu has provided the inertia for the dynamometer, but for the Opel, an approximation will be done. The approximation done is the following:

$$I_e = 2 \cdot Ixxw$$

This approximation is done so the inertia of the crankshaft and other main components of the engine are considered.

6.3 Research of alternatives

It has been found while researching for alternatives that only one model is able to be used in both engines. This is because of the flywheel size, as the Opel engine is a small flywheel, a lot of companies do not produce couplings for such small SAE sizes.

As seen in chapter 6.1.1, the coupling for the SISU engine can be kept, so if the coupling found cannot stand the stress with the SISU engine, there is no problem as the current coupling can be used.

The research of new alternatives is by no means an easy job, as the coupling needs some specifications, these being:

- Being able to be connected to the flywheel (SAE size).
- rpm limitations.
- Torque limitations.
- Critical speed limitation.

The first thing that has been done, is to check if the current brand that we have for the coupling has other models that could fit the requirements.

6.3.1 CENTAX-TEST

The model that has been found is CENTAX-TEST. The only drawback of the model is that it comes with a shaft attached, but after communicating with the company, it has been found that the shaft can be disattached from the coupling.

The CENTAX-TEST is based on a highly flexible rubber element, combinable with homokinetic joints, Cardan joints, slip joints, etc. in the case of the study it will be connected to a Cardan joint. It is an extremely adaptable design with high torsional flexibility. Dampens torsional vibrations and shocks and compensates axial, radial, and angular misalignments (CENTAX, 2022).

The properties of the coupling can be seen in the following figure.

CX-CV; CX-2x2, CX-UJB, CX-CVB							CX-CV, CX-UJB, CX-CVB		CX-2x2	
CENTAX size	Shore hardness	Nominal torque	Max. torque	Continuous vibratory torque	Relative damping	Max. speed	Allowable energy loss	Dynamic torsional stiffness	Allowable energy loss	Dynamic torsional stiffness
CENTAX Größe	Gummi-qualität Shore A	Nenn-drehmoment T_{KN} [Nm]	Max. Drehmoment T_{Kmax} [Nm]	Zul. Wechsel-drehmoment T_{KW} [Nm]	Relative Dämpfung Ψ	Max. Drehzahl n_{max} [min-1]	Zul. Verlust-leistung P_{KV} [W]	Dyn. Dreh-steifigkeit C_{dyn} [Nm/rad]	Zul. Verlust-leistung P_{KV} [W]	Dyn. Dreh-steifigkeit C_{dyn} [Nm/rad]
CX-11	45	150	450	37,0	1,00	8000 4000 *	68	320	136	160
	50	180	540	45,0	1,05		70	400	140	200
	55	200	560	50,0	1,05		72	500	144	250
	60	225	560	56,0	1,10		74	630	148	315
	65	240	560	60,0	1,10		76	780	156	390
CX-13	45	280	840	70,0	1,00	8000 4000 *	98	780	196	390
	50	330	990	82,0	1,05		100	975	200	488
	55	360	1080	90,0	1,05		102	1200	205	600
	60	400	1100	100,0	1,10		105	1500	210	750
CX-15	45	450	1120	112,5	1,00	8000 4000 *	146	1100	292	550
	50	520	1120	130,0	1,05		150	1400	300	700
	55	580	1120	145,0	1,05		154	1750	308	875
	60	640	1120	160,0	1,10		158	2200	316	1100
	65	700	1120	175,0	1,10		160	2750	320	1375
CX-17	45	700	2100	175,0	1,00	8000 5000 ** 4000 *	195	1700	390	850
	50	800	2400	200,0	1,05		200	2100	400	1050
	55	900	2400	225,0	1,05		205	2600	410	1300
	60	1000	2400	250,0	1,10		210	3250	420	1625
	65	1100	2400	275,0	1,10		215	4050	430	2025
	70	1200	2400	300,0	1,15		220	5050	440	2525
Values in grey are optional * without centrifugal protection ** value for CV-joint size 30							Werte in grau sind optional * ohne Schleuderschutz ** Wert für CV-Gelenk Größe 30			

Figure 38: Technical data of the CENTAX-TEST. Source: (CENTAX, 2022)

As seen in Figure 38, all the sizes of this model fit our requirements; the rpm is higher than the maximum rpm of the Opel engine, as well as the maximum torque (depending on the size) is greater than the SISU torque. The next step is to check what size is needed, to do this Figure 37 will be used.

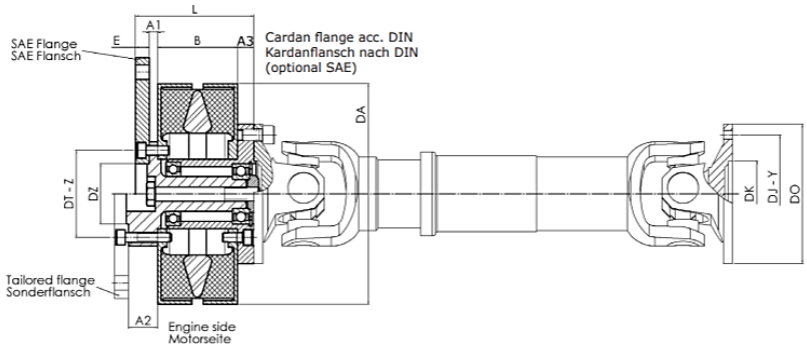

Size Größe	Nominal torque Nenndrehmoment T_{KN} [Nm]	DA [mm]	A1 [mm]	A2 [mm]	A3 [mm]	B [mm]	E	DT ±0,2 [mm]	Z	DZ [mm]	L	UJB sizes Kardan-größe	SAE Size Größe
CX-11	150-240	150	6	25	14	71	12	75,0	6x M8	52 H7/h7	103	100	6½
CX-13	280-400	170	6	25	14	64	12	75,0	12x M8	52 H7/h7	96	120	7½ 8
CX-15	450-700	190	6	25	14	71	12	75,0	12x M8	52 H7/h7	103	120	10 11½
CX-17	700-1200	220	6	25	14	84	15	101,5	8x45° x M10 + 4x90° x M10	68 H7/h7	119	120 150	11½

Figure 39: Sizes of the CENTAX-TEST. Source: (CENTAX, 2022)

It can be seen in the figure above that models CX-11, CX-13, and CX-15 can fit all the different SAE sizes including 7 ½ and 11 ½, which means that these models can be used for both the SISU engine and the Opel engine. Of these models, the one which is better

for our application is size CX-15, as the nominal torque varies from 450 to 700Nm, which is in the range of the maximum torque of the SISU engine.

One complication could come with the holes in the coupling because it comes with a shaft attached, the holes are made exclusively for that shaft, but that could be solved by designing an adapter.

The next step is to check the calculations to see if the coupling can be used.

6.3.2 Verification of the CENTAX-TEST

To do this, the procedure will be the same as in chapter 6.1.1. First, the calculations will be made for the SISU engine.

From Figure 38 can be taken the torsional stiffness of the CX-15, which in this case is 1400Nm/rad, which corresponds with a nominal torque of 520Nm having a shore hardness of 50. Having this said, putting the values in equation [3.4], the critical frequency is as follows.

$$n_c = \frac{60}{2\pi} \cdot \sqrt{\frac{1400 \cdot (0.624 + 1.8)}{0.624 \cdot 1.8}} = 524.89cpm$$

Using equation [3.6], the corresponding engine speed is:

$$N_c = \frac{524.89}{2} = 262.45rpm$$

Same as for the current coupling, this critical speed is lower than the idle speed of the engine, which means that the coupling selected is good for the operation.

Now that it has been checked that the SISU engine can operate with the CENTAX-TEST, the Opel engine needs to be checked. Using the same methodology as for the SISU engine, the critical frequency is checked.

$$n_c = \frac{60}{2\pi} \cdot \sqrt{\frac{1400 \cdot (0.296 + 1.8)}{0.624 \cdot 1.8}} = 488.1cpm$$

Using equation [3.5], the corresponding engine speed is:

$$N_c = \frac{488.1}{2} = 244.05rpm$$

In this case, as well as for the SISU engine, the critical speed is way below the engine idle speed, which means that this coupling can also be used for the Opel engine.

6.3.3 Design of the adapter

From Figure 39 can be seen that the Cardan size corresponding to the model CX-15 is size 120, the corresponding measurements of the Cardan shaft can be seen in the following figure.

DO [mm]	DJ [mm]	DK [mm]	Y [mm]
100	84,0	57 H7/h7	6 x M8
120	101,5	75 H7/h7	8 x M8
150	130,0	90 H7/h7	8 x M10

Figure 40: Measurements of the Cardan shaft. Source: (CENTAX, 2022)

In this case, it can be seen that the diameter where the bolts are located is 101.5mm. currently, the bolts of the owned Cardan shaft are in a diameter of 170mm, so an adapter that goes from 101.5mm to 170mm is needed.

The design of the adapter is presented in the following figure, as well as the dimensioning is presented in Appendix XIII.

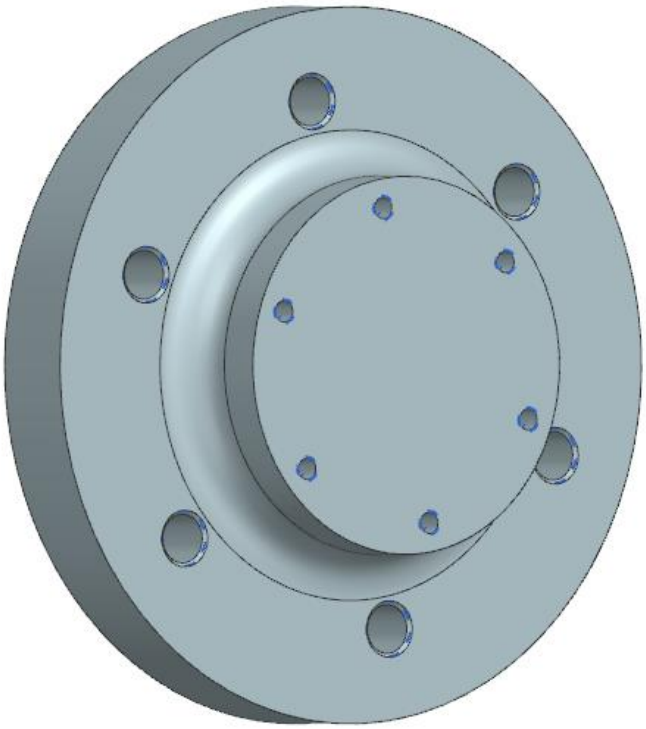

Figure 41: Design of the engine adapter. Source (Author's own)

It can be seen in Figure 41 that the holes are smaller on one side than on the other, this is because according to Figure 40, the holes in the coupling are size M8, while the ones that are in the Cardan shaft are M18. This means that the smaller part goes attached to the coupling and the wider part goes bolted to the Cardan shaft.

7 Setup adaptation to the proposed solutions

After presenting all the solutions to different elements from the setup that needed to be modified or changed, the project can focus on the adaptation of the infrastructure to the changes that have been done and the new engine that will be tested. Principally two main elements influence the required modifications, the first one, is the adaptation of the current engine bed for suiting the Opel engine and after that, adapting the new dynamometer to the part of the structure destined previously for the current water brake. In this way, the project will be divided on one side in the adaptation of the engine bed and the other for the adaptation of the dynamometer.

7.1 Adaptation of the engine bed

In this part, firstly it is required to know what will the Opel engine require to suit the current setup, for this reason, it is needed to know the measurements of the engine. As can be seen in Figure 42, this engine is currently attached to a structure that was used for its previous isolated testing.

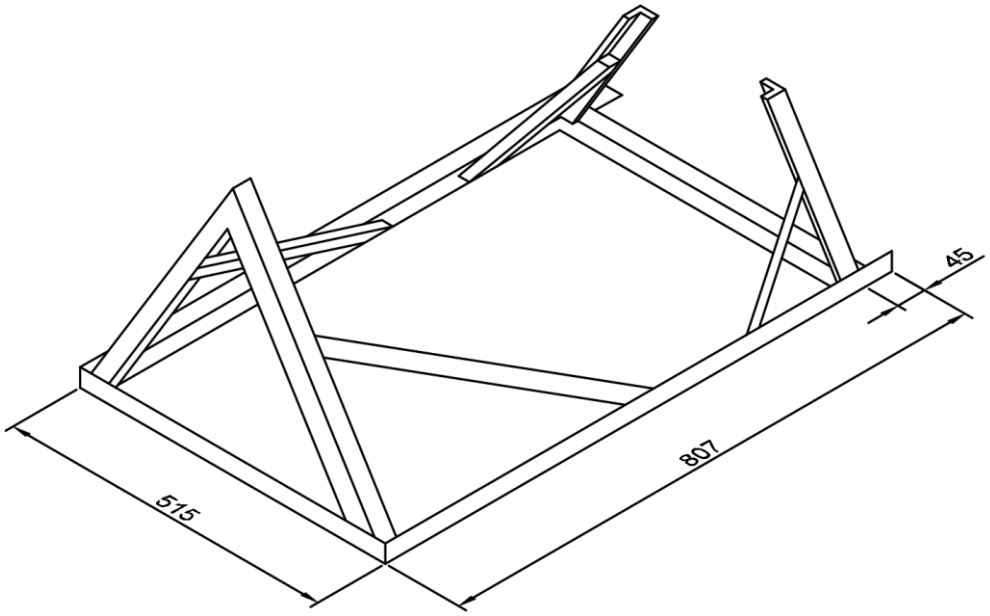

Figure 42: Container structure for the Opel engine with the measures of interest indicated. Height is not specified as it is not giving valuable information. Source (Author's own)

It is thought that keeping this structure could be helpful for its adaptation to the existing engine bed and also because it has an easier geometry. As the Opel engine suits inside it, it leads the study on focusing on the measurements of this structure as reference instead of the engine, which would be more complex to measure and adapt directly. Following, it is also required to take measurements of the current engine bed test to study the way to adapt it, see Appendix XVI. After checking carefully all the values, the adaptation of the new set will depend on those aspects that involve a modification of it. The following list will introduce the elements from the Opel engine that have motivated

the different adaptations of the current engine bed, or elements from the engine itself that have to be modified:

- Container structure dimensions.
- Output shaft position.
- Exhaust pipe and heat exchanger pipes.
- Heat exchanger.
- Opel engine exhaust pipe.

Following, all these aspects are going to be faced one by one. The way it will be done will be keeping the line that the project has followed since the beginning. Thus, it has been tried to maintain the current setup the most similar as it was, limiting, in this case, the total modifications that should be required. For this reason, the modification process will start by considering the initial facility and in each of the previously introduced points, a solution for suiting the Opel engine will be presented.

7.1.1 Adaptation of the Opel engine container structure

The adaptation for the container structure has been the first part that has been faced, after considering the different measures, for suiting the container structure in the current engine bed, it has room in terms of width but it would require extending the length of the part destined to the engine bed. Specifically, now, the availability for suiting the Opel engine (See Appendix XVI) is 786mm and 540mm referring to length and width, respectively. While checking the Opel dimensions requirements, it can be seen how the width is not a problem as it occupies 515mm however, length can bring issues as it is 807 mm. Having said that, it has been found that there is a part of the container of the structure that could be cut, specifically, the part from the iron profile that surpasses 45 mm from the end of the structure, see Figure 42. Thus, after this, the structure would look as shown in Figure 43.

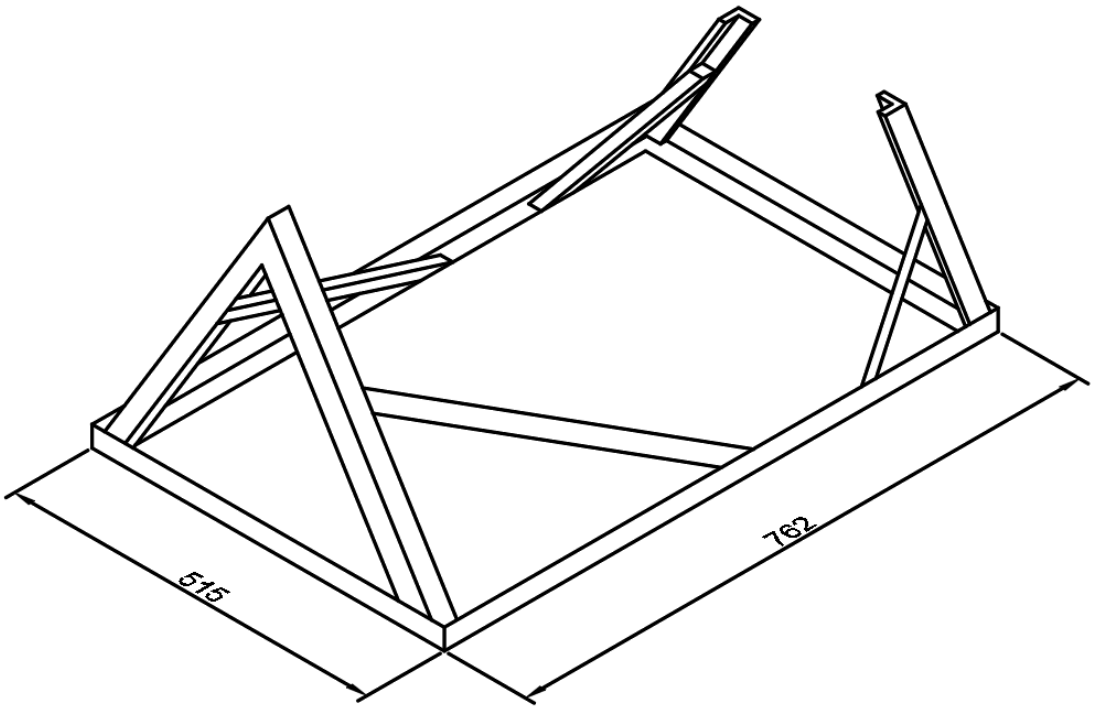

Figure 43: Opel engine container structure after removing 45 mm of the iron profile for saving space. Source (Author's own)

After this modification, the Opel engine's container structure would suit the current engine bed and would not require changes on it. Anyway, as it will be introduced in section 7.1.3, there will be other factors that will require modifications on it, however, if the factors to consider are reduced, as happens with this modification, the solution becomes less complex.

7.1.2 Adaptation for the output shaft

This modification has been motivated also to keep the structure as much similar as possible and also because if it was not kept that way, some modifications would be required on the other side of the facility, referring to the side of the dynamometer. Thus, the project wants to keep the engines in such a position that while being tested, have their outputs shafts in the same position, avoiding any movement from the Cardan shaft as it is unknown the value that it could be extended. For doing so, it is required to determine the place where the shafts are going to be placed.

7.1.2.1 Vertical positioning of the engines

Starting with the vertical positioning, the used reference will be the distance from the central axis of the output shaft of both engines to the structure where they are laying (Doing it that way omits the space occupied by the mountings, however, the vertical space required varies as they can be regulated). The SISU engine, shown in Figure 44 has a margin of 60mm.

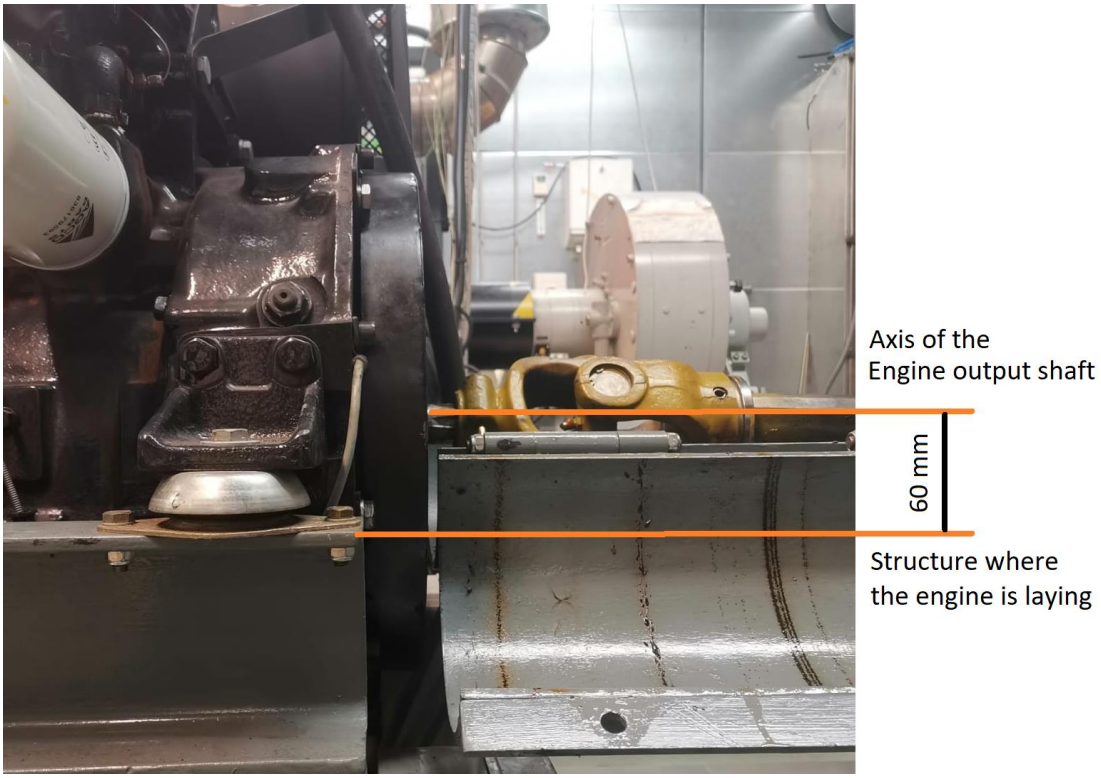

Figure 44: Vertical distance from the axis of the SISU engine output shaft to the structure where lays. Source (Author's own)

While the Opel engine, as shown in Figure 45, has a total distance of 300mm (275mm plus the mountings that would be configurated to occupy 25mm) from the axis of the output shaft to just under its mountings.

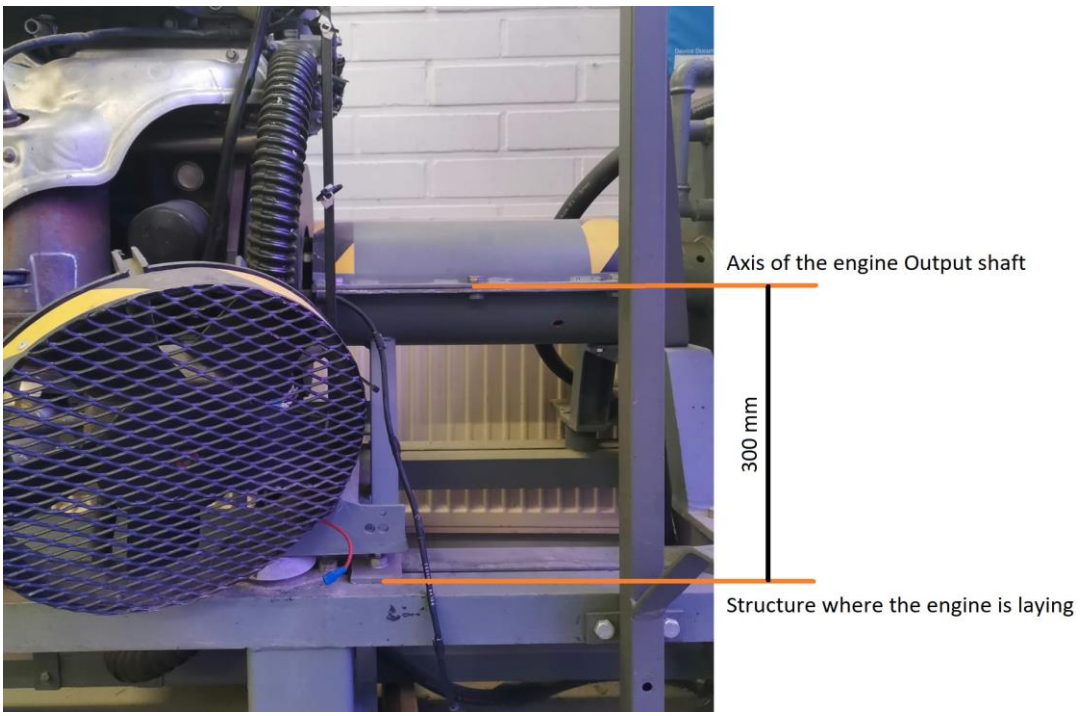

Figure 45: Vertical distance from the axis of the Opel engine output shaft to the structure where lays. Source (Author's own)

In this way, if both axes had to be in the same vertical position the Opel has to be placed lower than the SISU engine. As a proposed solution, analyzing the existing structure focusing on the engine bed (see Figure 46) and referencing the set on the lowest beam's surface.

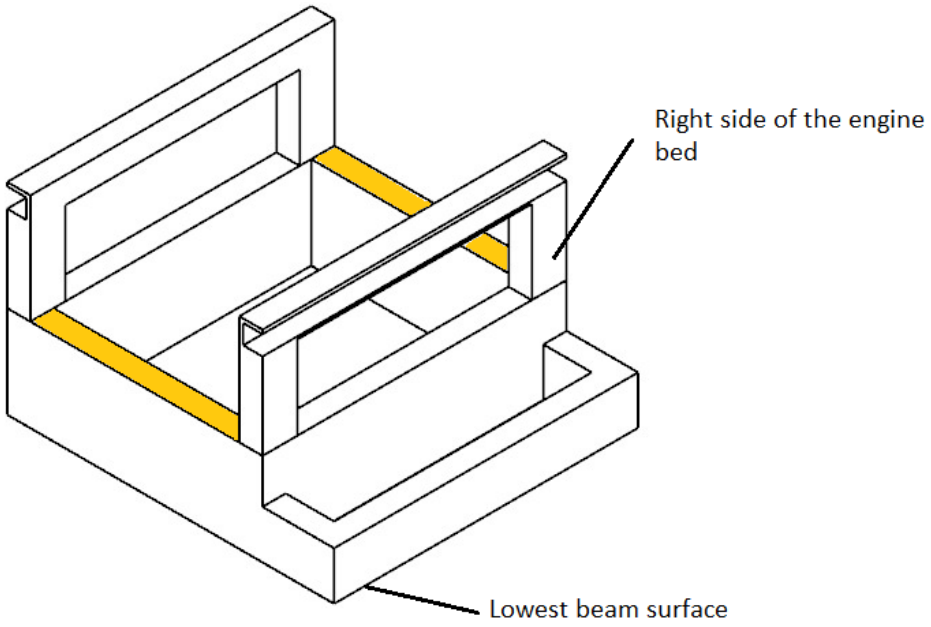

Figure 46: Current engine bed model highlighting in yellow where the beams used for the introduction of the Opel engine to the setup. Identification of the lowest beam and also the right side of the structure of the engine bed (will be used as reference below in the report). Source (Author's own)

The idea would be to add two beams that had the same length as the separation between the surfaces highlighted in yellow that would be used to lift the required measure to make both shafts coincide. The length of these beams is calculated in the end, specifically in section 7.1.3.

7.1.2.2 Horizontal positioning of the engines

In this case, this process is a little bit easier, as the Cardan shaft is going to be kept in the same position, for this reason, in this direction, the SISU engine will also remain in the same place. In this way, knowing the position of the Opel's output shaft concerning its container structure, it can be positioned. Figure 47 shows schematically that it is centred, thus to align both shafts the distances to each side of the current engine bed will be 12.5mm and 12.5mm.

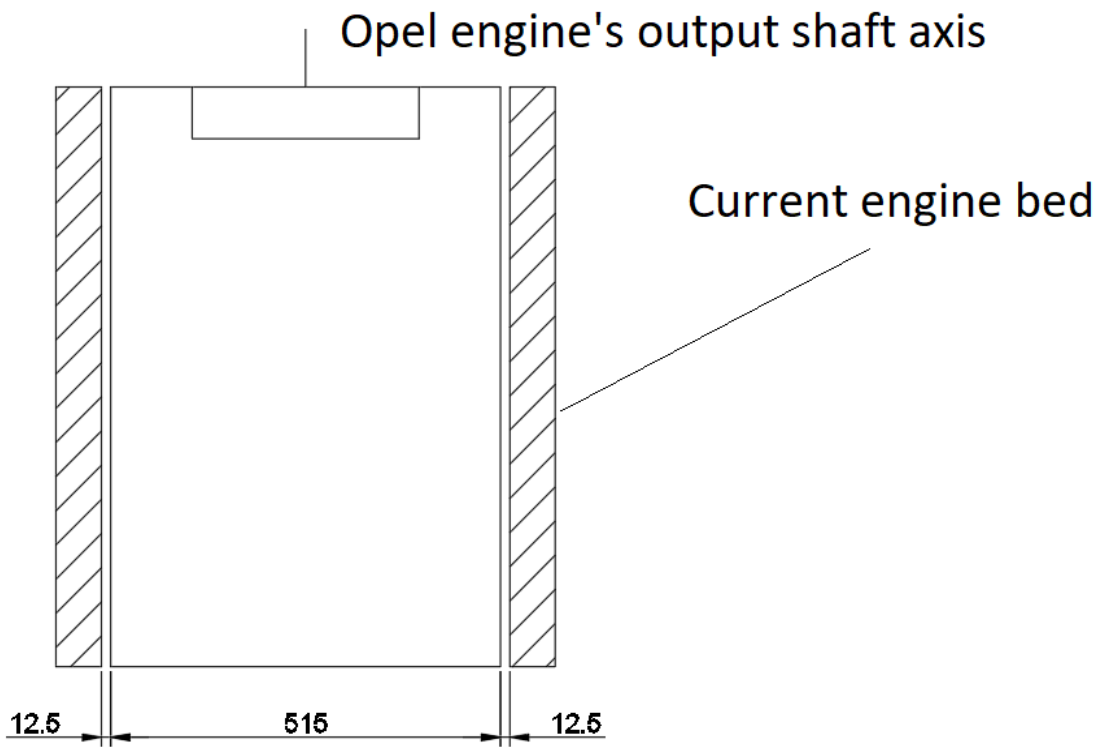

Figure 47: Schematic top view of the Opel engine structure for checking the horizontal positioning of the output shaft regarding the structure. Source (Author's own)

Finally, the separation of both beams will coincide with the current separation on the structure where the Opel engine is laying, 515mm between the outer sides of each one. Below, it is going to be checked what section is required for the beams to allow said separation.

7.1.2.3 Dimensioning of the beams' section

Thus, the next step is to dimension the section of these beams. Starting with the height, it is required to calculate the distance the Opel engine has to be lifted to make both shafts coincide. For the width of the section, the restriction will be the size of the mountings used for the Opel engine, which have to suit the used beam. Following all these considerations are going to be illustrated and calculated.

Starting with the height of the section, as introduced before, the Opel engine has to be placed lower than the SISU engine. Also, it will lay on two beams that will be attached to its structure (structure shown in Figure 42), having said that, the height of the section will be the total height from the axis of the output shaft to the lowest beam h_{axis}, minus the distance between the Opel output shaft's axis and its base h_{OPEL}, minus the height of the beams that form the base of the engine bed h_{beams}, minus the height of the beam where these will lay h_{beams2}, marked in yellow in Figure 46:

$$height = h_{axis} - h_{OPEL} - h_{beams} - h_{beams2} = 580 - 300 - 124 - 114 = 42mm$$

With this value, bot engine output shafts will be placed at the same height concerning the lowest beam of the base of the structure. Anyway, to make the calculations and the task of finding these beams easier, the final value will be 40mm.

In the case of the width, as introduced before, the limiting aspect for the width of the section is the mountings used for the Opel engine (see Appendix X), in this case, they require at least 96mm to fit completely in the section of the beam, for this reason, the beam will have a width of 100mm.

7.1.3 Adaptation for the exhaust and heat exchanger pipes

This part has been the biggest issue to adapt the current engine bed. Figure 48 shows how the engine has different pipes that come out from the container structure, requiring more space horizontally.

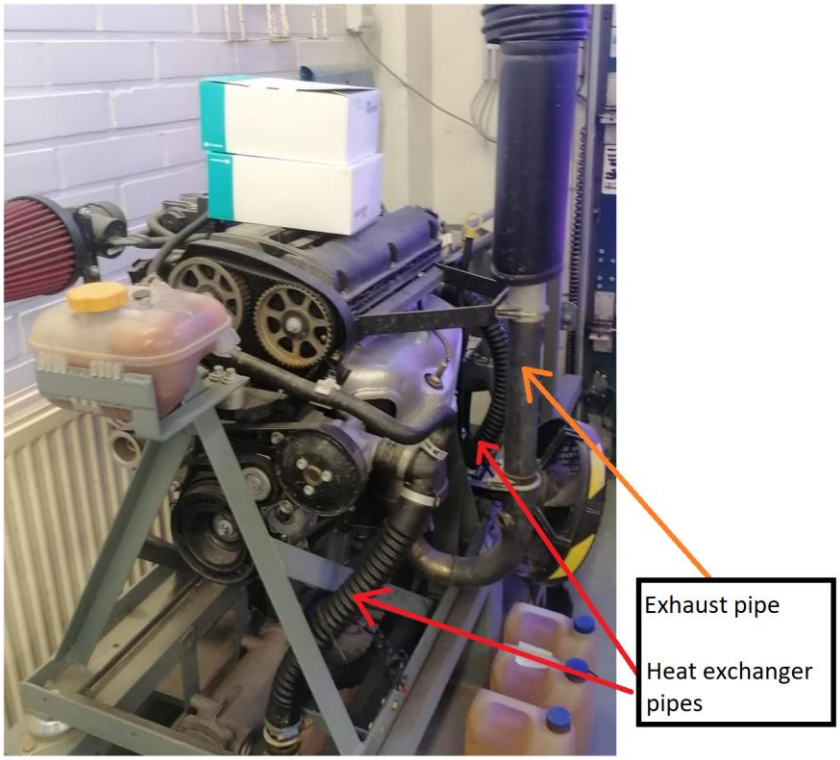

Figure 48: Identification of the pipes coming out from the Opel engine that will require modifications on the right side of the structure of the current engine bed. Source (Author's own)

In this way, the proposed adaptation of the engine bed for this is modifying the part identified in Figure 46 as the right side of the structure of the engine bed. The solution would consist of removing that part and designing two pieces that would raise from the basement of the structure. In this section, the project will focus on positioning the engines in the longitudinal direction of the output shafts and after that, designing these pieces to allow the SISU engine to be tested and at the same time, suit the Opel engine when it had to be tested too.

7.1.3.1 Longitudinal positioning of the engines on the engine bed

Starting with the positioning, it will be defined by where the SISU engine will be placed this is going to determine where said pieces will have to be placed. In this way, the first step is to find an element to reference the position of both engines. As there is not much accurate information (in terms of dimensions) about the inner part of the Opel engine flywheel cover, see Figure 49, the reference to place the SISU engine will be that part. This implies that both engines will have the cover of their flywheels in the same place.

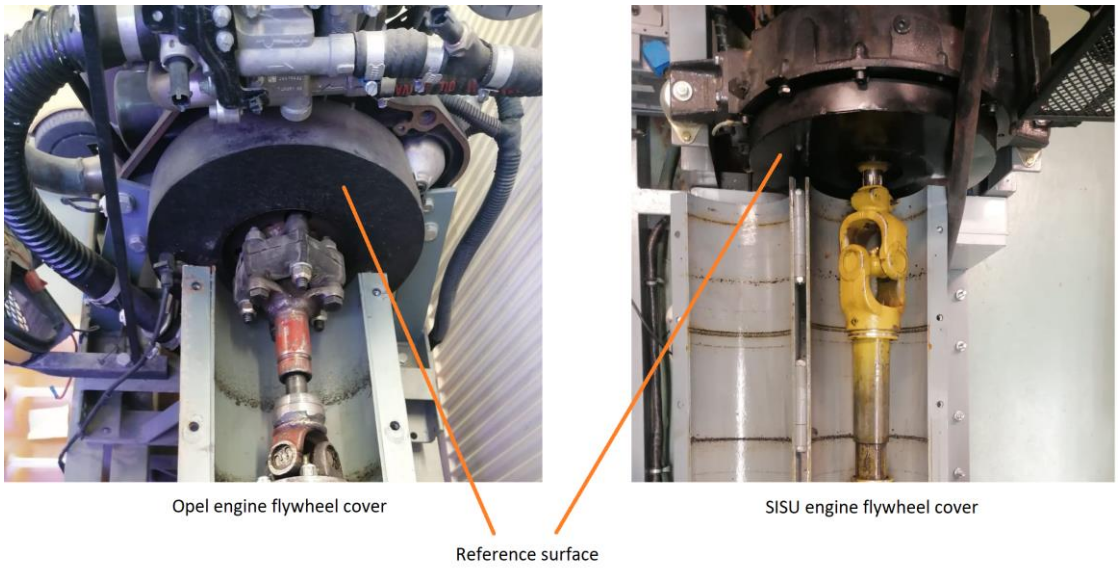

Figure 49: Identification of the reference to define the longitudinal position of both engines in the engine bed. The reference surface is the cover of the flywheel of both engines. Source (Author's own)

The motivation for doing so is that the Cardan shaft allows a certain margin as it can be extended longitudinally, in this way, the SISU engine position is determined. Now it is required to identify at what distance (longitudinally) will the different elements (pipes and mountings) be after this. Figure 50 shows in form of shading the parts that require space, in orange, the exact position where both engine flywheel covers will be placed are determined, as it can be seen, the Opel engine assembly starts a little before this, in this way, the distances are set since there.

Figure 51 shows where the SISU engine will be placed (Focusing on where its mountings will be placed longitudinally concerning the engine bed) and in this way, the position of the required pieces for it is determined.

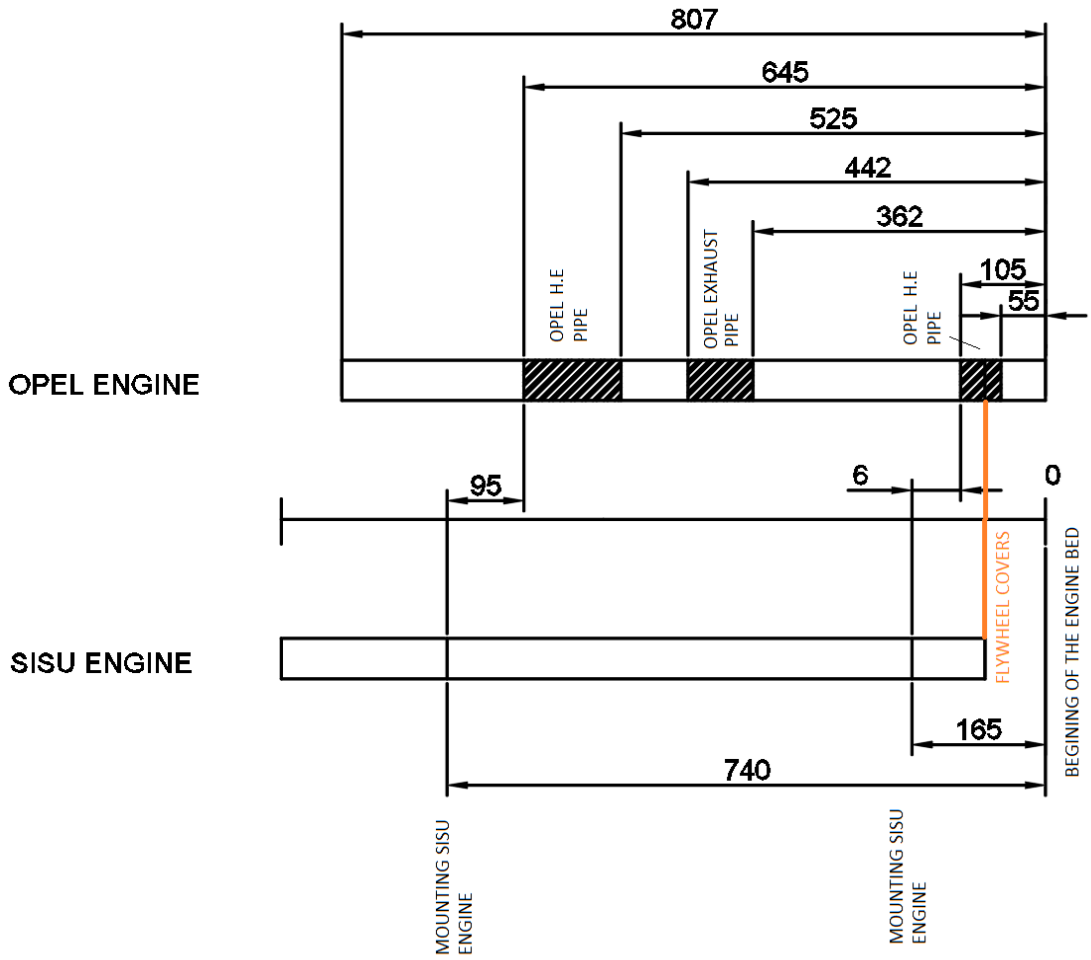

Figure 50: Identification of the longitudinal position of the different elements of interest in the section (Opel heat exchanger H.E pipes and also Opel's exhaust pipe). The graphs show in form of a line which regions are occupied by the different elements of the Opel engine. Also, the SISU engine mountings centre is identified. Source (Author's own)

The most important information that the figure above gives is the space available for suiting the pieces required for the SISU engine. As it can be seen, the room available for the mounting on the left is 95mm and for the one on the right 6mm. This is a problem as more space is required for suiting them (Introduced below in this section, a minimum value of 85mm), in this way, the solution will be designing the pieces such in a way that they can be removed in the case that the Opel engine has to be tested and then, relocated again when the SISU engine would be required to test.

7.1.3.2 Design of the pieces required to test the SISU engine

This section of the report will focus on the design of two pieces that will allow the SISU engine to be placed in the same engine bed but at the same time, give room for the Opel engine's pipes. The proposed solution is going to focus on keeping the rigidity of the setup while being as much simple as possible. Now, omitting the part from the setup that is going to be replaced, see Figure 51.

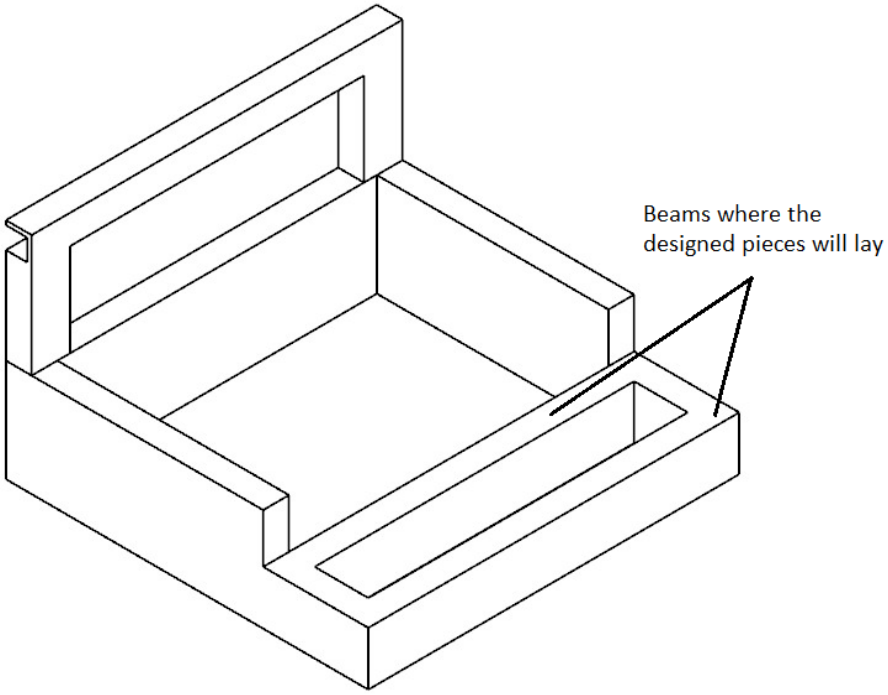

Figure 51: Engine bed removing the right side of the structure (identified in Figure 46). As it will be required below, it is identified where the designed pieces will be attached. Source (Author's own)

The idea is to use the current two beams from the base of the engine bed as the base for these pieces.

This would be used to design an iron plate where said pieces will be placed. After that, the pieces will be beams with a rectangular section that could suit the mountings for the SISU engine, and finally, to hold the engine, these will add another iron plate at the top as a way to cover the space. Figure 52 shows the three elements that will make up the pieces. Beforehand it should be noted that all the thicknesses of the different elements will be 10mm.

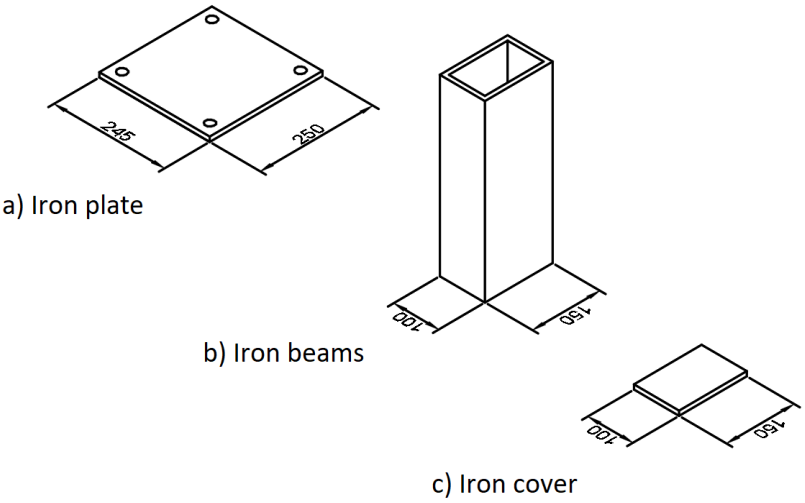

Figure 52: Elements that will form the pieces used for keeping the height of the SISU engine in the engine bed. Measures are indicated in mm (The justification of these values is introduced below). Source (Author's own)

Finally, after introducing the solution, it is required to dimension said pieces. Starting with the iron base, referred to as a) in Figure 52, its section will have to cover the distance between the two beams from the engine's bed base, see Figure 51, in this way, they will require to have a length of 305mm. As for the width, the limiting aspect is the position concerning the engine bed, as introduced in Figure 50, the mountings for the SISU engine are placed at a distance of 85 and 150mm from both ends, thus, if the base is going to be aligned with the centre of both mountings, it cannot surpass a total value of 170mm. The result of merging the three elements is shown in Figure 53.

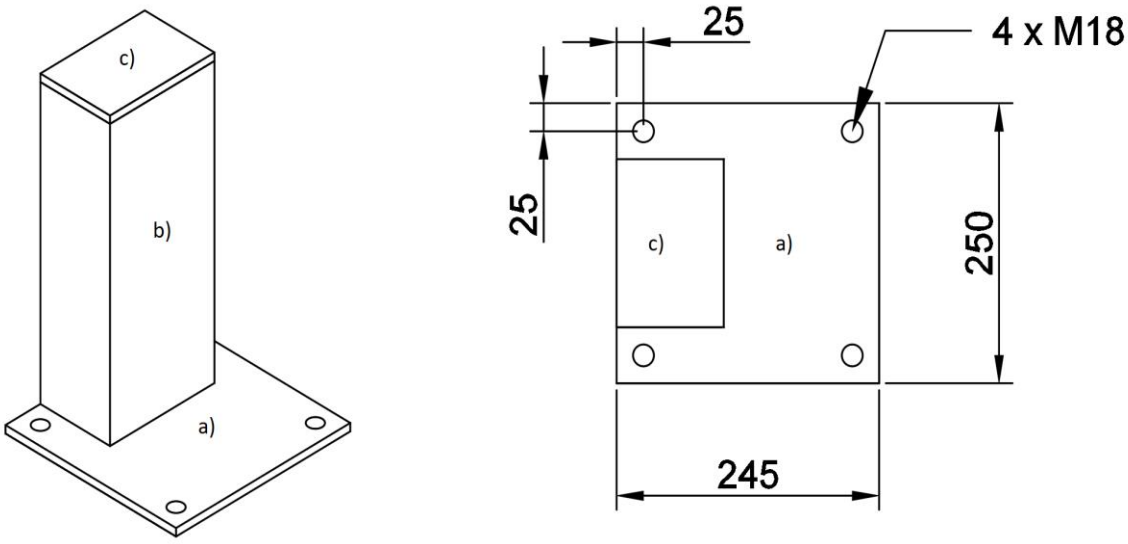

Figure 53: Assembly of the three parts introduced in Figure 52 that will be used for the SISU engine. In the top view, it is specified the positioning of the pieces, the shredded holes, and their dimension. Source (Author's own)

Here, the beam used to raise the vertical position of the SISU engine will have a section that suits the mountings, see Appendix IX, which requires at least a section of 136mm in length and 96mm in terms of width. In this way, the section will be 150mm long and 100mm wide. Regarding the height, the engine has to be at a level l_{eng} of 520mm concerning the base, considering the thickness, of the iron plates, and the beams of the structures that have a section of 124mm in height, the required length of the beamsl_{beams} will be:

$$l_{beams} = l_{eng} - 2e - h_{beams} = 520 - 20 - 124 = 376mm$$

As the last part of the design, the cover of the beams will have the same section. After this, it is known all the dimensions of the pieces, so the only part remaining is adapting the current engine bed for suiting them both.

7.1.3.3 Length adaptation of the engine bed

The available information about the current pieces and the different solutions have led the study to this final stage where the length of the engine bed will have to be modified (There has not been found a better solution that avoids would avoid it). This modification is motivated to suit the designed pieces, which require an iron plate to be attached to the engine bed. Analysing again Figure 50, and focusing on the SISU engine line. The centre of the mounting is placed at 740mm from the beginning of the engine bed, thus, if it is going to be centred with the designed assembly, the length of the engine

bed for suiting said the assembly will require to have 125mm plus the said 740mm, in this way, the total length of the engine bed will be 865mm, all this is shown Figure 54.

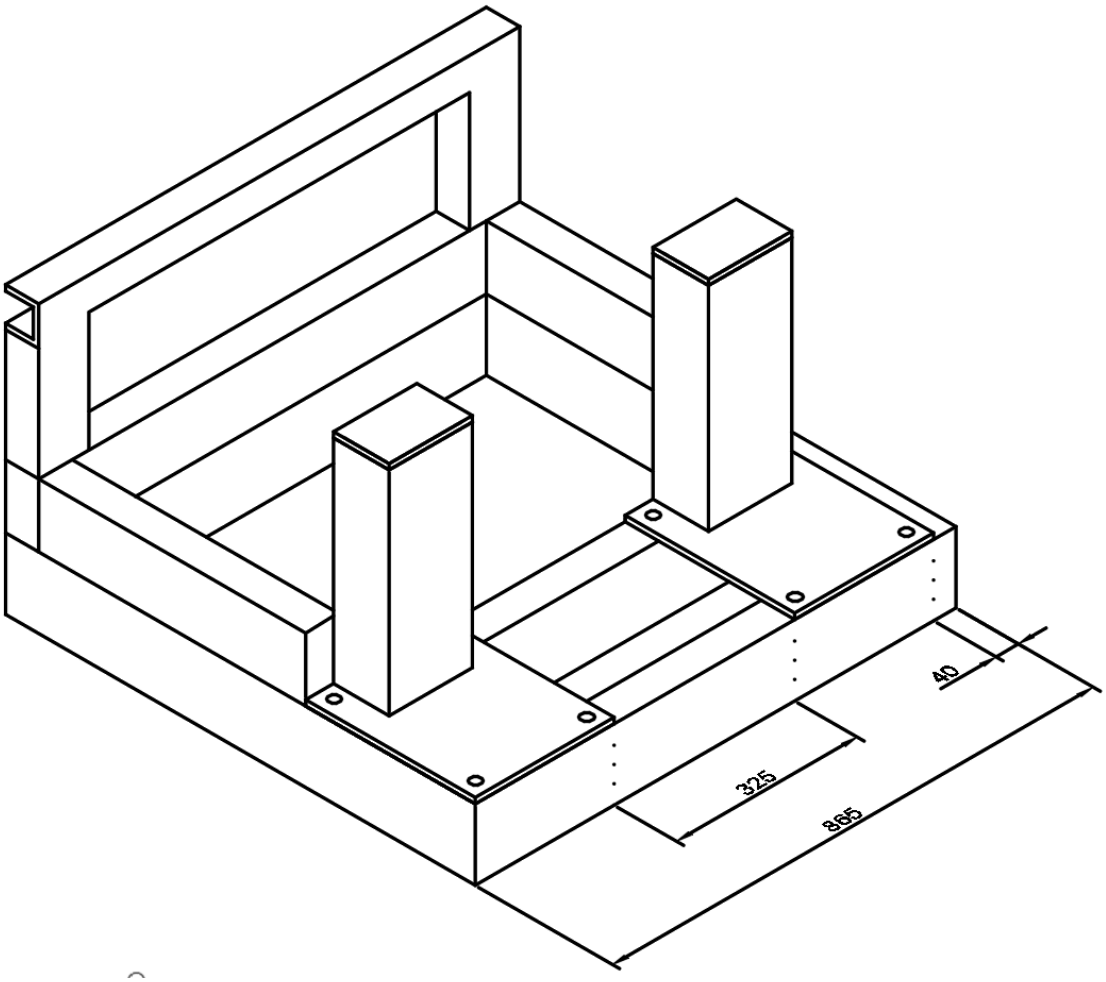

Figure 54: Engine bed with the designed pieces located. It is specified the distance to one of the sides and also the separation between each one. Source (Author's own)

After this adaptation, as was introduced in section 7.1.2, the length of the Opel engine beams (used to raise it) will be the same as the engine bed to allow them to lay on the pieces marked in yellow in Figure 46, thus, the length is going to be 865mm. Finally, the only required modification for the engine bed is the adaptation of the heat exchanger.

7.1.4 Heat exchanger

This required adaptation is related to the previous one as two of the pipes that come out from the Opel engine, shown in Figure 48, are entering the heat exchanger.

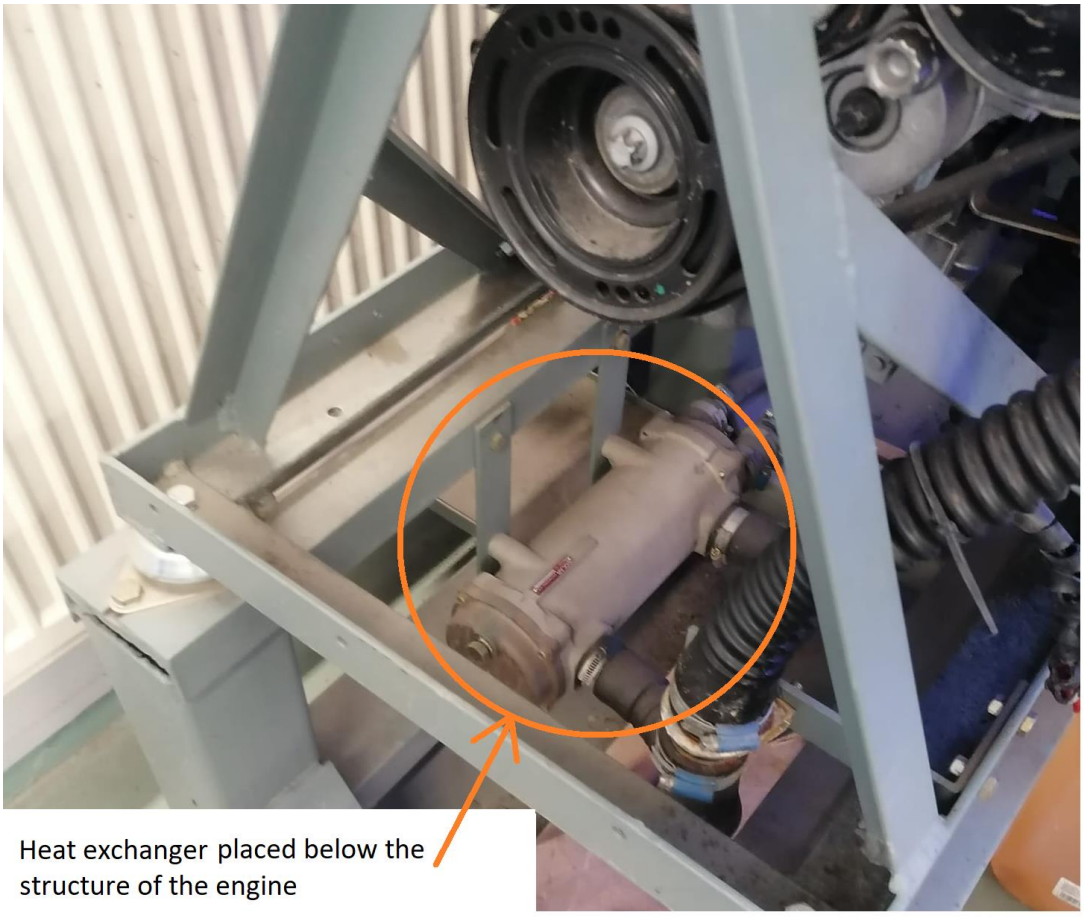

Figure 55: Heat exchanger of the Opel engine. Source (Author's own)

In this case, the solutions presented will have to be related to how all the modifications have reached this point. Thus, as it has been tried to keep the pipes from the heat exchanger with no modifications (that is why the engine bed has changed on its right side of the structure as shown in Figure 51) the best idea would be to keep the heat exchanger in the same relative position to the Opel engine structure once it would be placed on the engine bed for testing.

As seen in Figure 55, the heat exchanger is placed behind the structure that contains the Opel engine, specifically attached to the base where said structure lays. In this way, if this disposition has to be kept, the idea is to attach now the heat exchanger to the beams that will be used to raise the position of the Opel engine (see Figure 56).

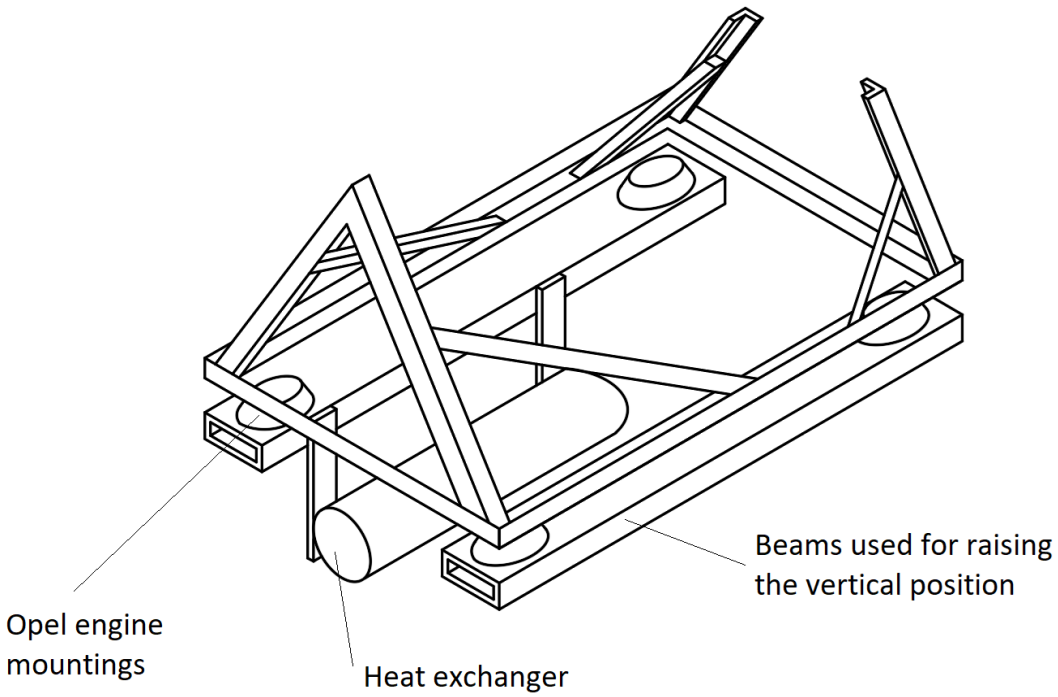

Figure 56: Adaptation of the heat exchanger to the beams used for raising the vertical position of the Opel engine. Source (Author's own)

Thus, checking if there is room for placing the heat exchanger behind the engine, placing it the beams that will be used for the Opel engine the same way it is now placed on the base that will be removed from, the available room behind h_b in the function of the vertical distance from the axis of the Opel's engine output shaft h_{axis}, the space occupied by the heat exchanger behind the structure $h_{H.E}$, and the space left between the base of the engine bed and the floor h_f will be:

$$h_b = h_{axis} - h_{H.E} + h_f = 580 - 300 - 250 + 80 = 110mm$$

The previous calculation shows that keeping the heat exchanger in the same relative position to the engine but now attached to the new beams would be 110mm above the floor.

All the detailed information about the new solutions will be shown in Appendix Appendix XV and Appendix XVII. To verify that the structure will hold all the forces, a simulation in NX is required.

7.2 Adaptation for the dynamometer

As said before, the height of the output shaft of the engine is 580mm from the basement. However, the height of the dynamometer needs to be kept in mind, as a lot of difference between the height of the dynamometer input and the output shaft could lead to a critical failure of the shaft.

It can be seen in ANNEX LANMEC, that the height of the input of the dynamometer (h_{input}) is 475mm. Thus, the difference in heights between the dynamometer and the engine is described in the next equation:

$$\Delta_h = h_{input} + h_{beams} - h_{axis} = 475 + 124 - 580 = 19mm$$

This difference in heights would be a problem in the case of having a rigid coupling, however, in the case of having a flexible coupling and a Cardan shaft, the setup allows certain misalignment.

Besides the height, another problem is the width of the dynamometer. The current testbed is 845mm wide and looking at the specs of the dynamometer it's seen that the total wide of the device is 935mm. However, this is not a problem, as the bolts of the dynamometer are located at 360mm from the centre of the dynamometer. Knowing that the dynamometer will be centred on the structure, the bolts will lie inside the structure.

Also, the length is another issue of the dynamometer. The bolts are separated 430mm from one another, and as seen in Appendix XVI, the beams are separated 720mm. To solve this problem two beams can be put as shown in Figure 58. The reason why the first beam is not used is that the input of the dynamometer is at 135mm from the bolts, and if the input of the dynamometer is wanted to be in the same position as it is currently, the dynamometer must go back.

Similar to what happened in Section 6.3.3, an adapter is needed. This is because, as it can be seen in Appendix VI, the bolts of the input to the dynamometer are in a diameter of 130mm, however, the Cardan shaft output has the bolts in a diameter of 170mm, therefore an adapter is needed. The following figure shows the design of the adapter:

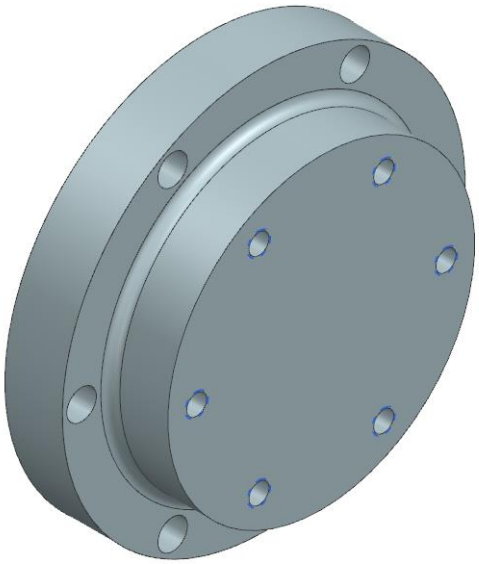

Figure 57: The adapter from the Cardan shaft to the dynamometer. Source (Author's own)

It can be seen in Figure 57 that the holes are differently sized. This is because the Cardans' shaft holes are M18, and the holes in the dynamometer are 10.5mm. The sizing of the adapter can be seen in Appendix XIV.

7.2.1 Simulation in NX

Following the previous considerations, the solution is 3D modelled in NX. The solution is shown in the next figure.

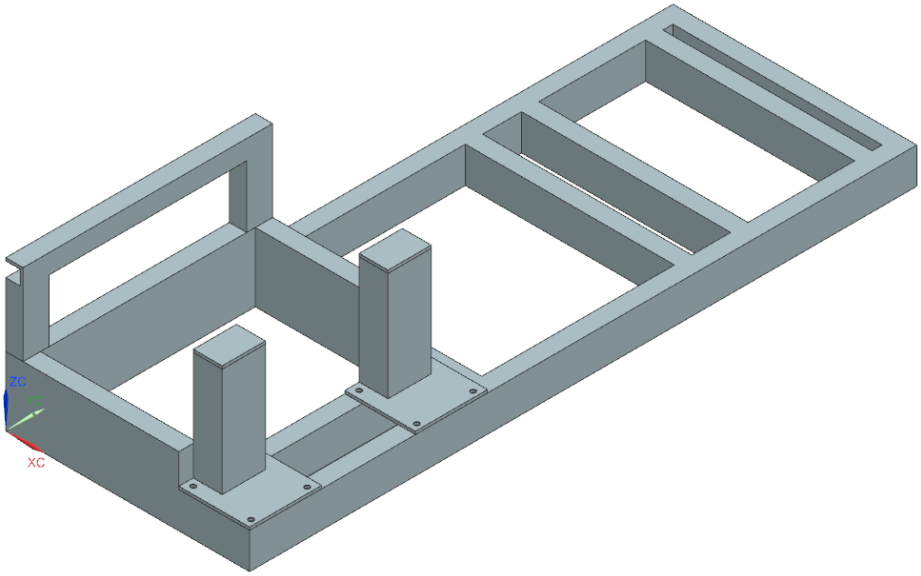

Figure 58: Isometric view of the new testbed. Source (Author's own)

The measurements of the new testbed are shown in Appendix XVII, as well as the measurements of the detailed pieces are in Appendix XV.

To see if the structure will hold when placing the engines, a structural analysis must be carried on. To do this, the program NX has a feature that does the simulation and calculates the displacement of the structure. By putting the constraints and the forces that will act on the structure, the software gives the results. The forces applied to the structure are shown in the next figure.

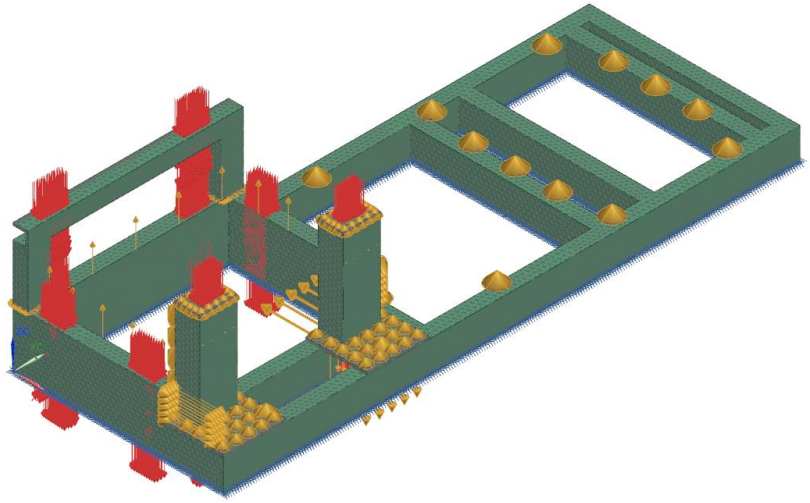

Figure 59: Forces applied to the structure. Source (Author's own)

It can be seen in Figure 59 the forces applied to the structure. The red arrows indicate the load of the engines, the ones which are in the beams and on the side is where the SISU engine lies, thus the load applied is the load of the engine. The other red arrows which are in the main structure, are loads of the Opel engine. The orange arrows appearing in the structure indicate the reactive forces between the components of the assembly.

It is noted that in Figure 59 appear all the loads at the same time, which in reality would not be possible, as both engines would not be placed at the same time. However, the simulations were done one by one, meaning that the figure is indicative.

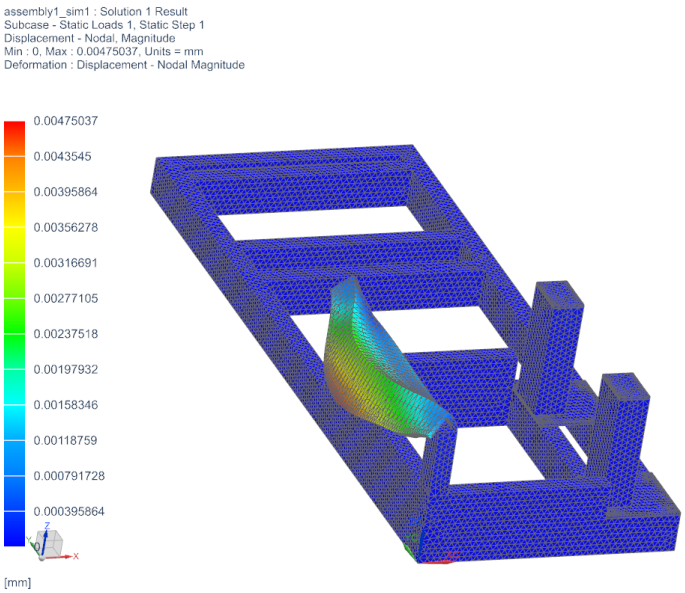

Figure 60: Displacement simulation when placing the engines in NX. Source (Author's own)

It can be seen in Figure 60 that the displacement of the structure is shown in colours, where red is the most displaced part, and blue is the least. It can be seen that the part that gets displaced the most is the left beam. Although it might seem that the displacement is unacceptable, the most displaced part is 0.004mm, which can be considered acceptable in this case. Also, the more deformed part is the part that has not been modified, so this will not cause any problem

The next figure shows the front view of the simulation.

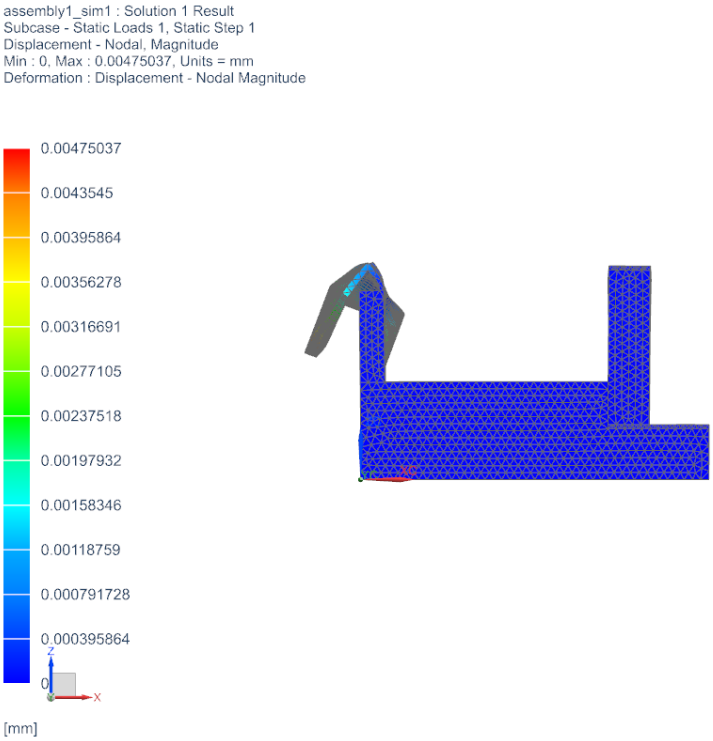

Figure 61: Front view of the deformation when placing the engines simulation in NX. Source (Author's own)

In Figure 61 can be seen that the beams that were added in the new version of the testbed get a bit tilted. However, the displacement of these beams is less than 0.0003mm, which compared to the already existing part, is almost neglectable.

These simulations are not 100% accurate and might have some variations in reality, as NX creates an idealized part of the assembly. Moreover, the test conditions are ideal and there are no temperature variations which is not true (as the engine runs faster more heat is produced). Also, the vibrations of the engine were not considered in these tests. However, they give a first approximation of what should the installers expect when placing the engines in their place.

In the previously shown figures, the Opel engine weight is also added. However, because it is located in a very stable zone (this being the base), it does not get deformed.

8 Results

Throughout the project, every section that occupied our study presents the results that have been obtained with its corresponding justification and discussion. However, in this chapter, a final analysis to put in perspective the outcome of the work will be presented.

Following the order in which the project was developed, the first result comes with the study and the selection of the dynamometer. After checking the current working conditions of the available (referred to as water brake while analysed), it has been verified how the issues with its performance highlighted before starting the project were a limitation for braking the engine at low speeds. Specifically, after transferring the data provided by the manufacturer of the current dynamometer and also the curves of torque and power of the engine, it has been observed that below 1500rpm, the torque produced by the engine is 502.93Nm, a value that surpasses the torque offered by the dynamometer at that speed. In this way, it is verified how below this value, the water brake is not offering proper testing conditions. Following, the next step was to search for a dynamometer that could work with both engines at the same time, principally, a model that could work with the high torque of the SISU engine and the high speed of the Opel engine. In this case, two different options were presented, firstly the model DW250 from Jiangsu Lanmec, and after it, the model DE200 from Taylordyno. Focusing on the DW250 (the alternative that has been selected with the back of a matrix of decisions using the following selection criteria: Budget, normal working conditions, workload, over-dimensioning, infrastructure adaptation and company customer service), it was checked how the principal requirements were met. Specifically, in the most unfavourable point (1000rpm), this dynamometer would be able to brake the SISU engine offering 550Nm against the 491.79Nm required. In this way, approximately, it would be working a 10% below his maximum working conditions. Thus, when the speed would increase, this margin would be increased in the rest of the range of speeds for the tests. Having said that, the indicative cost to purchase this equipment is currently 17500€ with an expected delivery time between 40 and 50 labour days.

Having found a feasible solution for the first stage of the project, the following part to analyse the obtained results refers the selection of the mountings. As done before, the same process has been followed, trying to keep material in case it was possible, the current working conditions have been checked in first place. It is important to highlight that each engine had his own mountings before the project was started. As for the SISU engine, the tests carried out on it advanced that at low speeds, the level of isolation was poor. After analysing it numerically with the back of the diagrams provided by the manufacturer, it has been verified how at the interfering frequency corresponding to the idle speed, 16.67Hz and 1000rpm, respectively, the level of isolation provided by the equipped mountings (RA100/M16 40 deg IRH) falls inside of the resonance zone, not offering any degree of isolation of the existing vibrations. Focusing on the Opel engine, even if there was not any indicative of this issue, with the back of the diagrams provided

by the manufacturer, it has been verified how the problem is with its mountings (RA125 EMA) is even bigger as the interfering frequency at idle speed, 12.83Hz at 770rpm, respectively, it falls deeper into the resonance zone. After these verifications, the process to follow was the same done with the dynamometer, finding alternatives that could improve the conditions of the tests. In this case, two alternatives were presented too, the first one, working with the same mountings for both engines and adapting the Opel engine interfering frequency to a value that made it possible, and the second one, based on finding a feasible model of mountings for each engine. However, after defining a matrix of decisions based on the following selection criteria: Price of the mountings, degree of isolation provided at idle speed, static deflection and modularity. It was observed that to make the first alternative feasible, the idle speed of the Opel engine needed to be modified from the current value of 770rpm to a higher value of 1000rpm. Presenting in this case an interfering frequency of 16.67Hz that would fall out of the resonance zone for the natural frequency associated with its vibrating behaviour (11.18Hz). In this way, even if it was possible, the fact of modifying the specifications of the Opel engine was a factor to avoid. For this reason, the second alternative has been selected, the results regarding it are using the Vulkan mountings VD 3 for the SISU engine, which will provide a level of isolation of the 70% at idle speed with a natural frequency of 7.91Hz. As for the Opel engine, the level of isolation at the idle speed that has been accomplished is a little worse, close to the 50% at a natural frequency of 7Hz approximately. For the presented solutions, it has not been found the exact price for each as we were not provided with its final price by the supplier, however, researching the market for similar models has allowed estimating a price of 150€ for each mounting of the SISU engine and 80€ in the case of the Opel, what means that the total amount for these solutions would be 920€. Regarding the shipping time, as these products are easier to acquire, 10 to 20 labour days would be required.

The next result comes with the flexible coupling. First, a study if the coupling used in the current setup could be used for both engines was done. After discussing that the coupling could not be used for both engines, a new coupling has been searched. In this case, only one coupling that could fit both engines was found, so a decision matrix was not needed. The final option was CENTAX-TEST, more specifically the model CX-15. This flexible coupling is based on a highly flexible rubber element which according to CENTAX, having a shore hardness of 50 can go up to 8000rpm, a value that surpasses the maximum rpm value that could be obtained from the Opel engine (6500rpm) and the nominal torque is 520Nm which is higher than the SISU engine maximum torque (510Nm). When using this rubber coupling it has been calculated that the critical frequency of the shaft is 524.89cpm when using the SISU engine, which corresponds with a critical speed of 262.45rpm, and a critical frequency of 488.1cpm when using the Opel engine, which in this case corresponds to 244.05rpm. These speeds are lower than the idle speeds of the engine, so it would be not a problem for the stability of the shaft, however, there would be no problem either if the critical speed would lie between the

idle speed and the minimum full-load speed. Having said that, the indicative cost to purchase this equipment is approximately 3750€ with an expected delivery time between 30 and 60 labour days.

The final result comes with the redesign of the testbed, where the main objective was to keep as much material as possible and be able to fit both engines. The main idea of the redesign is to keep the stand where the Opel engine is currently placed and put this stand in the SISU testbed. To do this, the structure had to be enlarged. Currently, the structure where the engine lies is 740mm and in the new setup, it is 855mm long. The width of the structure does not need to be modified, so it will remain 845mm. The new version of the testbed will keep one of the sides that it has (where the SISU engine lies in the current setup), and the other side will be replaced with two assemblies of two beams which will be bolted to the main structure. It is done this way because the Opel engine is wider and the heat exchanger has tubes that connect to the engine where the beams are. The dimensions of the new assemblies are seen in previous chapters as well as in the appendices.

Still analysing the structure of the whole setup, focusing on the part used for the dynamometer, some modifications have been proposed. In this case, two beams where the new dynamometer will be bolted have been added in order to maintain the dynamometer intake distance to the engine output. These two beams will support the structure and will be bolted to the dynamometer. Moreover, the dynamometer intake has bolts at a diameter of 130mm, whereas the Cardan shaft has them at 170mm, to solve this an adapter has been designed.

After analysing all the results from the different sections of the project, the final stage regards the simulation of how the structure will hold the weight of the engine. As the SISU engine is the heavier one, the study has focused on doing the simulations with it as it will be the less favourable case. To check that, the resulting setup was built in Siemens NX and structure analysis was carried on. This analysis verified that the proposed solution is feasible, showing how the part that would suffer the most in terms of deformation refers to the section of the engine bed that has not been replaced by the designed pieces. Focusing on the values, the deformations are not going over 0.004mm which for our structure is completely acceptable. Focusing now on said pieces, the situation is even better, it is known that the sections used for the beams that will form them are quite over-dimensioned but it is thought that it was the most simple solution. Having said that, the existing deformation in this part is 0.0003mm in the worst case, which verifies that the solution is completely secure and feasible. In the same way, checking the behaviour of the part of the structure that will be used for holding the Opel engine weight has shown how the solution avoids any deformations. For the proposed solutions in terms of structure and modifications of the engine bed and setup, an orientation budget checking the price of the meter of iron beams in the market, according to (WestcountryFabricationLtd, 2022), 550€ would be required

approximately. In this way, considering the price required for all the modifications and alternatives to the current engine laboratory, the total price for completing the project is 22720€. Although the values are not exact and the final price may vary, it gives an approximation to see that there is still a margin until the proposed budget of 30000€.

9 Discussion

With respect to the initial aims and objectives

To meet the aim of the project three objectives were established. The first and second proposed objectives were to analyse the existing dynamometers and their feasible alternatives existing in the market according to a budget. These objectives were greatly accomplished, as the found dynamometer accomplishes the specifications of both engines and the cost do not exceed the budget and there is still a budget left for other components.

With respect to the third objective, it was partially accomplished, as new mountings and couplings were found. Unfortunately, the providers of the information did not give the price of the materials, so in this case, it cannot be said that the objective was completely accomplished, but it is known that the project is still within budget thanks to the current margin.

Concerning the last objective, the design found could fit both engines separately and it is a reasonable design modifying the current testbed. It was designed in this way to not waste a lot of money or materials. After doing the simulations in NX it is seen that the structure gets deformed in the part that is already existing, so the deformations are allowable in this case, also, the maximum deformation does not exceed 0.003mm, so it is acceptable.

With respect to other published work

Comparing the work to other work published, this research had to deal with the fact that all the material in the current setup is old, which makes it hard to find information. This work also uses the same testbed, dynamometer, coupling and mountings for two different engines, one being diesel-fuelled and the other one being gasoline fuelled, while other works study the only one engine test facility.

Other work also is more specific about their work, focusing on just one part of the test facility. However, this work is more practical and does not focus only on one part but on all the aspects of the engine test setup.

For comparison, the indicative purchase cost of a new engine testbed ranges from 75000€ according to (Lanmec, 2022) to 125000€ from supplies (Machineseeker, 2015). These more modern installations are significantly more expensive than adapting the current engine testbed, also it is unknown if they could fit two different sized engines at the same time. However, they would enable the Novia team to get more information about the engines. This would be for the Novia laboratory team to decide.

With respect to the limitations of the work

There have been found some limitations to the existing documentation, as said before, the current setup is old, so the documentation about the engines and the Cardan shaft

was not so easy to find. Also, the fact of working with large multinationals makes communication a lot harder than with small companies.

Another limitation comes with the building of the pieces and the simulations in the program NX. The measures taken in the engine lab are not exact because the measurement instruments were not ideal, also the measures were taken from an assembly, while in an ideal case the pieces would need to be measured one by one separately with the correct instrument. This means that the tolerances of the pieces are unknown. Also, the simulations as it is said in Section 7.2.1, are an approximation, the pieces are idealized and so are the conditions of the simulation.

With respect to consistencies and inconsistencies

Focusing now on the consistencies and inconsistencies of the project, the research has achieved a valid concept of a testbed with a simple modifying strategy, suitable for both engines considering their characteristics and the testbed simulation shows logical results. However, there are some inconsistencies in the Opel information, the information was very limited and some assumptions about the engine parts had to be made, concretely the flywheel was not possible to measure and different references had to be taken. Another inconsistency comes with the budget, as it is not known if the budget has been exceeded or not.

10 Conclusions

Engine testing is a well-organized and comprehensive way to extract as much information as possible from an engine. Even if the apparition of different simulation software has become an alternative for this, the quality of the results in terms of being close to reality is still one step ahead in the case of real engine testing. For this reason, Novia UAS owns a very valuable facility for introducing to students this way of picking information. In that respect, it has been found that it is worthwhile for the university to improve the quality of the tests that can be carried out, motivating to conduct the research of the project to find an appropriate solution among the whole range of possibilities for all the elements that could improve the testing process.

The current setup has some limitations, according to the testing that has been done, below 1500rpm, the torque produced by the engine is 502.93Nm, which is higher than the dynamometer torque at that rpm, meaning that a new dynamometer is needed. The selected dynamometer is Lanmec DW250 and works at high speeds, surpassing the maximum rpm of the Opel engine (6500rpm) and at the same time offers the required torque for braking the SISU engine at its most unfavourable point (1000rpm), 550Nm against the 491.79Nm required. The cost of the new dynamometer is 17500€.

For the mountings, both engines currently present issues with isolating vibrations at idle speeds. The current used models are RA125 EMA and RA100/M16 40 deg IRH for the SISU engine and the Opel engine, respectively. The methodology used for finding a feasible option is based in finding the lowest required natural frequency (11Hz for the SISU engine and 9Hz for the Opel engine) once the interfering frequency is determined for each engine. Reached this point, the study has focused in finding alternatives to cover the requirements. Two feasible options have been presented, the first one tries to work with just one model of mountings (Vulkan mountings VD 3) that suits both engines in the case that the idle speed of the Opel engine is set at 1000rpm. However, the chosen alternative is focused on satisfying the performance of both engines without modifications on them. Thus, two models of mountings will be used, starting with the SISU engine, as introduced before, the selected model is VD 3 from Vulkan mountings, which provides a level of isolation of the 70% at idle speed. Regarding the Opel engine, the used model is M100 40 from Vulkan mountings, which provide a level of isolation of the 50% at idle speed. The estimated cost is 920€. l

The coupling that is currently installed in the setup is the CENTAX-V 35. This coupling works for the SISU engine, but because of its size, it would not work for the Opel engine, in the case of study, the SISU engine has a flywheel SAE size of 11 ½ and the Opel an SAE size of 7 ½. The substitute for the coupling is one of the same brands named CENTAX-TEST, which can be used for both engines. According to the calculations done, the resonant speed when using the SISU engine is 262.45rpm, which is lower than the idle speed of the engine, so it would not matter while operating. For the Opel engine, the critical speed is 244.05rpm, being also below the idle speed of the engine, meaning that

there is no problem while operating. An adapter needs to be designed, as the diameter of the bolted part of the coupling is different from the cardan shaft. The cost of the coupling is expected to be around 3750€.

The suggested redesign of the testbed allows both Opel and SISU engines to be placed in the stand, the main idea was to keep as much material as possible. The design is enlarged from 740mm to 855mm to fit the Opel engine. The width of the structure will remain 845mm. The new version of the stand will keep one of its sides (where the SISU engine is placed in the current setup), while the other will be replaced with two assemblies of two beams which will be bolted to the main structure. The part where the dynamometer lies is also modified, two beams where the dynamometer is bolted have been added to maintain the dynamometer intake distance to the engine output. Also, an adapter needs to be designed, as the diameter of the bolts is different for the cardan and the dynamometer intake. The new dimensioning of the engine bed has been verified with a simulation with NX, where it is shown that the new designed pieces and the current structure would deform, in the worst case, 0.0003mm and 0.004 mm, respectively. Approximately 550€ would be required for the proposed solution.

The final price of the proposed solution would be 22720€ which is under the proposed budget of 30000€.

11 References

7zap.com. (2022). *ENGINE ASSEMBLY (EXCHANGE) [FOR VAUXHALL] OPEL ASTRA-G + ZAFIRA-A*. [online] Available at: https://opel.7zap.com/en/car/t98/e/7/4-2/ [Accessed 10 Apr. 2022].

ATA (2018). *ATA - Modular Flow Management*. [online] ATA - Modular Flow Management. Available at: https://advancedta.com/blog/tp [Accessed 14 Mar. 2022].

Atkins, R. D. (2009). *An Introduction to Engine Testing and Development*. https://library.poltekpel-sby.ac.id/apps/uploaded_files/temporary/DigitalCollection/ODIyNjEyYmUyZWIyODRmY2ZhYmZiN2I0NTQxMWEyMGM0YjY3NjdmMA==.pdf

AURM441976B Test engines using a dynamometer Release: 1. (n.d.). [online] Available at: https://training.gov.au/TrainingComponentFiles/AUR05/AURM441976B_R1.pdf.

Auto-data.net. (2022). *1998 Opel Astra G Classic 1.6 Ecotec 16V (101 Hp) | Technical specs, data, fuel consumption, Dimensions*. [online] Available at: https://www.auto-data.net/en/opel-astra-g-classic-1.6-ecotec-16v-101hp-2395 [Accessed 10 Apr. 2022].

AZoM (2019). *How Eddy Current Brakes Work*. [online] AZoM.com. Available at: https://www.azom.com/article.aspx?ArticleID=18334 [Accessed 31 Jan. 2022].

Bartech Propulsion. (2022). *Couplings For Propulsion Systems | Geislinger UK Dealer*. [online] Available at: https://bartechpropulsion.com/service/couplings/ [Accessed 28 Mar. 2022].

Cardanshaftsindia.com. (2015). [online] Available at: https://Cardanshaftsindia.com/ [Accessed 28 Mar. 2022].

Coxon (2011). *The eddy-current dyno*. [online] High Power Media. Available at: https://www.highpowermedia.com/Archive/the-eddy-current-dyno [Accessed 28 Mar. 2022].

D.J.Dunn. (n.d.). *SOLID MECHANICS DYNAMICS TUTORIAL – FORCED VIBRATIONS*. [online] Available at: http://www.freestudy.co.uk/dynamics/forced%20vibrations.pdf.

Dspmindustria.it. (2021). *DSPM Industria-Sensori e Trasduttori*. [online] Available at: https://www.dspmindustria.it/img/cms/Smart_Working/bhb.pdf [Accessed 4 Feb. 2022].

DYNOmite Dynamometer. (2020). *DYNOmite Animated How-Water-Brakes-Work MAX Tutorial - DYNOmite Dynamometer*. [online] Available at: https://dynomitedyno.com/videos/dynomite-animated-how-water-brakes-work-max-tutorial/ [Accessed 6 Apr. 2022].

Fahad. (2015). *Water Brake Absorbing Dynamometer*. [online] Available at: https://es.scribd.com/document/251640992/Water-Brake-Absorbing-Dynamometer [Accessed 30 Jan. 2022].

ForceBwU (2021). *Oil Shear Technology - Force Control Clutches & Brakes with Oil Shear Technology*. [online] Force Control Clutches & Brakes with Oil Shear Technology. Available at: https://www.forcecontrol.com/the-iron-and-steel-technology-conference-expo/oil-shear-technology/ [Accessed 6 Feb. 2022].

ForceBwU (2021). *Oil Shear Technology - Force Control Clutches & Brakes with Oil Shear Technology*. [online] Force Control Clutches & Brakes with Oil Shear Technology. Available at: https://www.forcecontrol.com/home/oil-shear-technology/ [Accessed 4 May 2022].

Freestudy.co.uk. (2022). *Untitled 1*. [online] Available at: http://www.freestudy.co.uk/ [Accessed 6 May 2022].

Fuller, D. (2012). *OnAllCylinders*. [online] OnAllCylinders. Available at: https://www.onallcylinders.com/2012/05/11/dyno-duel-engine-vs-chassis-dynos-what-you-should-know/ [Accessed 30 Jan. 2022].

Globalspec.com. (2022). *Oil Shear Brakes Preventing Downtime from Force Control Industries, Inc.* [online] Available at: https://www.globalspec.com/FeaturedProducts/Detail/ForceControlIndustries/Oil_Shear_Brakes_Preventing_Downtime/324702/0 [Accessed 4 May 2022].

Gomog.com. (2022). *engine weights*. [online] Available at: https://www.gomog.com/allmorgan/engineweights.html#engine [Accessed 4 May 2022].

Grobbelaar, E., Richard, M. and Haines, W. (2017). The Development of a Small Diesel Engine Test Bench Employing an Electric Dynamometer. [online] Available at: https://core.ac.uk/download/pdf/188223699.pdf.

Hasnun, M. and Bin, A. (n.d.). *DESIGN OF A DYNAMOMETER-ENGINE COUPLING SHAFT IN PARTIAL FULFILMENT OF THE REQUIREMENTS FOR THE DEGREE OF MASTER OF ENGINEERING FACULTY OF ENGINEERING UNIVERSITY OF MALAYA KUALA LUMPUR 2012*. [online] Available at: http://umpir.ump.edu.my/id/eprint/3587/1/MOHD_HASNUN_ARIF_BIN_HASSAN_u.PDF [Accessed 27 Mar. 2022].

Hindawi.com. (2013). *Figure 9 | MR- and ER-Based Semiactive Engine Mounts: A Review*. [online] Available at: https://www.hindawi.com/journals/smr/2013/831017/fig9/ [Accessed 15 Mar. 2022].

Killedar, J.S. 2012. *Dynamometer - Theory and Application to Engine Testing*. USA: Xlibris. ISBN 978-1-4771-2006-4.

KRemington (2021). *Motor brakes work on oil shear*. [online] Windpower Engineering & Development. Available at: https://www.windpowerengineering.com/motor-brakes-work-on-oil-shear/ [Accessed 6 Feb. 2022].

Lanmec (2022). *DW series eddy current dynamometer-Lanmec magnetic powder clutch, torque speed sensor, magnetic powder brake, eddy current brake*. [online] Available at: https://www.lanmec.com/enPhoto_Show.asp?InfoId=230&ClassId=41&Topid=0 [Accessed 10 May 2022].

Lee, Y.H., Kim, J-s., Kim, K.J., Ahn, T., Choi, B-I., Lee, H.J., Woo, C.-S. . and Kim, K.-S. . (2013). Prediction of dynamic stiffness on rubber components considering preloads. *Materialwissenschaft und Werkstofftechnik*, [online] 44(5), pp.372–379. Available at: https://onlinelibrary.wiley.com/doi/abs/10.1002/mawe. [Accessed 15 Apr. 2022].

Ling, S.J., Moebs, W. and Sanny, J. (2016). *Eddy Currents*. [online] Opentextbc.ca. Available at: https://opentextbc.ca/universityphysicsv2openstax/chapter/eddy-currents/ [Accessed 31 Jan. 2022].

M. Vetr, T. Passenbrunner, H. Trogmann, Ortner, P., Kokal, H., Schmidt, M. and M. Paulweber (2017). Control oriented modeling of a water brake dynamometer. [online] undefined. Available at: https://www.semanticscholar.org/paper/Control-oriented-modeling-of-a-water-brake-Vetr-Passenbrunner/c258a004dbbd1011853cb6d86219651800e63846 [Accessed 12 Jun. 2022].

Machineseeker. (2015). *▷ Used Highly dynamic engine test bench, 4Q BETADyn / Schenck /ABB for sale - Machineseeker.com*. [online] Available at: https://www.machineseeker.com/betadyn+%2F+schenck+%2Fabb-m/i-7011129 [Accessed 10 May 2022].

MAGCRAFT Brand Rare Earth Magnets. (2015). *What are Eddy Currents?* [online] Available at: https://www.magcraft.com/blog/what-are-eddy-currents [Accessed 27 Mar. 2022].

Martyr, A. and Rogers, D. (2021). *Engine testing : electrical, hybrid, IC engine and power storage testing and test facilities*. [online] Oxford, United Kingdom ; Cambridge, Ma: Butterworth-Heinemann, An Imprint Of Elsevier. Available at: https://www.elsevier.com/books/engine-testing/martyr/978-0-12-821226-4 [Accessed 30 Mar. 2022].

Martyr, A. J., & Plint, M. A. (2007). Engine Testing. *Engine Testing*. https://doi.org/10.1016/B978-0-7506-8439-2.X5000-2

Mechanical Vibrations. Fourth Edition. J. P. Den Hartog. McGraw-Hill, New York, 1956. 67s. 6d. (1957). *The Journal of the Royal Aeronautical Society*, [online] 61(554), pp.139–139. Available at: https://www.cambridge.org/core/journals/aeronautical-journal/article/abs/mechanical-vibrations-fourth-edition-j-p-den-hartog-mcgrawhill-new-york-1956-67s-6d/BF19F602D073D34F8595208182AB6DDA [Accessed 9 Apr. 2022].

MER Equipment. (2014). *Understanding Torsional Vibration*. [online] Available at: https://merequipment.com/understanding-torsional-vibration/ [Accessed 14 Mar. 2022].

Morris, J. (1964). Practical Solution of Torsional Vibration Problems.W. Ker Wilson. Chapman & Hall, London. 1963. 880 pp. Diagrams; tables. 10 guineas. *The Journal of the Royal Aeronautical Society*, [online] 68(639), pp.211–211. Available at: https://www.cambridge.org/core/journals/aeronautical-journal/article/abs/practical-solution-of-torsional-vibration-problemsw-ker-wilson-chapman-hall-london-1963-880-pp-diagrams-tables-10-guineas/A9344D50B3D804C7A5CDD9A8326CA440 [Accessed 9 Apr. 2022].

Opel Astra H 1.6 2004- Z16XEP Car Repair Manual. (n.d.). Retrieved April 20, 2022, from https://www.carrepairdata.com/service/repair/manual/eng/opel/astra_h/1_6/2004-/z16xep/1598/77/

Placid Industries. (2020). *How Magnetic Particle Brakes Work > Placid Industries*. [online] Available at: https://placidindustries.com/engineering-resources/how-magnetic-particle-brakes-work/ [Accessed 4 Feb. 2022].

powderbulksolids.com (2019). *Oil Shear Brakes, Clutches, and Clutch Brakes*. [online] powderbulksolids.com. Available at: https://www.powderbulksolids.com/instrumentation-control/oil-shear-brakes-clutches-and-clutch-brakes [Accessed 6 Feb. 2022].

Power Test Dynamometer. (2022). *What is a Dynamometer?* [online] Available at: https://powertestdyno.com/what-is-a-dyno/ [Accessed 6 May 2022].

Raúl, I. & Maderna, I. (n.d.). *VIBRACIONES MECÁNICAS EN MOTORES DE COMBUSTIÓN INTERNA*. [online] Available at: http://ing.unne.edu.ar/imate/jornadasint/pub/t7.pdf.

Rpmrubberparts.com. (2015). *The Complete Engine Mount Design Guide | RPM Rubber Parts*. [online] Available at: https://www.rpmrubberparts.com/pillar/complete-engine-mount-guide [Accessed 18 Mar. 2022].

Sebastian, M. (2022). *CENTA Power Transmission - International Site - Products - CENTAX-V*. [online] Centa.info. Available at: http://www.centa.info/cx-v [Accessed 27 Apr. 2022].

Sisu Diesel (2022). Retrieved May 10, 2022, from www.sisudiesel.com

Steffka, M. and Trzcinski, D. (2007). Engine Component Effects on Spark-Ignition Caused Radio Frequency Interference (RFI). *SAE Technical Paper Series*. [online] doi:10.4271/2007-01-0360.

Stuska Dyno. (2022). *Stuska Dyno*. [online] Available at: http://www.stuskadyno.com/tech-notes/ [Accessed 6 Feb. 2022]. (Stuska Dyno, 2022)

Taylordyno. (2022). [online] Available at: https://www.taylordyno.com/wp-content/uploads/pdfs/SMS2029-DE200.pdf [Accessed 10 May 2022].

wegetit.eu (2022). / *AMC Mecanocaucho*. [online] Mecanocaucho.com. Available at: https://www.mecanocaucho.com/en-gb/noticias/consejo-amc/consejo/#adv1 [Accessed 15 Mar. 2022]

Appendix I SISU 420 DWRIE performance and specifications

SISU Diesel

1998-05-27 J.KALLIO

TK9807

420 DWRIE ENGINE

ISO 8178 without fan

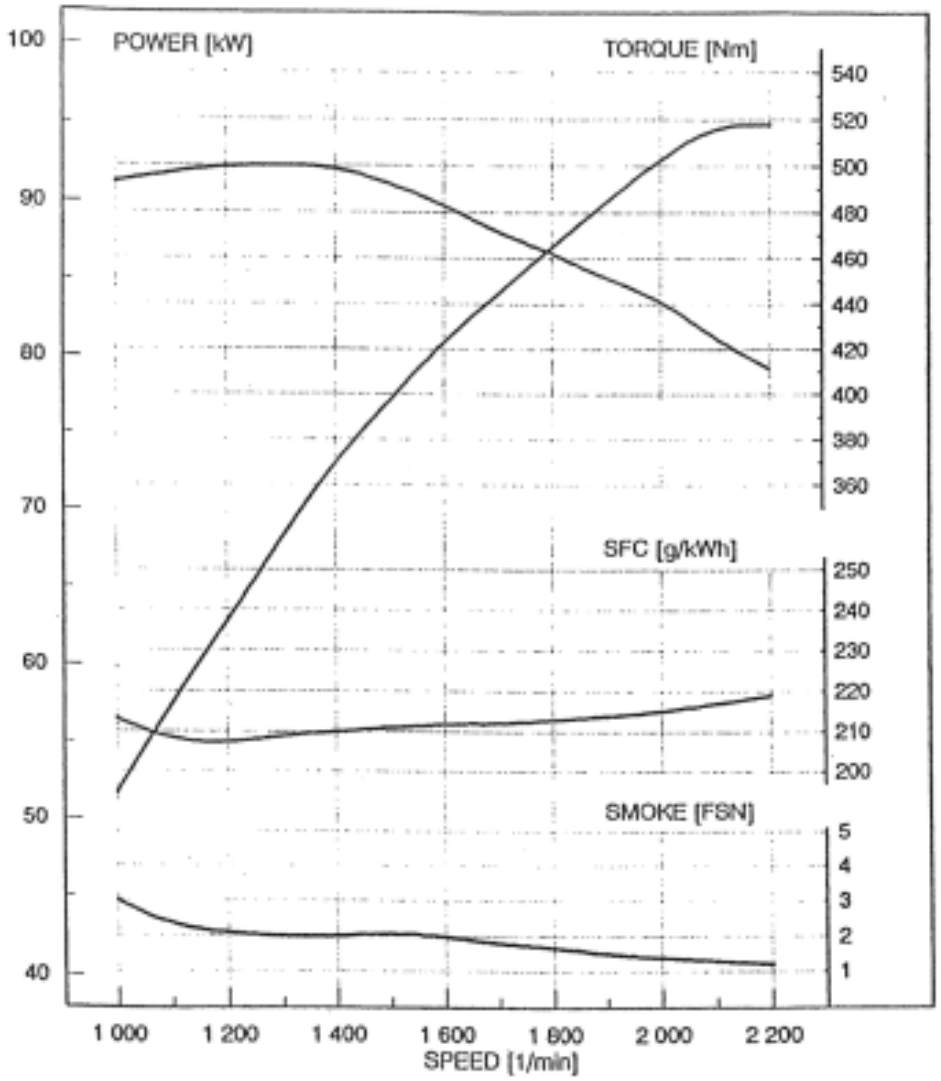

95 kW (129 hp) / 2200 rpm - 500 Nm / 1400 rpm - TBU 21 %
The power output is valid when the fuel density is 840 g/l at 15 C and fuel temperature is 35 C.
Power ouput of a new engine is about 3% lower.
Fulfils EPA 96 and 97/68/EC exhaust emissions for non-road mobile machinery.

From the performance curves supplied by the manufacturer, some data points are obtained. The next table shows the numerical values for said points.

Engine speed (rpm)	Power (kW)	Torque (Nm)
1000	51,5	491,79
1100	58	503,51
1200	64	509,30
1300	67,5	495,83
1400	73	497,93
1500	76,5	487,01
1600	80	477,46
1700	84	471,85
1800	86	456,24
1900	90	452,34
2000	92	439,27
2100	94,5	429,72
2200	95	412,36

Following, specifications of the SISU engine are shown, and the column of interest is the one referred to as 420 DWRIE.

ENGINE SPECIFICATIONS

Engine type	320D	320DS	420D	420DS	420DW	420DWI	620D	620DS	634DS
Number of cylinders	3	3	4	4	4	4	6	6	6
Displacement (dm^3)	3,3	3,3	4,4	4,4	4,4	4,4	6,6	6,6	7,4
Cylinder bore (mm)	108	108	108	108	108	108	108	108	108
Stroke (mm)	120	120	120	120	120	120	120	120	134
Compression ratio	16,5/18,5:1								
Combustion	direct injection								
Firing order	1–2–3			1–2–4–3			1–5–3–6–2–4		
Compression pressure bar[1]	24								
Weight kg[2]	275	280	335	340	340	345	500	510	515
Direction of rotation from the engine front	clockwise								

[1]) Minimum value at operating temperature and starting revs. Max permitted difference between cylinders 3,0 bar.
[2]) Without flywheel and electrical equipment.

Appendix II Opel Z16XEP performance

For the Opel engine, the performance information has been accessed directly from tabulations (automobile-catalog, 2013). The next table shows the different data points used

Engine speed (rpm)	Power (kW)	Torque (Nm)
1000	7,4	70,9
1100	9,3	80,6
1200	11,1	88,6
1300	13	95,5
1400	14,9	101,3
1500	16,7	106,4
1600	18,6	110,8
1700	20,4	114,7
1800	22,3	118,2
1900	24,1	121,3
2000	26	124,1
2100	27,8	126,6
2200	29,7	128,9
2300	31,6	131
2400	33,4	133
2500	35,3	134,7
2600	37,1	136,4
2700	39	137,9
2800	40,8	139,3
2900	42,7	140,6
3000	44,5	141,8
3100	46,4	143
3200	48,3	144
3300	50,1	145
3400	52	146
3500	53,8	146,9
3600	55,7	147,7
3700	57,5	148,5
3800	59,4	149,3
3900	61,3	150
4000	62,8	149,9
4100	64,3	149,8
4200	65,7	149,4
4300	67,1	149
4400	68,4	148,8
4500	69,7	147,8

4600	70,8	146,9
4700	71,9	146
4800	72,9	145
4900	73,8	143,8
5000	74,6	142,5
5100	75,3	141
5200	76	139,5
5300	76,5	137,8
5400	76,9	136
5500	77	133,7
5600	77	131,3
5700	77	129
5800	77	126,8
5900	77	124,6
6000	77	122,6
6100	76,7	120,1
6200	75,8	116,7
6300	74,2	112,5
6400	72	107,5
6500	69,3	101,8

Appendix III Water dynamometer performance data

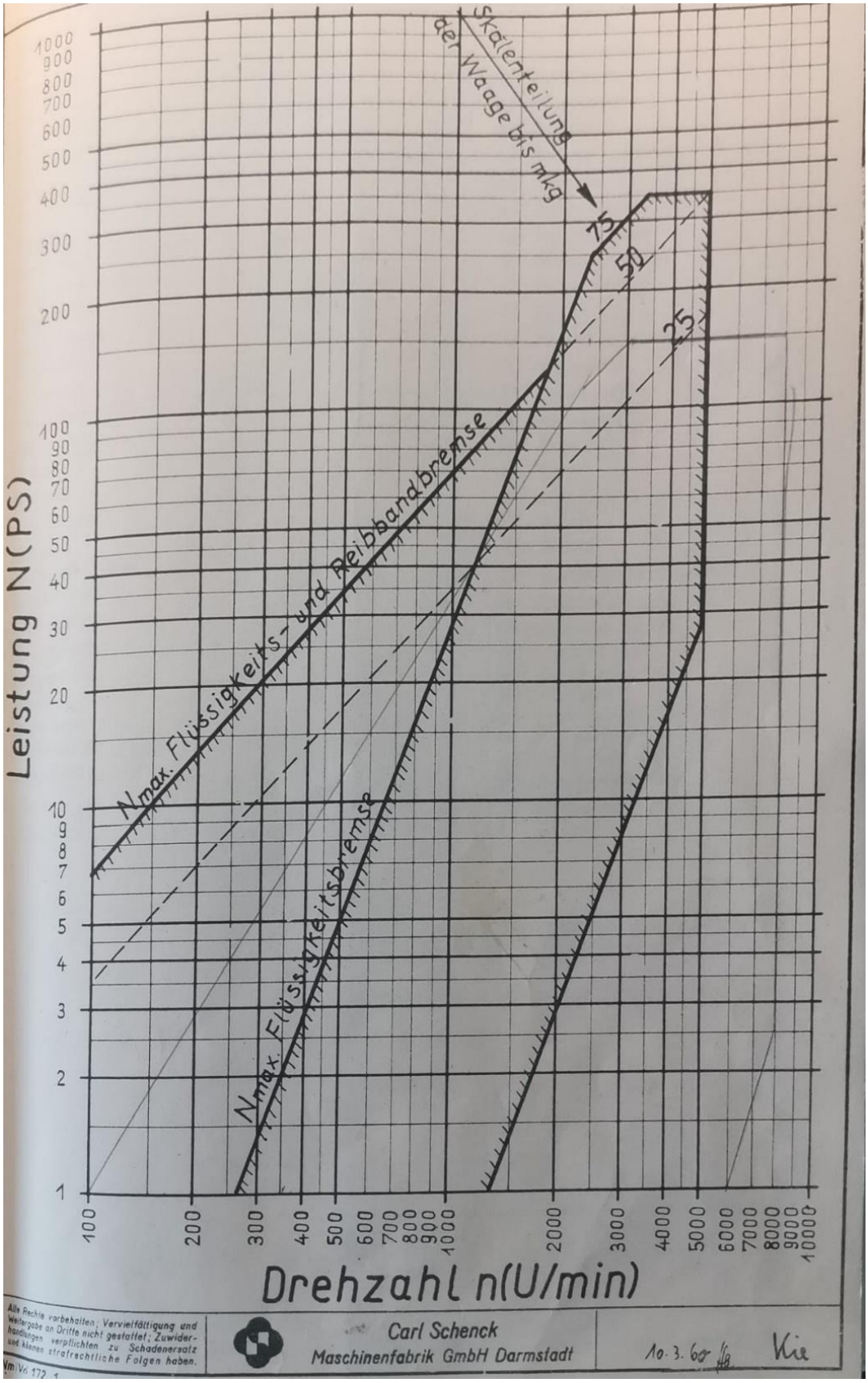

From the performance curves supplied by the manufacturer, some data points are obtained. The next table shows the numerical values for said points.

Speed (rpm)	Power (kW)	Torque (Nm)
300	1,09	47,11
400	2,17	70,43
500	3,68	95,49
600	5,88	127,32
700	8,46	156,88
800	11,03	179,05
900	16,18	233,43
1000	21,33	276,93
1250	36,78	381,97
1500	58,10	502,93
2000	119,15	773,49
2175	147,10	878,10
2470	183,88	966,53
3000	228,01	986,76
3500	257,43	954,93
3600	257,43	928,40
3700	257,43	903,31
3800	257,43	879,54
3900	257,43	856,99
4000	257,43	835,56
4100	257,43	815,18
4200	257,43	795,77
5000	257,43	668,45

Appendix IV Froude EC50TC performance data

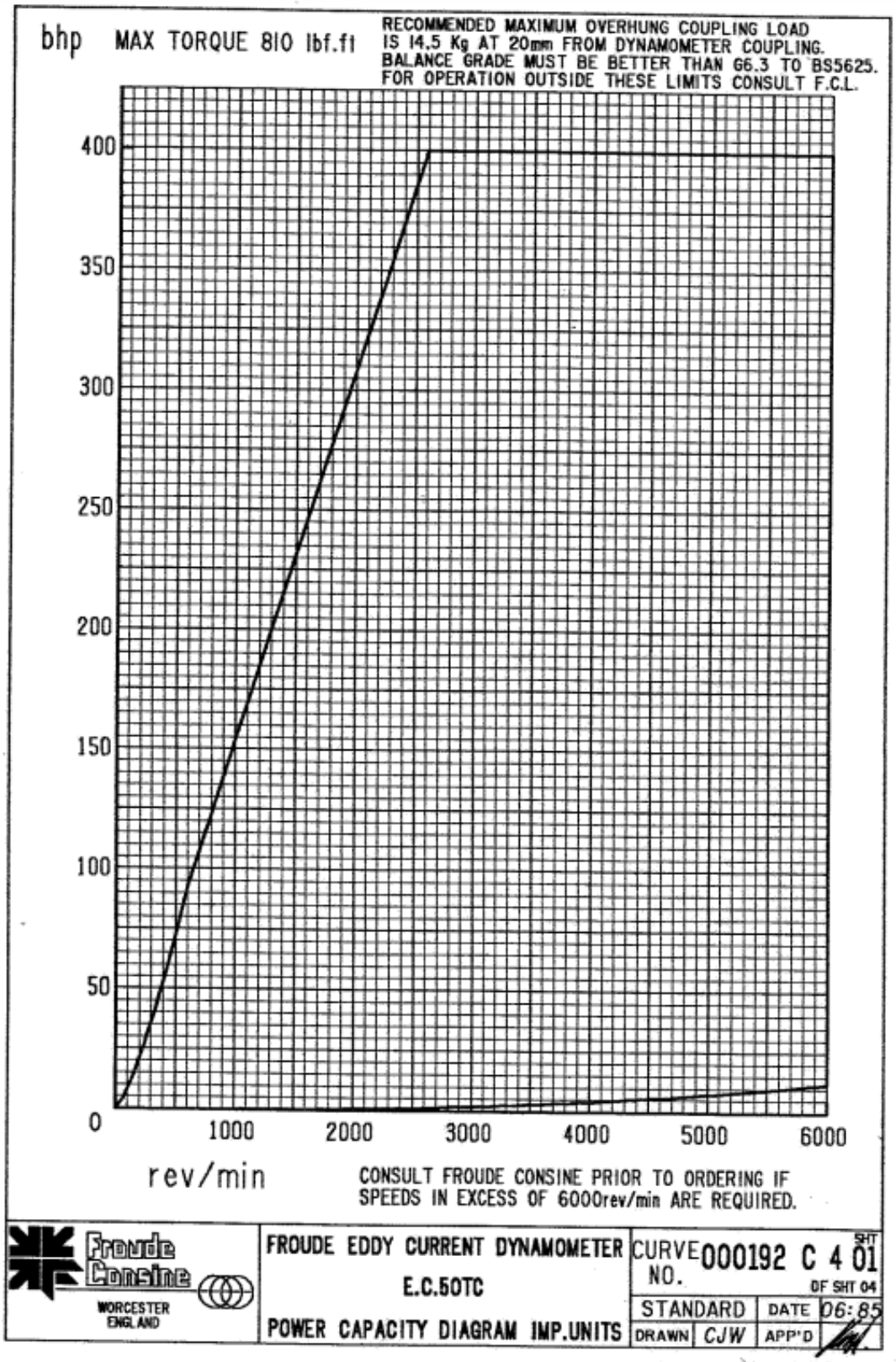

From the performance curves supplied by the manufacturer, some data points are obtained. The next table shows the numerical values for said points.

Speed (rpm)	Power (kW)	Torque (Nm)
0	298,40	0,00
100	3,95	377,56
200	14,92	712,38
300	26,11	831,11
400	40,28	961,71
500	53,71	1025,82
600	67,14	1068,57
700	79,08	1078,74
800	91,39	1090,83
900	102,95	1092,31
1000	114,88	1097,06
1100	126,07	1094,47
1200	138,01	1098,25
1300	149,20	1095,97
1400	160,39	1094,01
1500	171,58	1092,31
1600	182,77	1090,83
1700	195,45	1097,90
1800	206,64	1096,27
1900	219,32	1102,31
2000	230,51	1100,62
2100	242,45	1102,49
2200	252,89	1097,71
2300	264,83	1099,54
2400	278,26	1107,15
2500	289,45	1105,61
2600	298,40	1095,97
2700	298,40	1055,37
2800	298,40	1017,68
2900	298,40	982,59
3000	298,40	949,84
3100	298,40	919,20
3200	298,40	890,47
3300	298,40	863,49
3400	298,40	838,09
3500	298,40	814,15
3600	298,40	791,53
3700	298,40	770,14
3800	298,40	749,87

3900	298,40	730,64
4000	298,40	712,38
4100	298,40	695,00
4200	298,40	678,45
4300	298,40	662,68
4400	298,40	647,62
4500	298,40	633,22
4600	298,40	619,46
4700	298,40	606,28
4800	298,40	593,65
4900	298,40	581,53
5000	298,40	569,90
5100	298,40	558,73
5200	298,40	547,98
5300	298,40	537,64
5400	298,40	527,69
5500	298,40	518,09
5600	298,40	508,84
5700	298,40	499,91
5800	298,40	491,29
5900	298,40	482,97
6000	298,40	474,92

Appendix V Taylordyno DH21 performance data

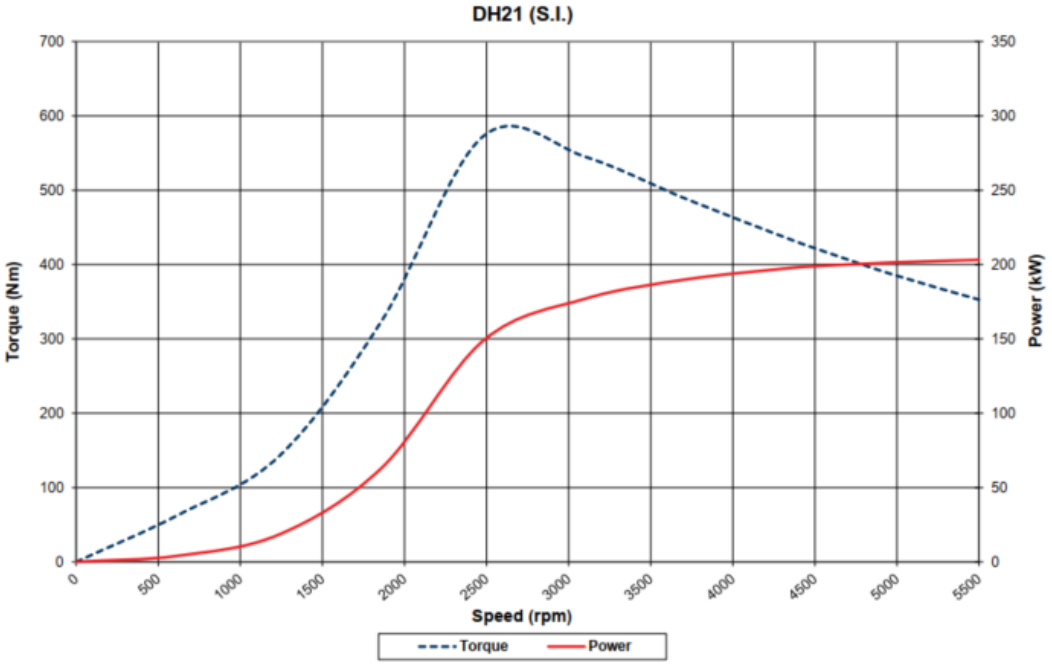

Appendix VI Lanmec DW250 performance data, specifications, geometry, and price information.

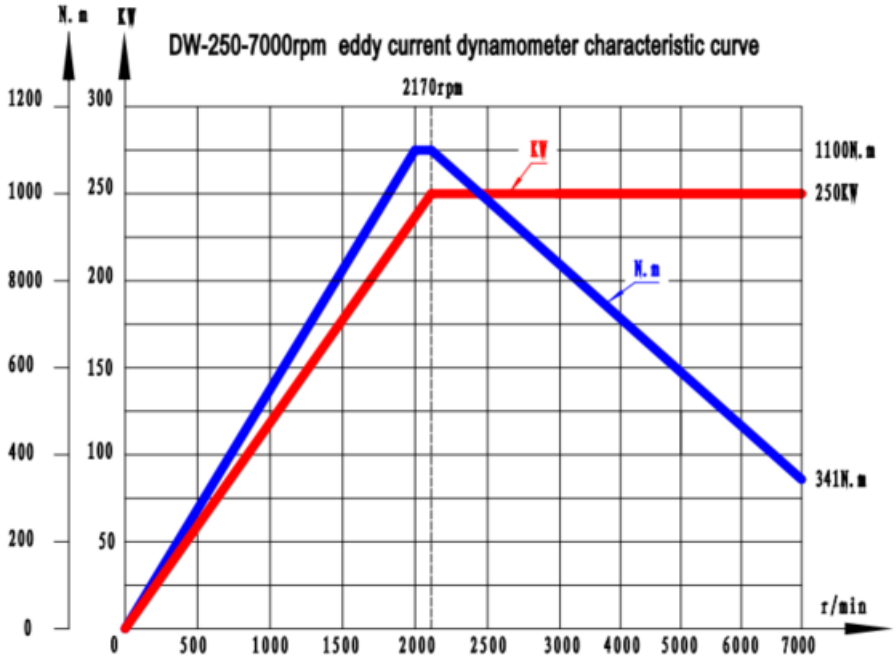

From the performance curves supplied by the manufacturer, some data points are obtained. The next table shows the numerical values for said points.

Speed (rpm)	Power (kW)	Torque (Nm)
0	0	0
500	55	285
1000	120	550
1500	175	805
2000	235	1100
2170	250	1100
2500	250	995
3000	250	825
4000	250	705
5000	250	595
6000	250	470
7000	250	341

Following, the geometrical data about the DW250 dynamometer is presented.

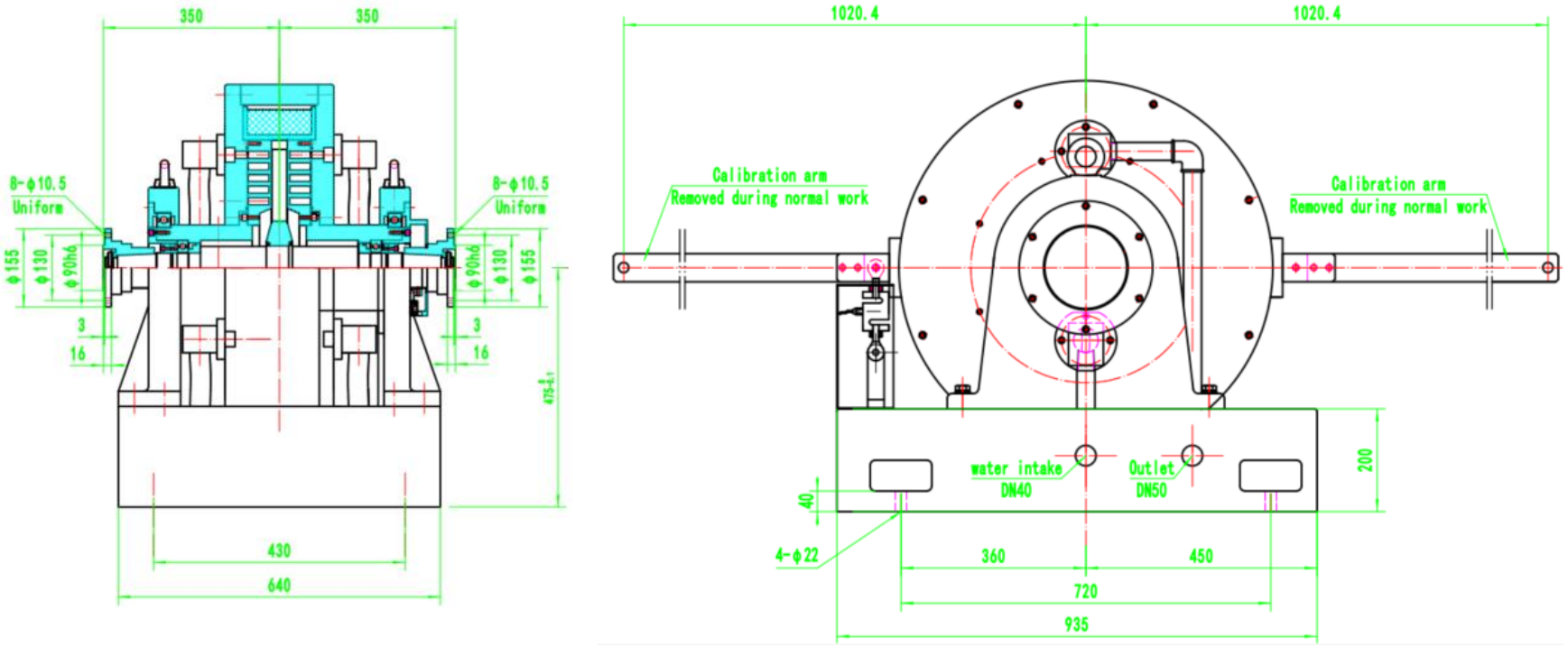

Following, is shown the budget provided by the manufacturer.

Lanmec® 兰菱科技 Test

INVOICE

Invoice No.: 20220228-01
Date: 28 February 2022

THE SELLER	THE BUYER
Company Name: Jiangsu Lanmec Electromechanical Technology Co., Ltd.	**Company Name:** Novia University of Applied sciences Finland
Contact Person: Nicole Yang	**Contact Person**: Pol estudis
Mobile Phone:86-13806277272	**Mobile Phone**:
Email: lanmec@lanmec.com	**Email:** arxiu.universitat.pol@gmail.com
Address: 11 ChaoYang Road(N), Haian, Nantong,Jiangsu, China	**Address:**
Phone: 86-513-88801556	

SL No	Product Descriptions	Quantity	Unit Price (USD)	Total Price (USD)	Remarks
1.	Eddy current dynamometer DW250(7000rpm) (Including calibration force arm, weight)	1	15500	15500	
2.	Torque speed power acquisition instrument CFY-10	1	1000	1000	
3.	Load controller SC-1D	1	1000	1000	
			Total EXW PRICE	17500	

Appendix VII Taylordyno DE200 performance data, specifications, and geometry.

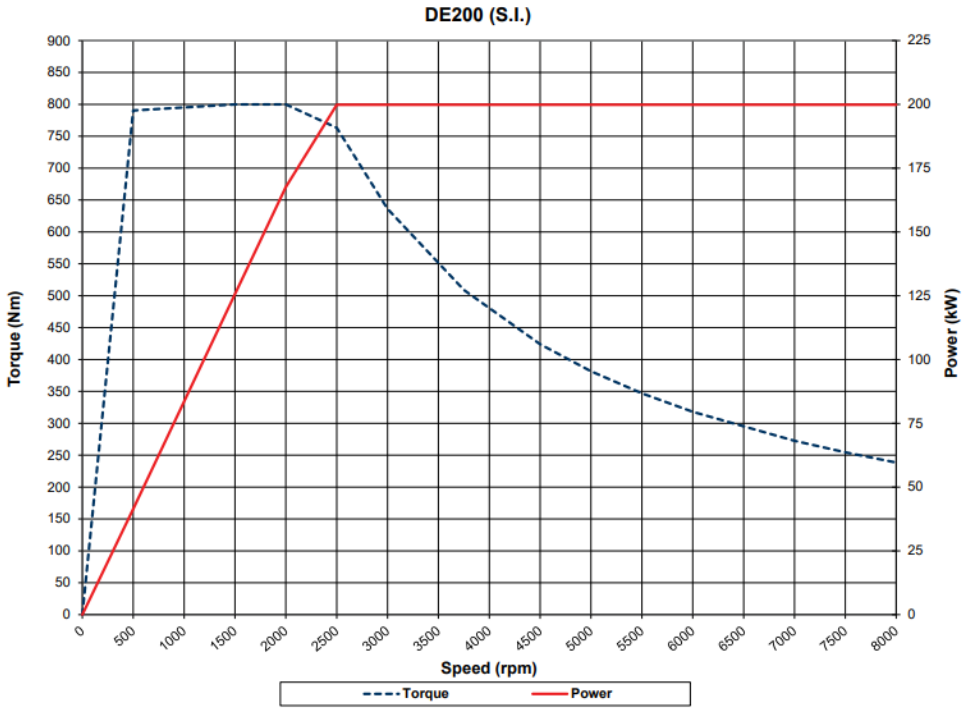

From the performance curves supplied by the manufacturer, some data points are obtained. The next table shows the numerical values for said points.

Speed (rpm)	Power (kW)	Torque (Nm)
0	0	0
500	39	790
1000	82	795
1500	125	800
2000	170	800
2500	200	760
3000	200	645
3500	200	550
4000	200	480
4500	200	425
5000	200	380
5500	200	350
6000	200	320
6500	200	298
7000	200	275
7500	200	252
8000	200	240

Following, the geometrical data about the DE200 dynamometer and other specifications is presented.

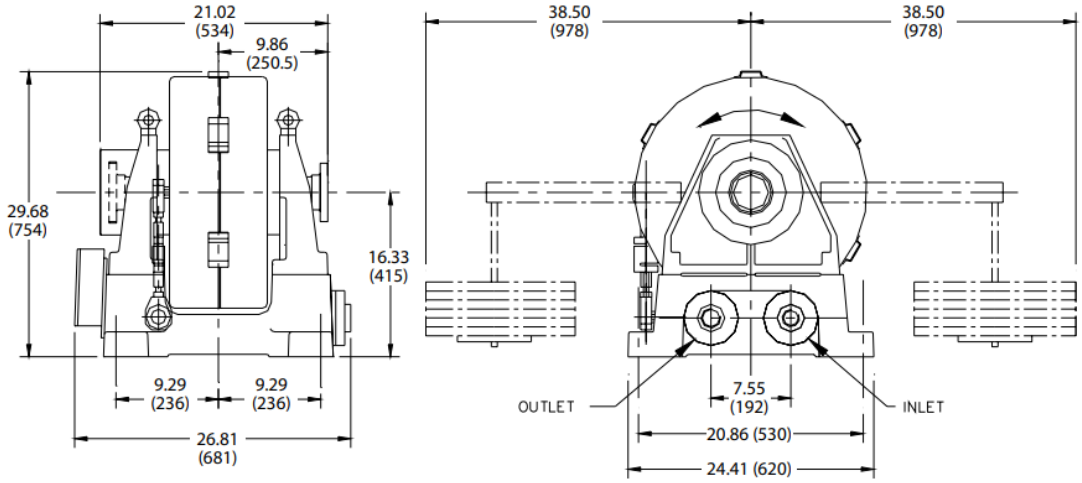

Specifications

Power:	268 hp (200 kW)
Torque:	590 lb-ft (800 Nm)
Speed:	8,000 rpm
Water Use*:	37 gpm (140.1 lpm)
Inertia Value:	8.28 lb·ft^2 (0.349 kg·m^2)
Shipping Weight:	1,863 lb (845 kg)
Rotation:	bi-directional

**No Cooling System*

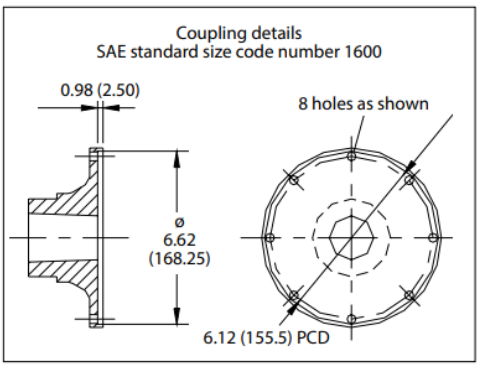

Appendix VIII Trelleborg AB mountings technical information.

This appendix is used for introducing the diagrams of the current mountings used for both engines. They are shown in form of adaptation in the report, however here the original version is presented.

Firstly, the diagrams corresponding to the mountings used in the SISU engine are shown. They have been used in section 5 of the report as a way to back the study.

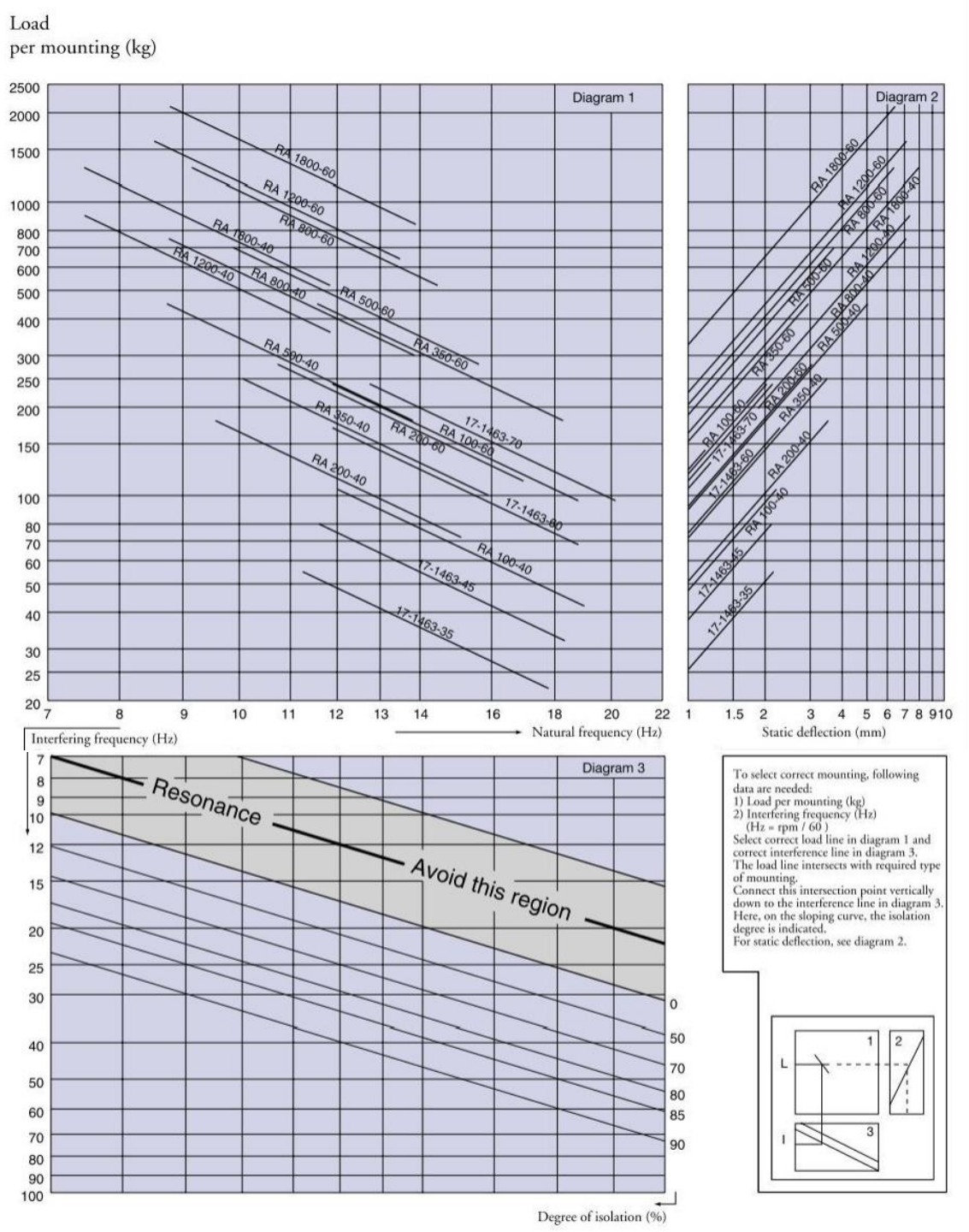

Following, the diagrams corresponding to the mountings used in the Opel engine are shown, the exact model is RA 125 EMA:

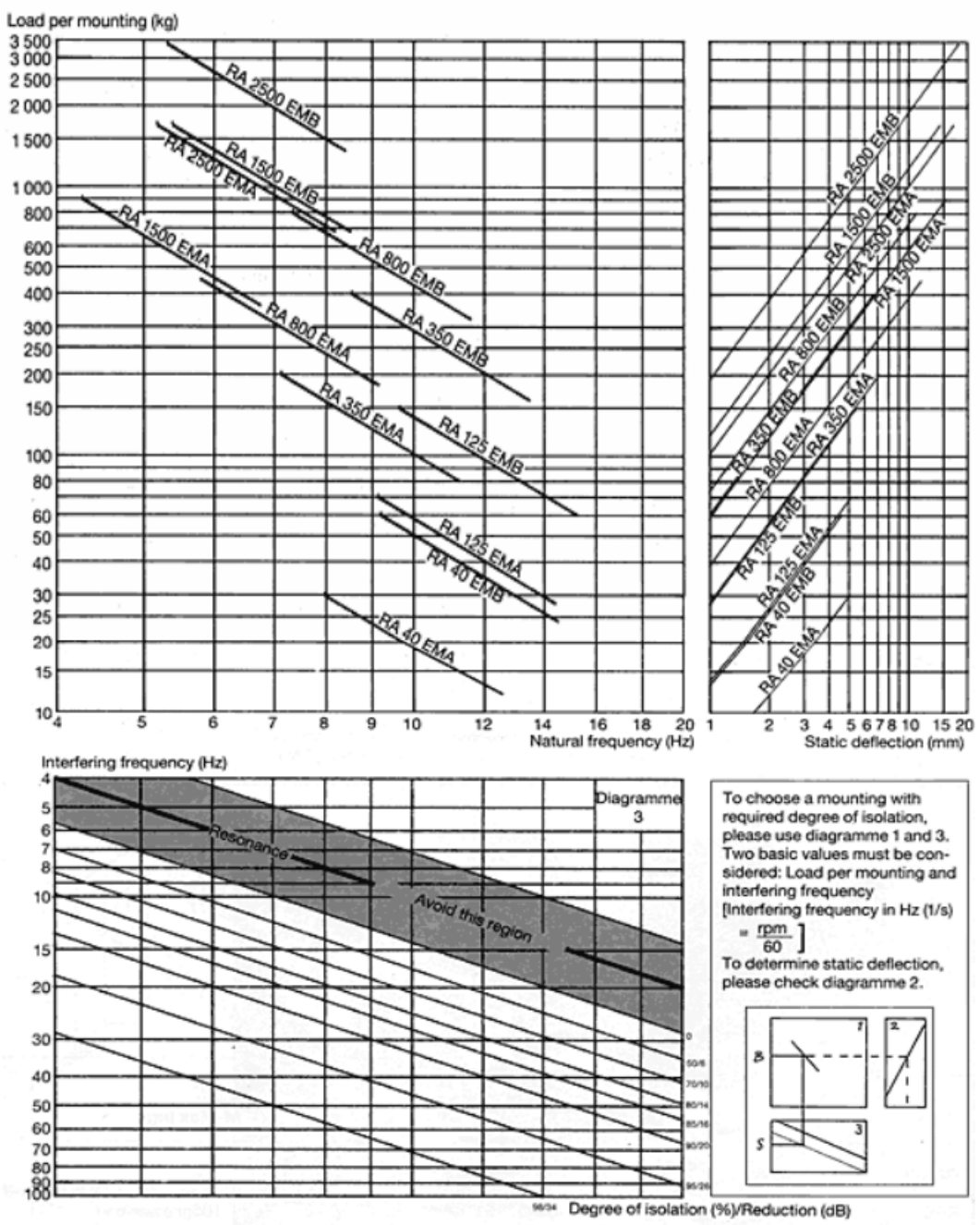

Appendix IX Vulkan mountings technical information.

These mountings are the option that has been used to isolate the vibrations coming out from the SISU engine. Firstly, technical information about their performance is shown.

VD SERIES

BAUGRUPPE DIMENSION GROUP
VD

LEISTUNGSDATEN PERFORMANCE DATA

		$F_{z, Nominal}$ [1]	$C_{z, Nominal}$
		[kN]	[kN/mm]
Baugruppe Dimension group	Elementsteifigkeit Element stiffness	Vertikale Nennlast Vertical nominal load	Vertikale statische Steifigkeit bei Nennlast Vertical static stiffness at nominal load
VD 3	22	0,75	0,15
VD 3	24	0,95	0,19
VD 3	26	1,10	0,23
VD 4	22	2,30	0,85
VD 4	24	2,80	1,35
VD 4	26	3,30	1,75
VD 5	22	3,40	0,45
VD 5	24	6,20	0,80
VD 5	26	7,40	0,95
VD 8	22	4,70	1,50
VD 8	24	6,20	2,00
VD 8	26	9,20	2,80
VDC 10	22	6,80	1,55
VDC 10	25	11,00	2,60
VDC 10	27	14,00	3,85
VDC 20	22	12,00	3,41
VDC 20	25	20,00	5,56
VDC 20	27	25,00	7,14

[1] Die Nennlast beträgt 75% der Höchstlast und ist für die erste Auslegung zu verwenden. VD 4 Lager haben die gleiche Schwingungsdämpfung wie VD S3 Lager.

[1] Nominal load is 75% of maximum load and to be used for first selection purposes. VD 4 mounts have the same anti-vibration performance as VD S3.

The geometric data about the selected dynamometers for the Opel engine is shown below.

VD SERIES

BAUGRUPPE DIMENSION GROUP
VD

GEOMETRISCHE DATEN GEOMETRIC DATA

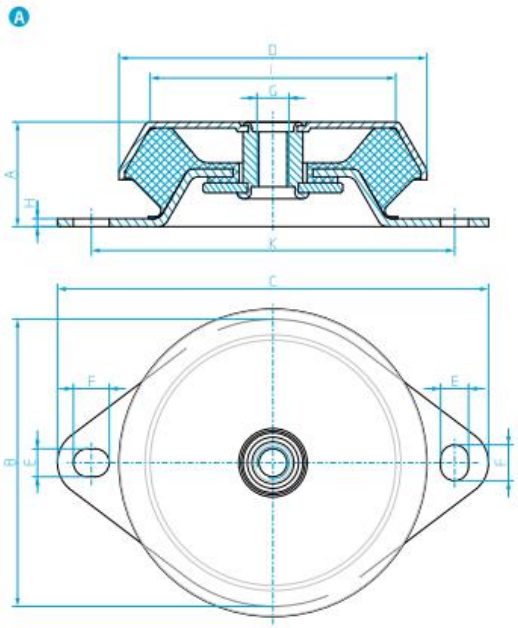

Baugruppe Dimension group	Abbildung Figure	Abmessungen Dimension					
		A	B	C	D	E	F
		[mm]	[mm]	[mm]	[mm]	[mm]	[mm]
VD 3	A	35,50	63,00	110,00	Φ34,00	9,00	16,00
VD 4	A	35,00	88,00	144,00	Φ53,00	10,00	10,00
VD 5	A	52,50	144,00	216,00	Φ 54,00	14,00	18,00
VD 8	A	48,50	154,00	226,00	Φ 44,00	18,00	24,00
VDC 10	B	63,00	170,00	170,00	Φ 54,00	14,00	19,50
VDC 20	B	73,50	190,00	190,00	Φ 74,00	16,00	23,00

Appendix X Trelleborg AB mountings used for the Opel engine technical and geometric information.

The following sheet shows the technical data about the mountings that will be used for the Opel engine, the model selected is M 100 40 IRH, which refers to the part number 10-00100.

TRELLEBORG INDUSTRIAL AVS

TRELLEBORG

M-Mounting

Technical Drawing

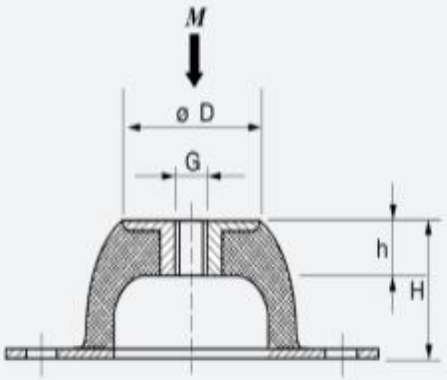

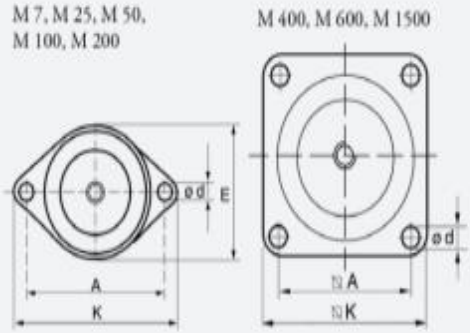

Product Data

DRAWING No.	PART No.	TYPE	DIMENSIONS (mm)								MAX LOAD (kg)	WEIGHT (kg)
			D	E	A	K	H	h	d	G		
17-4056	10-00139	M 7 40 IRH	18	43	50	64	20	7	7	M6	3.5	0.02
17-4057	10-00140	M 7 60 IRH	18	43	50	64	20	7	7	M6	9	
17-4047	10-00094	M 25 40 IRH	33	56	66	85	25	11	8	M8	20	0.07
17-4048	10-00095	M 25 60 IRH	33	56	66	85	25	11	8	M8	50	
17-4052	10-00096	M 50 40 IRH	45	76	92	114	35	14	10	M10	40	0.16
17-4053	10-00097	M 50 60 IRH	45	76	92	114	35	14	10	M10	80	
17-4041	10-00100	M 100 40 IRH	53	96	110	136	40	15	11.5	M10	70	0.26
17-4042	10-00099	M 100 60 IRH	53	96	110	136	40	15	11.5	M10	150	
174044	10-00102	M 200 40 IRH	58	101	124	151	45	13	11.5	M10	130	0.42
17-4045	10-00103	M 200 60 IRH	58	101	124	151	45	13	11.5	M10	220	
17-4050	10-00104	M 400 40 IRH	78	-	120	150	63	18	14.5	M12	280	1.06
17-4051	10-00105	M 400 60 IRH	78	-	120	150	63	18	14.5	M12	500	

Appendix XI SISU 420 DWRIE flywheel and flywheel housing technical information and geometry.

FLYWHEEL AND FLYWHEEL HOUSING SAE 3

Flywheel housing	8366 47440	(M18x1,5-6H for sensor)	
Flywheel housing	8366 64216	(2 x M18x1,5-6H for sensor)	
Flywheel	8361 24197	J = 0,45 kgm^2	SAE 11,5"

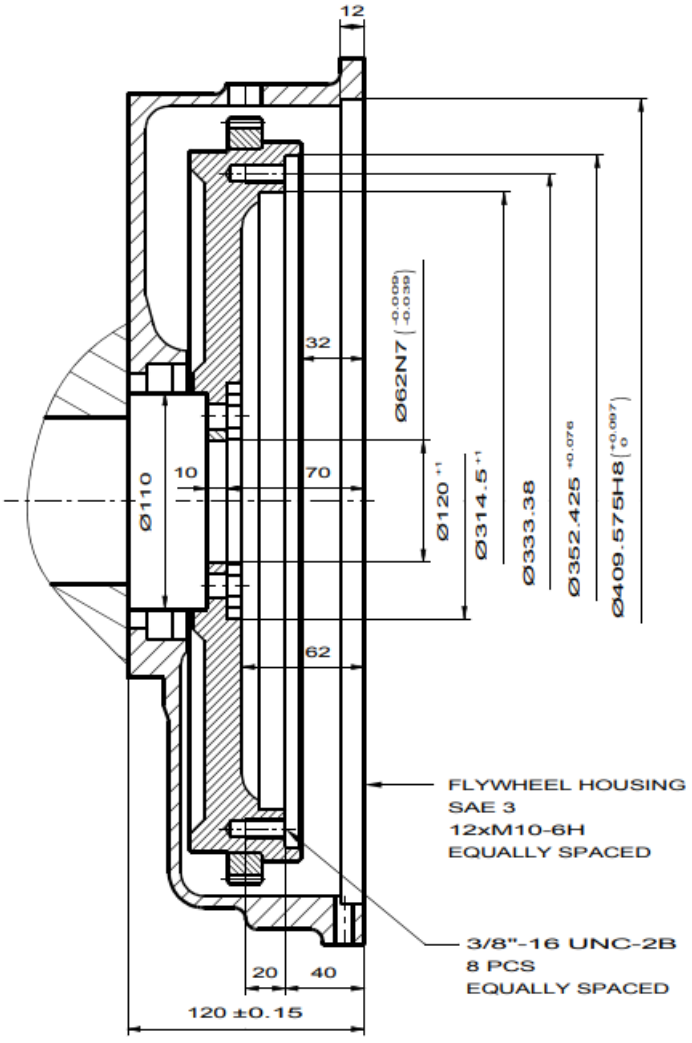

Appendix XII Opel Z16XEP flywheel.

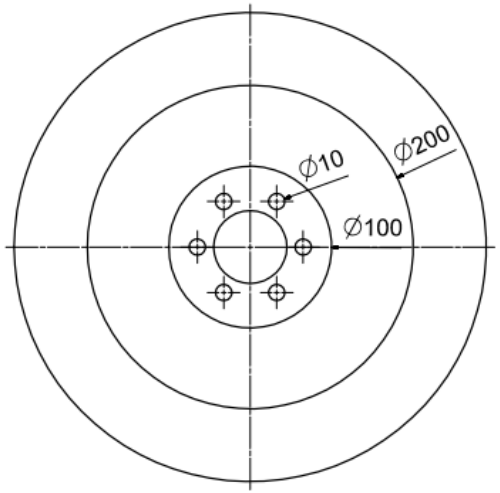

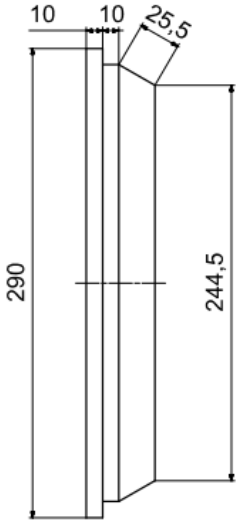

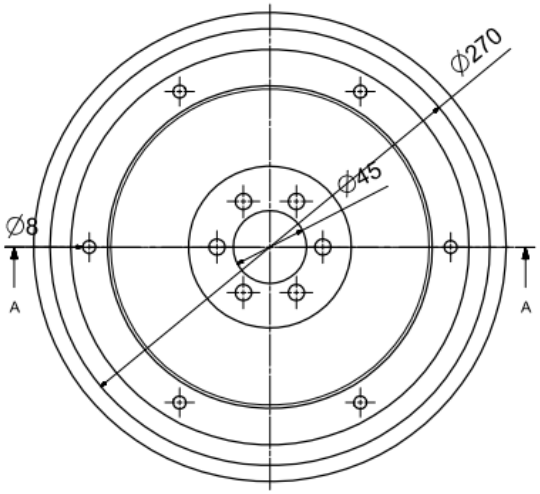

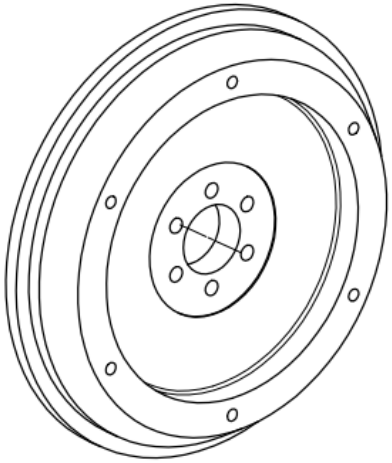

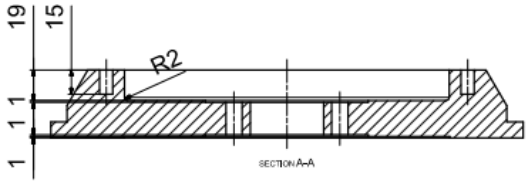

Appendix XIII Adapter for the engine flexible coupling.

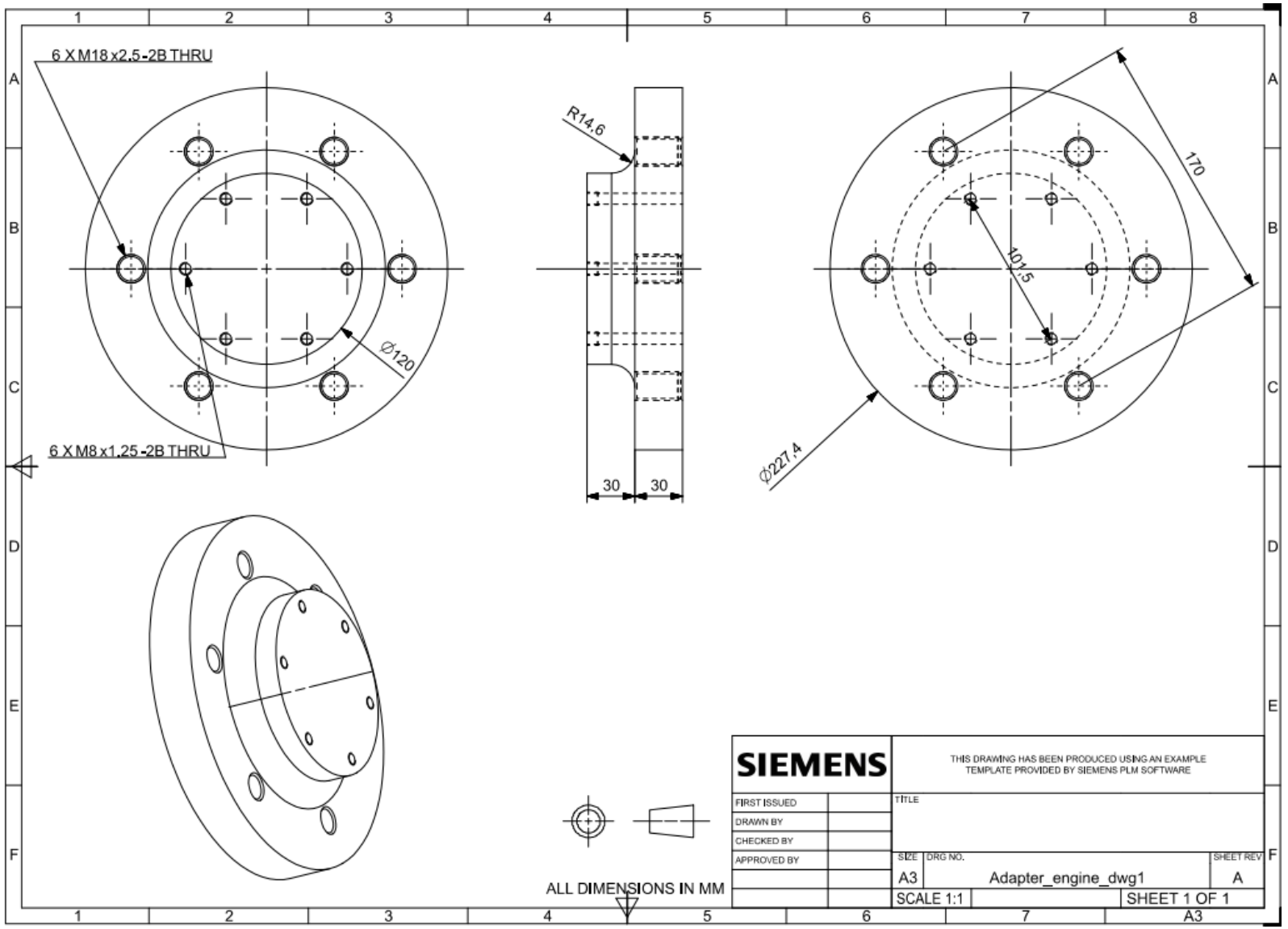

Appendix XIV Adapter for the coupling of the dynamometer with the Cardan shaft.

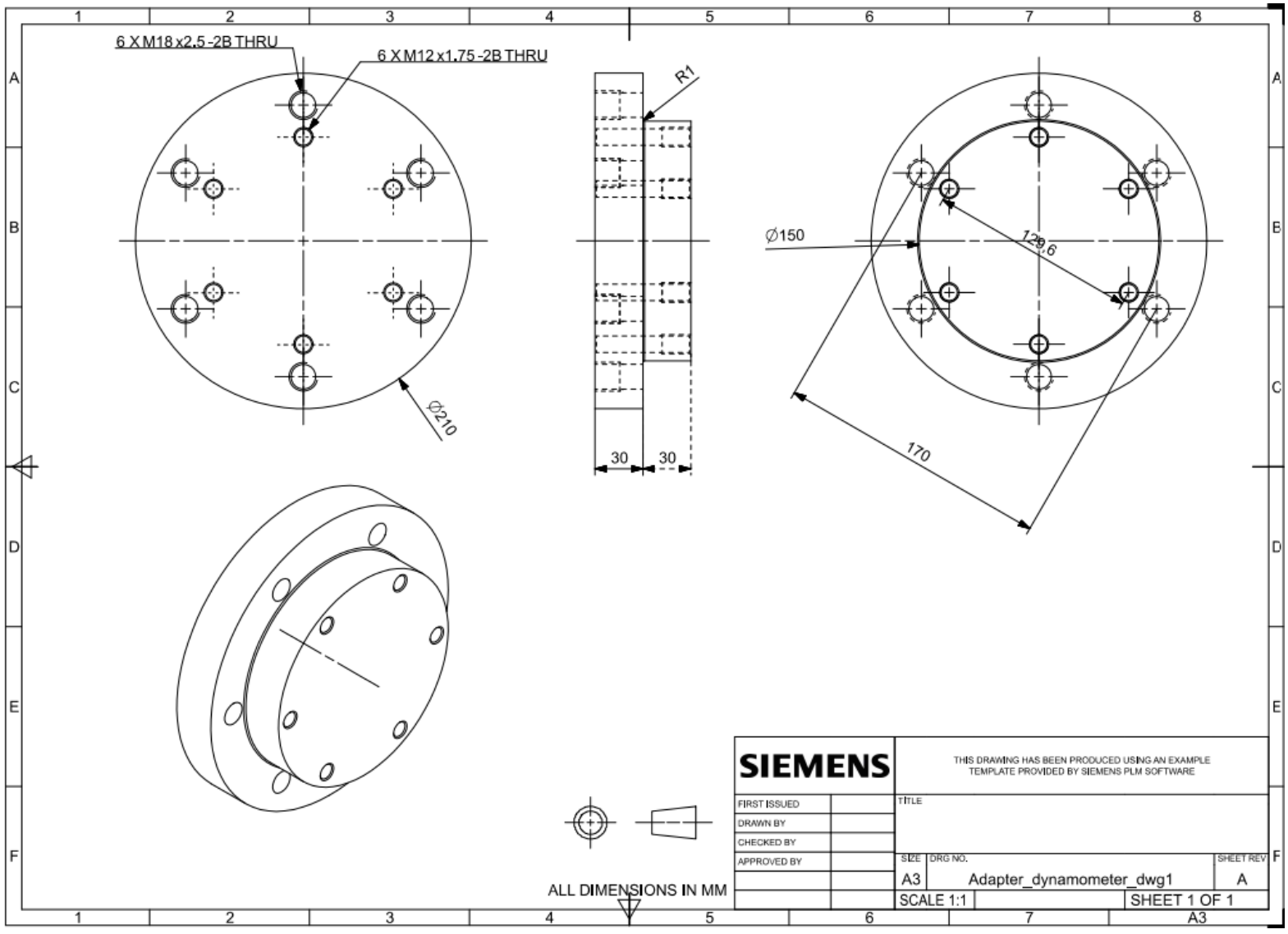

Appendix XV Pieces used for raising the position of the SISU 420 DWRIE.

Following, the different pieces that will for the assembly used for substituting the right side of the structure of the engine bed test are used. Following the iron base of the pieces identified as a) in Figure of the report is shown.

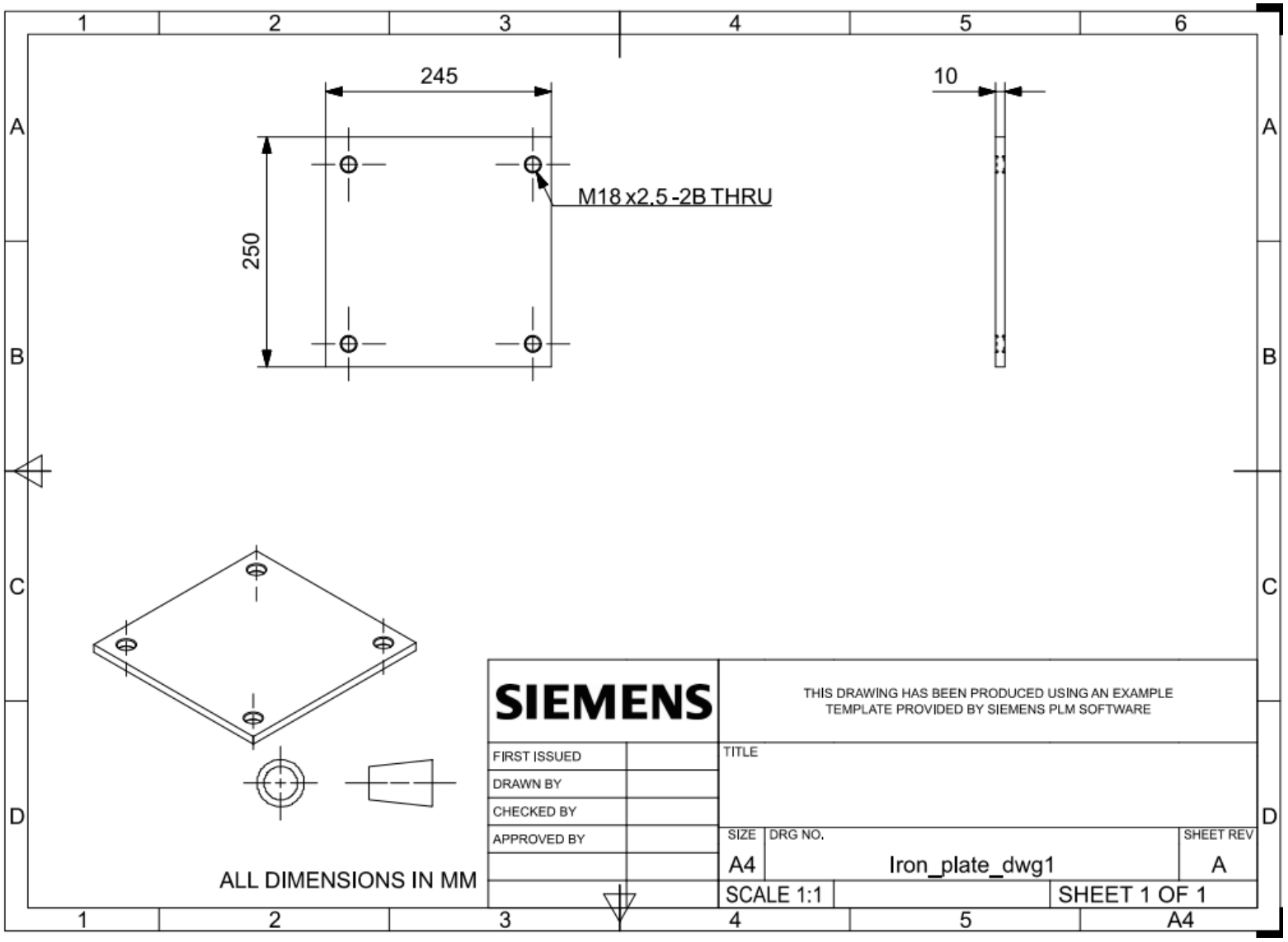

Following, the beam identified as iron beam b) in figure is shown.

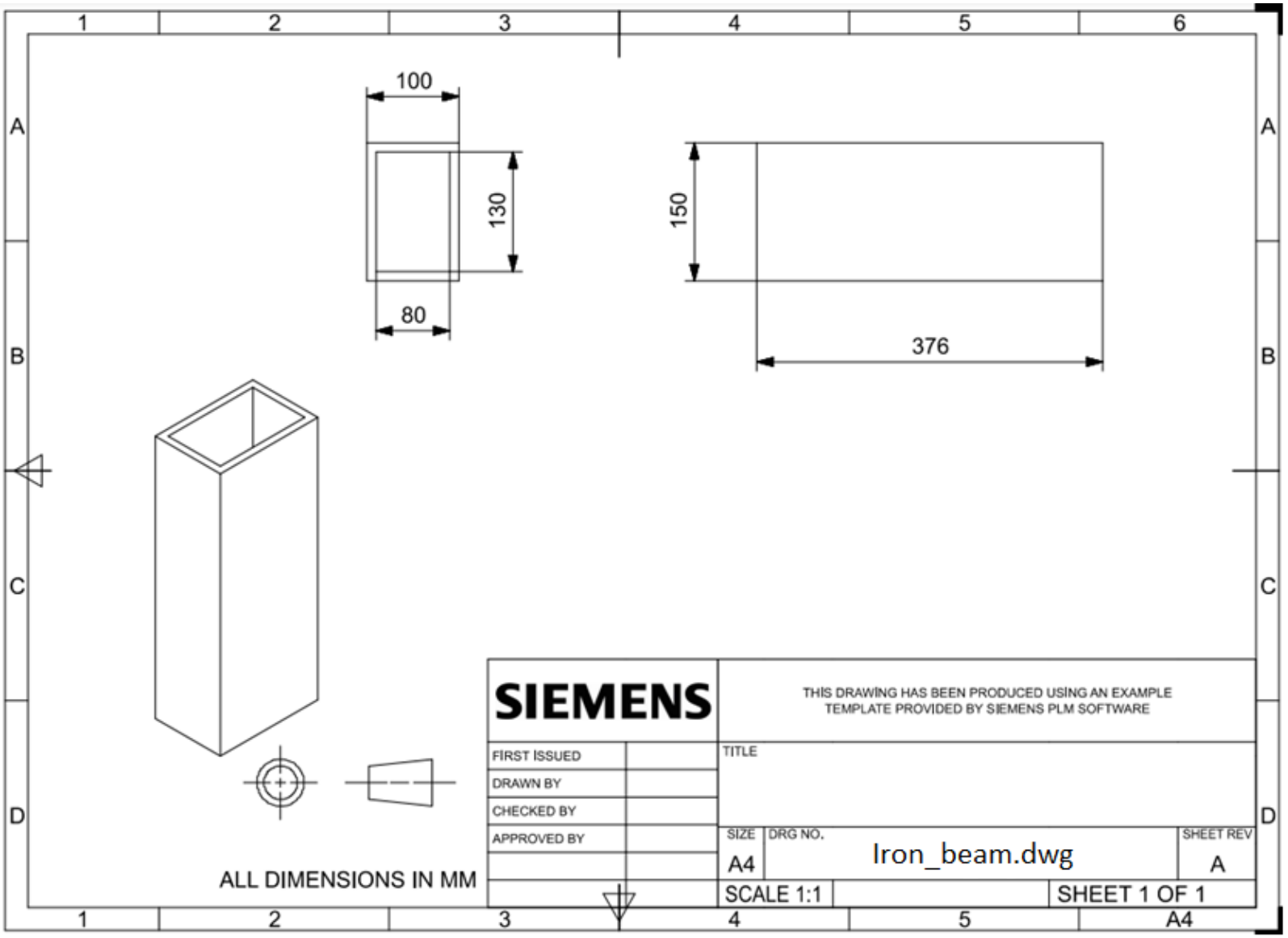

Following, the iron cover identified as c) in figure of the report is shown.

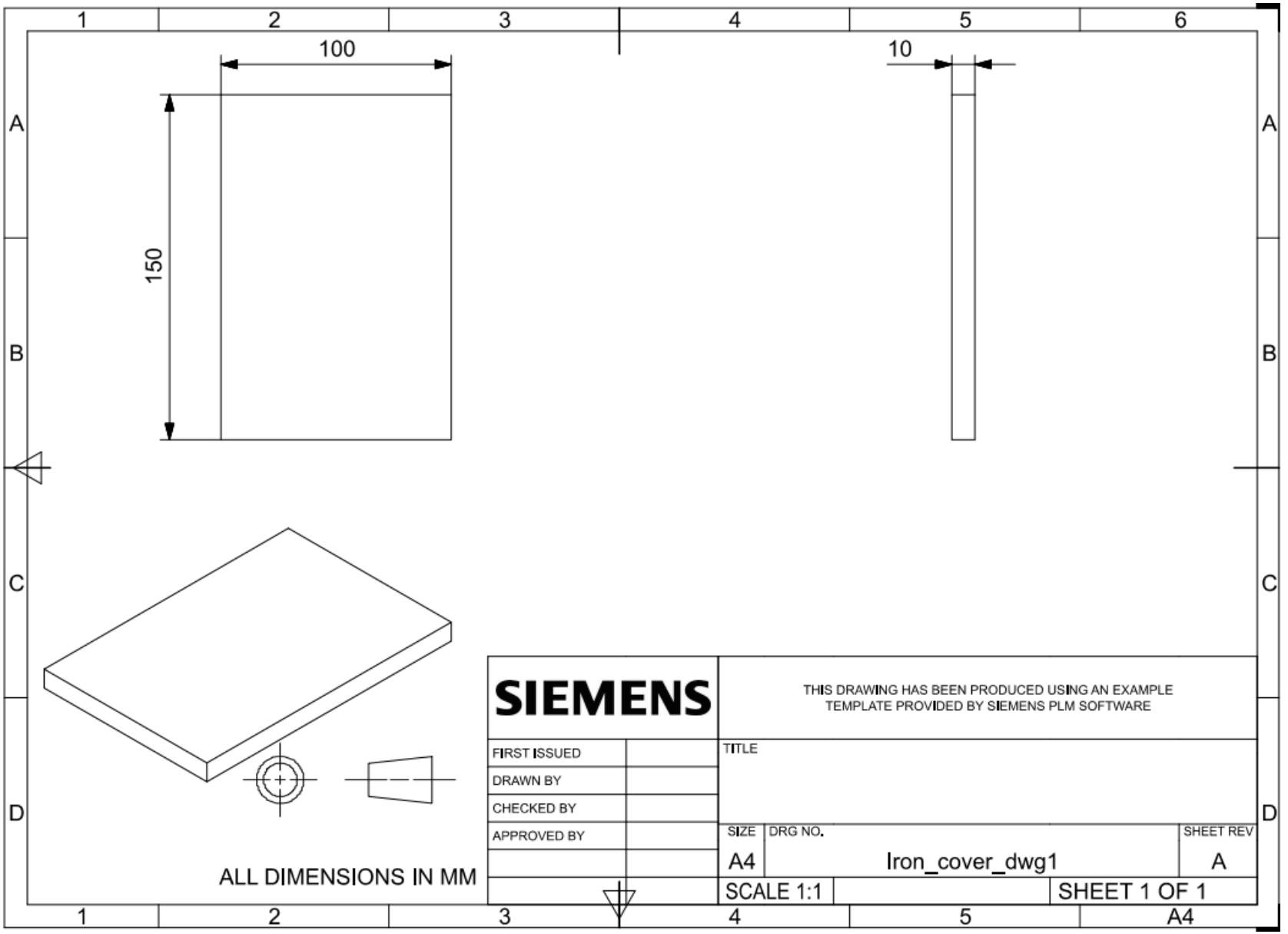

Appendix XVI Current engine bed test measurements.

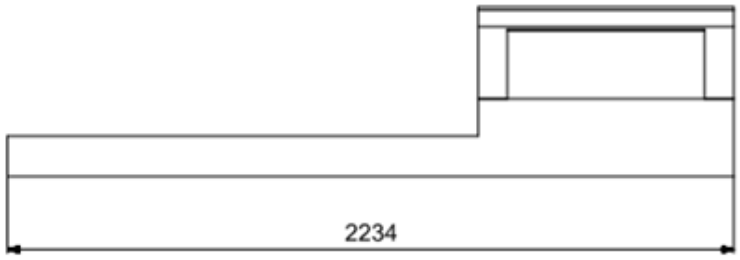

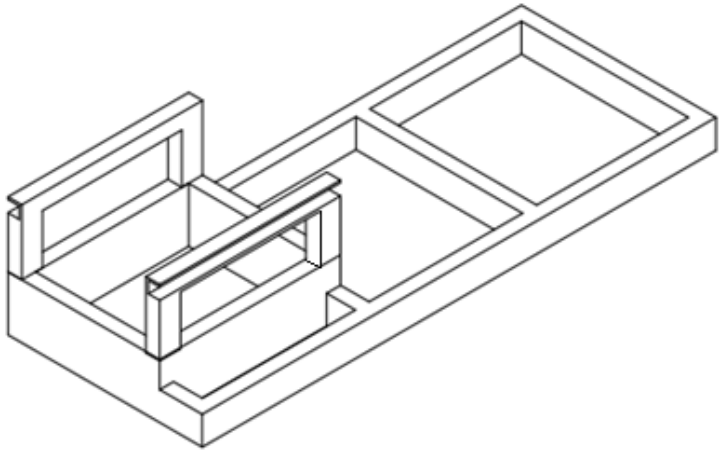

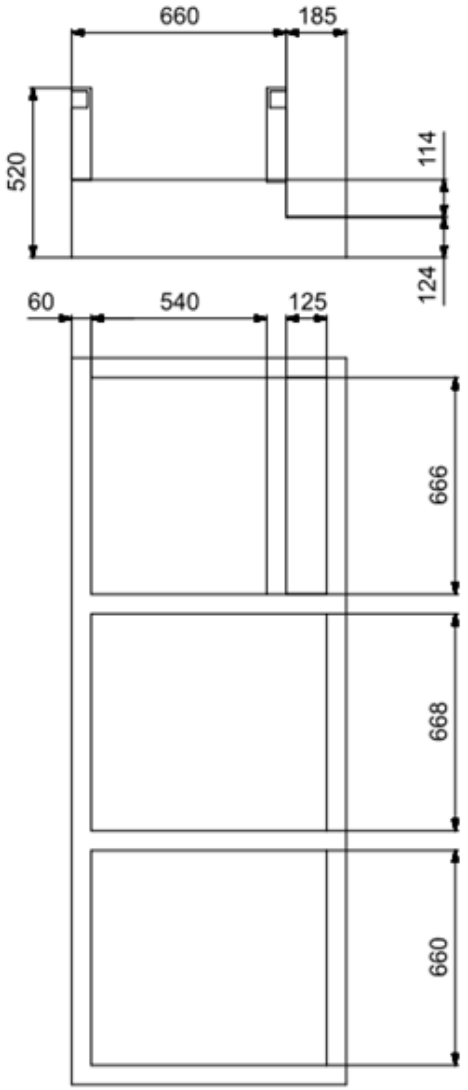

Appendix XVII New engine bed test measurements.

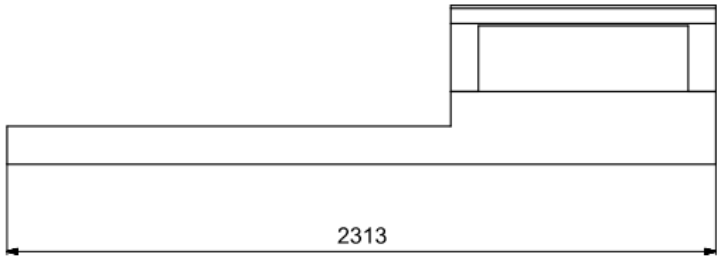

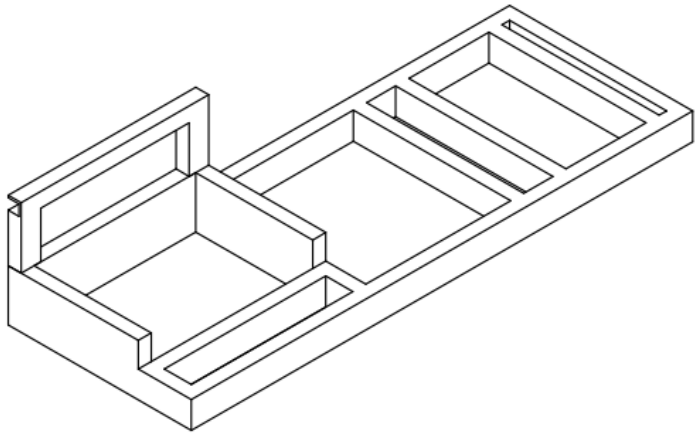

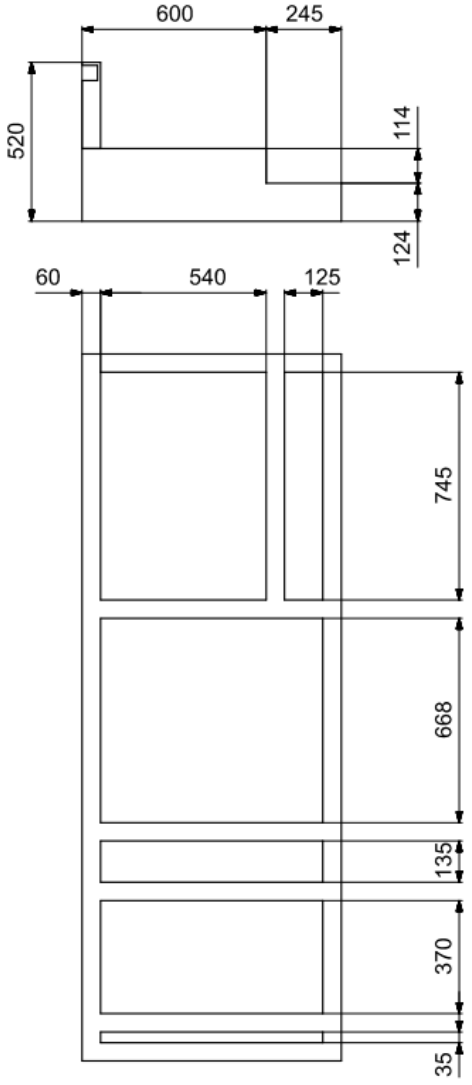

Appendix XVIII Shared folder

A shared folder with all files used during the thesis is available at Novia University of Applied Sciences. There can be found all GT-Power files as well as Excel files with all the basic simulation parameters and extra calculations.